USING ^{10}BE TO CONSTRAIN EROSION RATES OF BEDROCK OUTCROPS GLOBALLY AND IN THE CENTRAL APPALACHIAN MOUNTAINS

A Thesis Presented

by

Eric William Portenga

to

The Faculty of the Graduate College

of

The University of Vermont

In Partial Fulfillment of the Requirements
for the degree of Master of Science
Specializing in Geology

May 2011

Accepted by the Faculty of the Graduate College, The University of Vermont, in partial fulfillment of the requirements for the degree of Master of Science, specializing in Geology.

Thesis Examination Committee:

_____ Advisor
Paul R. Bierman, Ph.D.

_____
Laura E. Webb, Ph.D.

_____ Chairperson
Donna M. Rizzo, Ph.D.

_____ Dean, Graduate College
Domenico Grasso, Ph.D.

Date: **December 10, 2010**

ABSTRACT

Bedrock outcrops are features of landscapes around the world. Outcrops are the backbone of mountain chains and their presence along ridgelines often marks the boundary between drainage basins. As mountain belts are uplifted, material removed from outcrops by erosional processes is transported through the drainage basin via fluvial processes. Though outcrops are common and these fluvial processes on-going, the rates at which these phenomena occur are poorly constrained on millennial timescales and longer.

In situ production of ^{10}Be occurs when cosmic-rays trigger spallation reactions in mineral structures at Earth's surface; thus, the concentration of ^{10}Be can be used to infer residence times within the uppermost few meters of the crust. These concentrations can be used to model erosion rates in a variety of Earth surface materials that geologists sample, most commonly rock from the top surfaces of outcrops and fluvial sediment taken from active stream channels.

This thesis compiles publically available measurements of ^{10}Be from outcrops (n = 418) and fluvial sediment ($n = 1110$), published in 82 studies, in a global meta-analysis. I do statistical analyses of environmental, physical, and topographical parameters to determine their relationship with erosion rates for various lithologic, climatic, and seismic settings. Erosion rates from drainage basins (average = 209 ± 33 m My^{-1}) are two orders of magnitude higher than the average outcrop erosion rate (12 ± 1.3 m My^{-1}); median erosion rates follow the same pattern (53 and 5.2 m My^{-1} for drainage basins and outcrops, respectively). I conclude that 33% of global outcrop erosion rate variability is explained by six parameters (latitude, elevation, relief, mean annual precipitation and temperature, and seismicity) and that 56% of drainage basin erosion rate variability is explained by nine parameters: the same six listed above and basin slope, percent vegetation, and basin area.

This global context provides the background in which I am able to compare a subset of samples I collected from bedrock ridges in the central Appalachian Mountains ($n = 72$). Average erosion rates of 15 ± 1 and 9.7 ± 0.7 m My^{-1} for bedrock outcrops in the Potomac and Susquehanna River Basins, respectively are similar to outcrop erosion rates previously determined for the region. Outcrop erosion rates are similar to those inferred for sub-basins of the Potomac River, but outcrops erosion rates are half as rapid as those inferred for sub-basins of the Susquehanna River. The average outcrop erosion rate for the field area (13 ± 1 m My^{-1}) is slower, but comparable to denudation rates effective over timescales, $>10^{6}$ years, inferred from apatite fission track thermochronology and (U-Th)/He dating. By integrating my results with those of other studies, I am able to infer an overall lowering rate of tens of meters per million years for the central Appalachian Mountains.

Data presented here have significant implications for understanding erosion rates on multiple geographic and temporal scales: Mine is the first global analysis of bedrock outcrop and drainage basin erosion rates inferred from ^{10}Be. With the data I have collected, the long-term ($>10^{6}$ years) landscape evolution for the central Appalachian Mountains is better constrained by the integration of long-lived denudation rates and more recent erosion rates.

I dedicate this thesis to my family, who have always been there to support me.

I also dedicate this thesis in loving memory of my mother, Ann Rogalla Portenga, who taught me how to learn, laugh, live, and love.

The world misses your music.
And as always: Go Blue!!

Acknowledgements

Paul Bierman and I chatted on the phone three years ago and at the time I don't think I had a clue what I was getting myself into! I have been given the opportunities to gain lecturing experience in front of his classes, travel to numerous destinations for field work and to attend conferences, work in both a state-of-the-art laboratory facility at UVM and at the Lawrence Livermore National Laboratory, better understand the processes that shape our planet, and collaborate on projects for which I never thought I had the aptitude. For his guidance, genuine advice, and counsel, I am thankful.

Special thanks go out to my committee members: Donna Rizzo, for teaching me something new about statistics every time we meet and Laura Webb, for helping me get the writing of this thesis off the ground two years ago.

Special mentions go out to Luke Reusser and Lee Corbett for all of their help, advice, comments, laboratory instruction, and computer skills. Thanks to Charles Trodick, who spent two weeks in the field with me, collecting samples and camping in, sometimes, less than ideal conditions. I also thank all of the graduate students in our department: I know I talk a lot in the office and I thank you for your patience in putting up with my abhorrence for silence while you were trying to get work done.

TABLE OF CONTENTS

LIST OF TABLES

Chapter 3: Paper for submission to GSA Bulletin

Motivation for Studying Bedrock Outcrop Erosion Rates

Many regions around the world are typified by the presence of bedrock outcrops. Yet, as common as exposed bedrock may be, the rates at which it erodes are poorly constrained (Saunders and Young, 1983). It is important to understand how bedrock outcrops erode as they are the backbones of mountain ranges, they are one source from which sediment is generated, and they set the tempo of landscape evolution.

Prior to the past twenty years, erosion rate estimates were made in various ways, each of which incorporates many assumptions. Rates of drainage basin denudation have been inferred from measuring sediment yields of rivers (Dole and Stabler, 1909; Judson, 1968). Studies such as these, however, assume that short-term measurements are indicative of long-term denudation and that sediment transport dynamics within a drainage basin are not affected by human impact within the same drainage basin; both of these assumptions have been refuted (Kircher et al., 2001; Trimble, 1977). One of the earliest methods of understanding bedrock outcrop erosion rates involved measuring the depth of text incision and sharpness of edges on exposed tombstones in New England cemeteries (Matthias, 1967). Rahn (1971) did not measure erosion rates from tombstones; rather, he used the relative erodability of various lithologies of tombstones and suggested that bare rock on the landscape followed the same trend.

There are many techniques for measuring the rate at which landscapes erode, each being appropriate for certain timescales. Methods such as apatite fission track thermochronology (AFTT) and (U-Th)/He dating have been used to estimate denudation

rates of mountain ranges on the $>10^6$ year timescale (Ehlers and Farley, 2002; Reiners and Brandon, 2006). Over the past twenty years, advancements in accelerator mass spectrometry (AMS) allowed cosmogenic radionuclides such as ^{10}Be, ^{26}Al, and ^{36}Cl to be used for bedrock and basin-wide erosion studies on 10^3-10^6 year timescales (e.g. Elmore and Phillips, 1987; Bierman and Nichols, 2004; Gosse and Phillips, 2001). Cosmogenically derived erosion rates allows for observations of landscape evolution to be made on a more recent timescale than can AFTT or (U-Th)/He methods.

Many cosmogenic radionuclide erosion rate studies focus on basin-wide erosion rates and include few, if any, bedrock samples. Globally, bedrock outcrop erosion rates are less than basin-wide erosion rates inferred from the cosmogenic signature of fluvial sediments. Very few studies focus solely on bedrock outcrop erosion rates (e.g. Nishiizumi et al., 1991; Cockburn et al., 2000; Bierman and Caffee 2001; Bierman and Caffee 2002; Lal et al., 2003); most bedrock outcrop samples come from studies focused on drainage basin erosion rates and bedrock outcrop data are used for a loose comparison (e.g. Matmon et al., 2003; Reuter, 2005; Sullivan, 2007; Clapp et al., 2000; Clapp et al., 2001; Clapp et al., 2002). Though sample populations for bedrock outcrops and drainage basins are not equal, comparisons between the two have been used in an attempt to understand how overall landscapes erode, but these results may be biased in favor of the larger drainage basin sample population.

In the central and southern Appalachian Mountains, three studies with very small numbers of exposed bedrock samples (Reuter, 2005; Sullivan, 2007; Duxbury, 2009) suggest that outcrops erode more slowly than the basins in which they are located. One

Appalachian study (Matmon et al., 2003) suggests that exposed bedrock and basin-scale erosion rates are similar. Understanding the difference between bedrock outcrop and drainage basin erosion rates is important because outcrops account for such a small percentage of a basin's area, that erosion rates determined for a drainage basin are not representative of bedrock outcrops; thus, outcrops must be studied separately. The purpose of these studies is to understand the relationship between bedrock outcrop and drainage basin erosion rates globally and to increase the number of bedrock outcrop erosion rates in the Potomac and Susquehanna River basins so that a more robust relationship between the two sample types can be observed and understood in the central Appalachian Mountains.

Production of Cosmogenic Nuclides

Cosmogenic [10]Be is produced through multiple pathways (Bierman, 1994; Lal, 1991). For bedrock outcrop erosion studies, [10]Be, produced through spallation by cosmic rays, is the most useful (Nishiizumi et al., 1986). High-energy neutrons interact with particles in the atmosphere creating secondary neutrons which then strike Earth; their interactions with [16]O atoms produce [10]Be. These spallation interactions are more common at Earth's surface and decrease exponentially with depth according to the equation by Lal (1991):

$$P_x = P_0 e^{(-\frac{x\rho}{\Lambda})}.$$

The production rate (P_x) at a depth (x) is determined by the production rate at the surface (P_0), the density of the material (ρ), and the absorption mean free path (Λ).

Surface production rates are low, ~5 atoms g^{-1} yr^{-1}, and describe how quickly cosmogenic

nuclides are created, but do not take into account the nuclide's half-life (1.36 My for

^{10}Be; Nishiizumi et al., 2007). With this factor taken into account, the equation below is

used to estimate bedrock erosion rates from measured isotope concentrations (Lal, 1991):

$$N = \frac{P_0}{(\frac{\rho\varepsilon}{\Lambda}+\lambda)} e^{\frac{x\rho}{\Lambda}},$$

where N is the nuclide concentration, λ is the decay constant, and ε is the erosion rate.

Latitude and altitude control the cosmic ray flux and thus the production rate of

cosmogenic nuclides. Correction factors for latitude and elevation have been determined

by Lal and Peters (1967) and must be applied to raw ^{10}Be concentrations before model

erosion rates can be determined. The most widely used scaling schemes are more recent

(e.g. Lal, 1991; Stone, 2000; Dunai, 2001).

The advancement of technologies such as AMS allows erosion rates to be

measured directly through the analysis of cosmogenic nuclides – ^{10}Be being the most

common for bedrock studies (Elmore and Phillips, 1987; Nishiizumi et al., 1986). AMS

is the most appropriate method of measurement for cosmogenic radionuclide

concentrations because it has a low detection limit for these nuclides (Granger and Riebe,

2007; Lal, 1988; Lal and Peters, 1967). Any mineral containing ^{10}Be can be used for

erosion studies as long as absorbed atmospheric ^{10}Be can be removed (Nishiizumi et al.,

1990; Ivy-Ochs et al., 2007). Quartz quickly emerged as the optimal mineral phase to use

in bedrock studies because of its prevalence, resistance to atmospheric ^{10}Be adsorption,

simple chemical formula, low Al content, and measurable quantities of cosmogenic ^{10}Be

(Bierman, 1994).

Applications of Cosmogenic Radionuclides with Bedrock Outcrop Erosion Rates

The use of cosmogenic ^{10}Be in determining erosion rates has grown considerably since the late 1980s (e.g. Nishiizumi et al., 1991; Brown et al, 1995; Small et al., 1997; Clapp et al., 2000; Nichols et al., 2006). Many studies have involved either obtaining basin-wide erosion rates using stream sediments or determining how bedrock weathers under a mantle of sediment or soil (e.g. Brown et al., 1995; Clapp et al., 2001; Granger et al., 2001; Heimsath et al., 2006); many fewer studies present the erosion rates of exposed bedrock (e.g. Nishiizumi et al., 1991; Cockburn et al., 2000; Hancock and Kirwin, 2007).

This shortage of cosmogenic data from bedrock outcrops limits our understanding of how landforms change through time in different geographic settings and prevents rigorous comparison to results from other methods such as AFTT and (U-Th)/He dating, although such comparisons have been made (von Blanckenburg et al., 2004; Cockburn et al., 2000; Granger et al., 2001). Studies in which bedrock outcrop erosion is not the primary focus have compared basin-wide erosion rates to various environmental parameters such as mean annual precipitation (e.g. Matmon et al., 2003; von Blanckenburg et al., 2004; Henck, 2010), elevation (e.g. Heimsath et al., 2006), and basin slope (e.g. Matmon et al., 2003; von Blanckenburg et al., 2003; Palumbo et al., 2009) with varied success. With a few exceptions, correlations have not been explored in studies focusing solely on exposed bedrock (Bierman and Caffee, 2001, 2002). All existing studies were made on local or regional scales; bedrock outcrop erosion rates have not yet been compiled into a single global database.

Many studies in which exposed bedrock erosion rates were compared to basin-wide erosion rates show bedrock eroding more slowly than the basin as a whole (e.g. Brown et al., 1995; von Blanckenburg et al., 2004; Reinhardt et al., 2007; Kober et al., 2009). In contrast, in the Great Smoky Mountains, Matmon (2003) found a landscape where the average erosion rates of outcrops were indistinguishable from the basin-wide average erosion rates.

Outcrop erosion rates have also been used in studies comparing exposed bedrock erosion to that of covered bedrock, whether it be by boulders (Granger et al., 2001), soil (Heimsath et al., 1997), or sand (Clapp et al., 2001). Bare rock in the American Sierra Nevada erodes slower than bedrock covered by boulders and colluvium (Granger et al., 2001). In northern California, Heimsath et al. (1997) found the highest bedrock erosion rates under a thin mantle of soil whereas exposed bedrock eroded more slowly. Similar results were found in basins along the southeastern Australian escarpment (Heimsath et al., 2006, 2000). In Arizona and New Mexico, slopes covered by sand and colluvium were also found to have higher erosion rates than those of exposed bedrock in the same basin (Clapp et al., 2001, 2002). The higher erosion rates of shielded bedrock has been attributed to the ability of colluvium, soil, and sand to retain moisture, which facilitates chemical and biological weathering whereas most water runs off exposed bedrock (Granger et al., 2001; Clapp et al., 2001, 2002).

Many studies focusing only on bedrock outcrop erosion rates have been done on passive margins in arid environments (e.g. Bierman and Caffee, 2001; Bierman and Caffee, 2002; Cockburn et al., 2000; Hancock and Kirwan, 2007). Samples taken from

inselbergs on Australia's Eyre Peninsula exhibit slow erosion rates (~4 m My[-1] on average, but as low as ~40 cm My[-1]) suggesting that these landforms have changed little throughout the Cenozoic (Bierman and Caffee, 2002). Along the Namibian Escarpment, erosion rates of ~6.5 m My[-1] (Cockburn et al., 2000) and ~3 m My[-1] (Bierman and Caffee, 2001) were measured on samples from inselbergs and outcrops along the escarpment. Other arid environments not on passive margins also show erosion rates as low as ~10 m My[-1] (Nichols et al., 2006; Clapp et al., 2000). Antarctic outcrops produce some of the lowest erosion rates with an average of ~1.2 m My[-1] and a low of 12 cm My[-1] (Nishiizumi et al., 1986, 1991).

Bedrock summits in many western United States mountain ranges are eroding at rates only slightly higher than rock in arid environments: ~8.7 m My[-1] in the Wind River Range, WY; ~13.2 m My[-1] in the Beartooth Mountains, MT; and ~9.2 m My[-1] in the Front Range, CO (Small et al., 1997). Summit erosion rates in the passive margin Appalachian Mountains are within the range of their western counterparts (~6.5 m My[-1]) even though they are in a much older and less tectonically active environment (Hancock and Kirwin, 2007).

Exposed bedrock erosion rate data from the Appalachian Mountains are limited to a few exposures primarily within basin-wide studies (Table DR1 in Appendix B). Exposed bedrock erosion rates range from ~2.5 – 50 m My[-1], with an average of 27 m My[-1] (n=29; Hancock and Kirwin, 2007; Duxbury, 2009; Reuter, 2005; Matmon et al., 2003; Sullivan, 2007).

This thesis first provides a global context to which results from further bedrock outcrop and drainage basin studies can be compared. Second, I explore erosion rates from bedrock outcrops in the central Appalachian Mountains. I consider their geospatial relationships to each other and ^{10}Be-inferred drainage basin erosion rates from the same region, long-term methods of landscape denudation. I then compare them to global erosion rates of bedrock outcrops from similar settings.

Understanding Earth's Eroding Surface with ^{10}Be

Eric W. Portenga*
Department of Geology
University of Vermont
Burlington, VT 05405

Paul R. Bierman
Department of Geology and Rubenstein School of the Environment and Natural
Resources
University of Vermont
Burlington, VT 05405

Luke Reusser
Department of Geology and Rubenstein School of the Environment and Natural
Resources
University of Vermont
Burlington, VT 05405

*Corresponding Author: contact at eporteng@uvm.edu

Abstract

For more than a century, Geologists have sought to measure the distribution of erosion rates on Earth's dynamic surface. Since the mid-1980s, measurements of ^{10}Be, an *in situ* produced cosmogenic radionuclide, have been used to estimate outcrop and drainage basin-scale erosion rates at >80 sites around the world. Here, we compile and standardize published ^{10}Be erosion rate data (n= 1528) in order to understand how, on a global scale, pre-human or background erosion rates vary between climate zones, tectonic settings, and different rock types.

The conversion of bedrock to sediment in drainage basins occurs more quickly (mean = 209 m My^{-1}; median = 53 m My^{-1}; $n = 1110$) than on sub-aerially exposed outcrops alone (mean = 12 My^{-1}; median = 5.2 m My^{-1}; $n = 418$) likely reflecting the acceleration of rock weathering rates under soil. Drainage basin and outcrop erosion rates both vary by climate zone, rock type, and tectonic setting. On the global scale, environmental parameters explain erosion rate variation better when they are combined in multiple regression analyses. Drainage basin erosion rates are explained well by considering nine environmental parameters ($R^2 = 0.56$); slope is the most powerful regressor. Outcrop erosion rates are less well explained ($R^2 = 0.33$), and no one parameter dominates. Erosion rates are best explained when small geographic areas are considered or when analysis is done using subpopulations of climate zone, lithology, or tectonic regime.

10

Introduction

   Measuring the rate and spatial distribution of erosion on millennial timescales is
fundamental to understanding how landscapes evolve through time and for placing
human environmental impacts in context (Hooke, 1994, 2000). Yet, Geoscientists are
largely lacking the data to develop a global model that can predict, with accuracy or
precision, the background rate and spatial distribution of erosion on Earth's dynamic
surface. We are even less able to predict how erosion rates respond to changes in
boundary conditions including tectonic and climatic forcing. Understanding how rates of
erosion are related to complex, non-linear feedbacks between multiple Earth systems
including the solid Earth, climate, and biosphere is prerequisite to developing such a
model.

   Throughout the 20th century, geologists used a variety of tools to measure rates of
erosion (e.g., Saunders and Young, 1983). The most common approach equated sediment
yield with erosion rate (Dole and Stabler, 1909; Judson, 1968). Such an approach
presumes that human impact is inconsequential and that short-term measurements of
sediment flux are representative of long-term flux rates – both assumptions have been
repeatedly questioned (e.g. Wilkinson, 2005; Kirchner et al., 2001; Trimble, 1977) and
various modeling approaches implemented (Syvitski et al., 2005) to overcome limitations
of sediment yield data.

   Until recently, no one method of measuring pre-human or background erosion
rates directly was globally applicable. The development of Accelerator Mass
Spectrometry (AMS) and the measurement of cosmogenic radionuclides (Elmore and

Phillips, 1987), the concentration of which reflects near-surface residence time and thus the pace of surface processes (Bierman and Nichols, 2004), has changed everything. Now, there is a widely applicable method for measuring erosion rates over millennial timescales. Since 1986, *in situ* produced cosmogenic radionuclides, most commonly ^{10}Be produced in quartz, have been used to model the rate at which exposed bedrock outcrops and drainage basins (defined as the contributing area of a watershed upstream from where fluvial sediment is collected) erode over geomorphically meaningful timescales (e.g. Bierman and Caffee, 2002; Bierman and Caffee, 2001; Bierman and Steig, 1996; Granger et al., 1996; Nishiizumi et al., 1986; Schaller et al., 2001; Small et al., 1997). Such modeling is based on the known behavior of cosmic rays that produce ^{10}Be, an otherwise exceptionally rare isotope, within the uppermost several meters of Earth's surface (Lal, 1991).

Many local and regional-scale cosmogenic nuclide studies, now numbering >80, indicate that individual environmental parameters can influence millennial-scale erosion rates although the results are not uniform. In order to understand the relationship between erosion rates and metrics quantifying environmental parameters (e.g. climate, topography, biogeography, and tectonic setting), we compiled all publically available outcrop and drainage basin erosion rates inferred from measurements of ^{10}Be (Figure 1). After correcting the data for changes in calculation parameters used over the last 24 years, we compared erosion rates and a variety of environmental parameters, both individually and using multivariate statistical methods. The result is a description, at a global scale, of the relationship between these parameters and the erosion rate of both

outcrops and drainage basins. Such relationships are important for understanding the

behavior of Earth's sedimentary system over a variety of spatial and temporal scales as

geologists seek to understand human impacts on erosion and sediment generation

(Hooke, 1994).

Methods

We compiled all publicly available *in situ* ^{10}Be erosion rate data (Fig. 1; Tables

DR-1, 2, & 3 in Appendix B). For bedrock outcrops, we included only unshielded

samples collected from horizontal or sub-horizontal surfaces and in areas that had not

experienced extensive recent glacial cover. For each sample, we collected data necessary

to recalculate erosion rates (Table DR-1 in Appendix B). In some cases, information was

provided in the original publications; in other cases, we contacted authors directly.

Samples in this compilation required recalculation because constraints on production

rates, neutron attenuation path length, and the ^{10}Be half-life have improved over time and

values used in individual studies vary.

We used the CRONUS on-line calculator for erosion rate estimates (Balco et al.,

2008; http://hess.ess.washington.edu/). Effective elevation, or the production-rate

weighted average elevation for a basin, and effective latitude were determined (see

methods, Appendix A), enabling us to use the CRONUS calculator for determining

drainage basin erosion rates. CRONUS-calculated erosion rates for outcrops and basins

strongly and significantly correlate to their original published erosion rates (Figure DR-1

in Appendix A).

We compared erosion rates for outcrops and drainage basins to various environmental and physical parameters (Table DR4 in Appendix B). We extracted data from global datasets using ArcGIS. Not all global coverages extend to Antarctica. Antarctic climate data were modified from Monaghan et al. (2006); seismicity data could not be gathered for Antarctica and so those sites are excluded from some of our analyses. Outcrop lithologies are described using varying amounts of detail in individual studies; for our purposes, it is only possible to consider lithologies in general terms, delineating three main rock types: igneous, metamorphic, and sedimentary. Bivariate analyses were carried out for numeric parameters; Analyses of Variance and Student's t-Tests were carried out for nominal data. We performed forward stepwise regressions for each global dataset and for each subgroup of nominal data categories using JMP software (version 8.0). Parameters were entered into the test based on their ability to statistically improve the regression; if a variable did not significantly improve the regression, it was omitted from the test. These parametric statistical tests assume a normal sample distribution. Because both and basin-scale erosion rate distributions are highly skewed (Figure 2), we log-transformed all erosion rate data before performing statistical tests; this transformation normalized the distributions well.

Results

Outcrop Erosion Rates

Outcrops ($n = 418$) erode at an average rate of 12 ± 1.3 m My^{-1}. The median erosion rate is 5.2 m My^{-1}, reflecting the highly skewed distribution (Fig. 2B). In

bivariate global comparisons (Figure DR-2 in Appendix A), outcrop erosion rates are unrelated to absolute latitude, elevation, or seismicity. Globally, outcrop erosion rates co-vary weakly with relief and mean annual precipitation (MAP); the highest outcrop erosion rates occur where mean annual temperature (MAT) is ~10°C.

Analysis of Variance shows that outcrops in seismically active regimes erode similarly (14 ± 1.6 m My^{-1}, $n = 55$) to those in seismically inactive areas (12 ± 1.3 m My^{-1}, $n = 363$) but that outcrop erosion rates differ by lithology and climate (Figure 3). Erosion rates of sedimentary (19 ± 1.9 m My^{-1}; $n = 106$), and metamorphic outcrops (13 ± 1.7 m My^{-1}; $n = 82$) are statistically similar and faster than the erosion rate of igneous outcrops (8.6 ± 0.9 m My^{-1}; $n = 230$). The average outcrop erosion rate in temperate climates (26 ± 2.6 m My^{-1}; $n = 75$) is significantly higher than those in any other climate zone. Outcrops in polar climates erode most slowly (3.9 ± 0.39 m My^{-1}, $n = 31$). Median values show similar trends (Figure 4).

A forward stepwise regression shows that 33% of the variation in the global population of outcrop erosion rates can be described by five parameters of which latitude is most important regressor (Fig. 4). For individual climate zones, lithologies, and seismic regimes, the relevant parameters and their weighting vary greatly (Fig. 4, Table DR-5 in Appendix B).

Drainage Basin Erosion Rates

On average, sampled drainage basins erode at 209 ± 33 m My^{-1} ($n = 1110$). The distribution is highly skewed with a median erosion rate of 53 m My^{-1} (Fig. 2C). At the

global scale, basin slope yields the strongest bivariate correlation with erosion rates ($R^2 =$ 0.33, Figure 5; Figure DR-3 in Appendix A). Basin relief, mean elevation, and seismicity also have significantly positive, bivariate correlations. MAT has a very weak negative correlation. There is no significant bivariate correlation between basin erosion rates and latitude, MAP, or basin area (Fig. DR-3 in Appendix A). The latter is important as it indicates that changes in sediment delivery ratio do not appear to affect estimation of erosion rates cosmogenically, in contrast to estimates made on the basis of sediment yield (Walling, 1983).

Analysis of Variance (Fig. 3) indicates that the average erosion rate for seismically active basins (364 ± 54 m My^{-1}, $n = 219$) is significantly higher than in seismically inactive basins (171 ± 27 m My^{-1}, $n = 891$). The average drainage basin erosion rate in polar climates (550 ± 130 m My^{-1}; $n = 69$) is higher than in all other climate zones. Arid region drainage basins erode most slowly (103 ± 17.6 m My^{-1}; $n = 224$). Results are less clear for lithology. On average, metamorphic terrains erode more rapidly than other lithologies but ANOVA results on log-transformed data do not show separability (Fig. 3).

Forward stepwise regressions of basin erosion rates show that eight parameters describe 56% of variability in the global data set (Fig. 4). For nearly every basin-scale subcategory, basin slope is the most significant regressor. The remaining parameters are highly variable in terms of their regression power. Basin area, MAT, and elevation have low weights for all subcategories in which they appear.

Discussion

Compilation of 1528 measurements of *in situ* produced [10]Be provides the first

broad view of pre-human erosion rates (Figs. 1, 2). Erosion rates determined

cosmogenically are within the range determined previously using other techniques such

as (U-Th)/He dating and fission-track thermochronology (e.g. von Blanckenburg et al.,

2004; Cockburn et al., 2000). Compiled outcrop erosion rates are slow and, with the

exception of rare cases (i.e. Chappell et al., 2006), do not exceed 140 m My[-1], similar to

rock weathering rates measured in the past (Saunders and Young, 1983). Compiled basin-

scale erosion rates are also mostly within previously published ranges as quantified by

measuring chemical, bed, and suspended loads of rivers. Some cosmogenic studies in

tectonically active zones have indicated erosion rates higher than previously reported (i.e.

Binnie et al., 2006; Binnie et al., 2008; DiBiase et al., 2009).

Spatial Distribution of Existing Samples

Our compilation is global; however, large portions of Earth remain unsampled

meaning that the data are non-uniformly distributed (Fig. 1); drainage basin cosmogenic

data represent only 2.3% of the world's land area. Latitudes with large sample

populations, between 30 – 50° north and south, correspond to Europe, the United States,

and Australia — easily accessible locations. There are sampling gaps between 50 – 70°

latitude, both north and south. Low latitude samples are also rare. Exceptions include

large sample populations from basins and outcrops in Namibia and the Bolivian Andes

(i.e. Bierman and Caffee, 2001; Cockburn et al., 2000; Insel et al., 2010; Kober et al.,

2007; Kober et al., 2009; Safran et al., 2005; Wittmann et al., 2009). Refining the relationships presented in this study will happen only when these large spatial data gaps are filled.

Both outcrop and drainage basin erosion rates have highly skewed distributions (Fig. 2) with most samples indicating relatively slow rates of erosion. This skewed distribution probably reflects the rapidity of erosion in tectonically active zones where mass is supplied to orogens by plate convergence and removed by rapid erosion of threshold slopes (Montgomery and Brandon, 2002; Zeitler et al., 2001). In contrast, slower, isostatically driven rock uplift supplies mass for erosion in the tectonically stable zones that make up most of the world (Hack, 1975, 1979).

Studies with a large number of samples in one region (i.e. Bierman and Caffee, 2002; DiBiase et al., 2009; Henck, 2010; Safran et al., 2005; Schaller et al., 2001) are helpful in creating large sample populations for statistical analyses; however, sample adjacency leads to biases in data interpretation because of the scale dependence of correlation. For example, outcrops in "cold" climates come from numerous locations, geographically ($n = 111$) and the stepwise multivariate regression accounts for only 11% of the variability of erosion rates whereas 52% of variability of outcrop erosion rates in "polar" climates is explained (Fig. 4). This high correlation is most likely the result of all 31 polar outcrop samples coming from a single, small geographic area.

Most [10]Be measurements have been done in quartz-rich rocks and sediment because quartz retains *in situ* [10]Be and has a simple composition so nuclide production rates are easily calculated. Not all rocks are quartz-bearing; thus, the global data set does

18

not represent all lithologies. [10]Be can be extracted from other minerals (Ivy-Ochs et al.,

2007; Nishiizumi et al., 1990) expanding the area where erosion rates could be measured.

Application of other isotope systems (such as [21]Ne, [3]He and [36]Cl) offers the potential to

constrain better the effect of lithology on erosion rates (Kober et al., 2009); however,

uncertainties in cross-calibration of production rates between different isotope systems

could introduce biases into the data analysis.

Basins Erode More Rapidly than Outcrops

Average outcrop erosion rates are more than ten times slower (12 m My^{-1}) than

those inferred from drainage basin studies (209 m My^{-1}). Comparison of median values

(5.2 versus 53 m My^{-1}) shows a similar relationship. Within each seismic regime, climate

zone, and lithology, drainage basins erode more rapidly than outcrops (Fig. 4). Though

bedrock outcrops are found within drainage basins, they typically occupy such a small

percentage of space within the drainage basin that basin-averaged erosion may not

represent erosion rates for those outcrops. There are 19 study sites where both outcrop

and basin erosion rates have been measured (Figure DR-4 in Appendix A). At ten of

these sites, statistical analysis indicates that drainage basins erode more rapidly that

outcrops; at the other nine sites, drainage basin and outcrop erosion rates are statistically

inseparable. In no case does a Student's t-Test indicate that outcrops erode more rapidly

than the adjacent basins. These results ultimately suggest that soil cover, even if it is quite

shallow, speeds the rate of rock weathering. Other factors such as rock structure and

bioturbation also may speed the rate of erosion, but these factors have not been quantified globally.

Influence of Spatial Scale on Erosion Rate Correlation

Scale appears to determine which environmental parameters are related to outcrop and drainage basin erosion rates. Correlations observed on the local scale (tens to hundreds of square kilometers) are often not observed or are much weaker on the global scale. For example, locally, in Australia, the lowest measured outcrop erosion rate from sampling sites on Australia's Eyre Peninsula and in central Australia correlate well with MAP ($R^2 = 0.98$; Bierman and Caffee, 2002). On the global scale, however, there is little correlation; MAP does not factor into the multivariate analysis for outcrop erosion in arid regions (Fig. 4). On a basin scale, erosion rates have been shown to correlate well with average basin elevation in individual studies (Heimsath et al., 2006; Palumbo et al., 2009). This bivariate relationship is weak at the global scale ($R^2 = 0.14$, Fig. DR-3 in Appendix A) and elevation is at most a lightly weighted regressor in all of the multivariate regressions (Fig. 4). We suspect the scale-dependence of bivariate correlations is caused by the spatial autocorrelation of a variety of difficult-to-quantify factors such as bedrock structure and strength. Collecting such data along with samples for cosmogenic analysis would likely improve our understanding of controls on bedrock erosion rates.

Mean basin slope is the one parameter significantly related to drainage basin erosion rates at both the local (e.g. Matmon et al., 2003; Palumbo et al., 2009; von

Blanckenburg et al., 2004) and global level; however, scale remains important. For example, mean basin slope produced the strongest bivariate correlation (Fig. 5) with drainage basin erosion rates at the global scale (total basin area = 3.3 x 10^6 km^2, R^2 = 0.33). The regression explains more variability if only the Appalachian Mountain crest data are included (6.9 x 10^4 km^2, R^2 = 0.49) and gets even better if the data included are restricted to the Appalachian Plateau (786 km^2, R^2 = 0.75). Although bivariate analysis may be useful at local and regional scales, such regressions are of lesser use at global scales. Multivariate analysis is needed because many environmental metrics, such as slope, relief, and MAP, spatially co-vary.

Correlation of Physical and Environmental Parameters to Erosion Rates

Compiling and analyzing the global [10]Be dataset shows that the most successful understanding of erosion rate, in the absence of site-specific studies, will come from multivariate analyses of drainage basin data (Fig. 4, Table DR-5 in Appendix B). In general, analysis of data by climatic, tectonic, or lithologic sub-populations, provides better correlation (higher R^2 value) because of the autocorrelation of erosion rates. Multivariate analysis explains almost twice as much variance in drainage basin erosion rates as in outcrop erosion rates suggesting that there are other, unconsidered parameters controlling outcrop erosion rates (such as rock strength and joint spacing).

Topographic metrics (relief and slope) are clearly related to drainage basin erosion rates. On the global scale, relief and slope both produced significant bivariate correlations with drainage basin erosion rates. In the multivariate analyses, slope was the

predominant regressor in nearly every subdivision of categorical data (Fig. 4), and was the predominant regressor for the global basin-scale multivariate regression. Relief is unimportant for most categories of outcrops, except for sedimentary rocks. Elevation is not important for outcrops or for basins.

Seismicity, a proxy for tectonics, is positively related to drainage basin erosion rates in bivariate regression, multivariate regressions, and in the comparison of tectonically active and inactive basins (Fig. 4; Fig. DR-4 in Appendix A). This relationship likely reflects the weakening of rocks through seismic shaking, fracture density, and perhaps base-level lowering (Riebe et al., 2001b). Multivariate regressions for both outcrops and basins in tectonically active areas show high R^2 values.

Although individual climate metrics are weakly related to erosion rates (Fig. 4), consistent with the findings of Reibe et al., (2001a), erosion rates of both outcrops and basins vary significantly by climate zone (Fig. 3). MAP is frequently cited as a parameter controlling erosion rates and a relationship is often observed in local and regional studies of both outcrop and drainage basin erosion (e.g. Bierman and Caffee, 2002; Bierman and Caffee, 2001; Henck, 2010; von Blanckenburg et al., 2004). Although MAP may produce a strong correlation at the local scale, only weak correlations are observed globally and multivariate analyses suggest MAP does not play an important role in explaining erosion rates for either outcrops or basins. MAT is a significant regressor for many basin sub-categories but its weighting is usually low (Fig. 4). MAT carries high weighting for some sub-categories of outcrops. Latitude, a climate proxy, is significant in most basin sub-categories. Vegetation is generally unimportant.

22

Implications for Landscape Evolution

The ten-fold offset between rates of outcrop erosion and those of drainage basins suggests that ridgelines, where outcrops are common, erode less rapidly than the surrounding basins. The offset between outcrop and drainage basin rates of erosion implies that relief is increasing in many study areas as ridges (where outcrops are more common) are lowered less rapidly than basins. This offset cannot continue forever. Ridgelines will eventually be consumed from their margins.

Outcrop and drainage basin erosion rates are controlled by different processes and occur in different physical, chemical, and hydrological environments. Outcrops are situated above the landscape and exposed to a limited suite of what must be largely ineffective sub-aerial erosion processes that both physically and chemically wear away exposed rock. The stability of outcrops is likely due to the dry microclimate they create as precipitation rapidly runs off exposed rock surfaces. The conversion of bedrock to regolith results from linked chemical and physical processes that include hydrolysis, weathering induced by organic acids, and the ability of soil to hold water in contact with rock between precipitation events. A thin mantle of soil appears to create conditions most favorable for the conversion of bedrock to soil — the "humped" soil production function (Heimsath et al., 1997, 1999).

Cosmogenic data show that millennial-scale erosion rates differ between climate zones. Thus, substituting time for space, glacial-interglacial climate cycles probably changed erosion rates and thus the flux of sediment shed off the landscape. Erosion rates are generally high for both outcrops and basins in temperate and cold climate zones,

peaking where the MAT is ~ 10°C (Figs. DR-2, 3 in Appendix A). Temperatures in these

climate zones fluctuate throughout the year with numerous freeze-thaw cycles that may

facilitate frost cracking on outcrops and cryoturbation on basin hillslopes (Delunel et al.,

2010; Hales and Roering, 2007). This hypothesis is testable. Paleo-erosion rates should

be higher than modern rates in areas where warmer climates cooled significantly during

the Pleistocene.

Future Prospects

Accurate global mapping, understanding, and prediction of background erosion

rates is critical because erosion is the means by which sediment is generated, fresh rock is

exposed to CO_2-consuming weathering reactions, soil is created, landforms change over

time, and mass is moved from the continents to the oceans and eventually recycled *via*

the process of subduction and volcanism. Earth's ability to support billions of inhabitants

depends critically on the resiliency of the soil system and the purity of surface waters,

both of which erosion affects directly.

Compiling more than 20 years of cosmogenic analyses clearly shows their value

in measuring background rates of erosion around the world, understanding how such

rates are related to environmental parameters, and laying the groundwork for predicting

long-term sediment generation rates at a variety of spatial scales; yet, the same

compilation demonstrates spatial biases in the existing data set, providing both

justification and guidance for filling these data gaps. Multivariate regressions, using

widely available environmental data, explain much of the variance in drainage basin

erosion rates. Outcrop erosion rates are less well explained suggesting that important

controlling parameters, related to rock strength, need to be measured and considered in

any predictive model.

Acknowledgements

References Cited

Balco, G., Stone, J. O., Lifton, N. A., and Dunai, T. J., 2008, A complete and easily
        accessible means of calculating surface exposure ages or erosion rates from [10]Be
        and [26]Al measurements: Quaternary Geochronology, v. 3, p. 174-195.

Bierman, P., and Nichols, K., 2004, Rock to sediment - Slope to sea with 10-Be - Rates
        of landscape change: Annual review of Earth and Planetary Sciences, v. 32, p.
        215-255.

Bierman, P. R., and Caffee, M., 2002, Cosmogenic exposure and erosion history of
        ancient Australian bedrock landforms: Geological Society of America Bulletin, v.
        114, no. 7, p. 787-803.

Bierman, P. R., and Caffee, M. W., 2001, Slow rates of rock surface erosion and
        sediment production across the Namib Desert and escarpment, Southern Africa:
        American Journal of Science, v. 301, no. 4-5, p. 326-358.

Bierman, P. R., and Steig, E., 1996, Estimating rates of denudation and sediment
        transport using cosmogenic isotope abundances in sediment: Earth Surface
        Processes and Landforms, v. 21, p. 125-139.

Binnie, S. A., Phillips, W. M., Summerfield, M. A., and Fifield, L. K., 2006, Sediment
        mixing and basin-wide cosmogenic nuclide analysis in rapidly eroding
        mountainous environments: Quaternary Geochronology v. 1, p. 4-14.

Binnie, S. A., Phillips, W. M., Summerfield, M. A., Fifield, L. K., and Spotila, J. A.,
        2008, Patterns of denudation through time in the San Bernardino Mountains,

California: Implications for early-stage orogenesis Earth and Planetary Science Letters, v. In Press.

Chappell, J., Zheng, H., and Fifield, K., 2006, Yangtse River sediments and erosion rates from source to sink traced with cosmogenic [10]Be: Sediments from major rivers: Palaeogeography, Palaeoclimatology, Palaeoecology, v. 241, no. 1, p. 79-94.

Cockburn, H. A. P., Brown, R. W., Summerfield, M. A., and Seidl, M. A., 2000, Quantifying passive margin denudation and landscape development using a combined fission-track thermochronology and cosmogenic isotope analysis approach: Earth and Planetary Science Letters, v. 179, no. 3-4, p. 429-435.

Delunel, R., Beek, P. A. v. d., Carcaillet, J., Bourlès, D. L., and Valla, P. G., 2010, Frost-cracking control on catchment denudation rates: Insights from in situ produced [10]Be concentrations in stream sediments (Ecrins–Pelvoux massif, French Western Alps): Earth and Planetary Science Letters, v. 293, p. 72-83.

DiBiase, R. A., Whipple, K. X., Heimsath, A. M., and Ouimet, W. B., 2009, Landscape form and millennial erosion rates in the San Gabriel Mountains, CA: Earth and Planetary Science Letters, v. 289, p. 134-144.

Dole, R. B., and Stabler, H., 1909, Denudation: USGS Water Supply Paper, v. 234, p. 78-93.

Elmore, D., and Phillips, F., 1987, Accelerator mass spectrometry for measurement of long-lived radioisotopes: Science, v. 236, p. 543-550.

Granger, D. E., Kirchner, J. W., and Finkel, R., 1996, Spatially averaged long-term erosion rates measured from in situ-produced cosmogenic nuclides in alluvial sediments: Journal of Geology, v. 104, no. 3, p. 249-257.

Hack, J. T., 1975, Dynamic equilibrium and landscape evoluion, *in* Melhorn, W. N., and Flemal, R. C., eds., Theories of landform development: Binghamton, N.Y., SUNY Binghamton,, p. 87-102.

-, 1979, Rock control and tectonism, their importance in shaping the Appalachian highlands: U.S. Geological Survey professional paper, v. 1126-B, p. 17.

Hales, T. C., and Roering, J. J., 2007, Climatic controls on frost cracking and implications for the evolution of bedrock landscapes: Journal of Geophysical Research, v. 112.

Heimsath, A., Chappel, J., Finkel, R. C., Fifield, K., and Alimanovic, A., 2006, Escarpment Erosion and Landscape Evolution in Southeastern Australia: Special Papers-Geological Society of America, v. 398, p. 173.

Heimsath, A. M., Dietrich, W. E., Nishiizumi, K., and Finkel, R. C., 1997, The soil production function and landscape equilibrium: Nature (London), v. 388, no. 6640, p. 358-361.

-, 1999, Cosmogenic nuclides, topography, and the spatial variation of soil depth: Geomorphology, v. 27, no. 1-2, p. 151-172.

Henck, A. C., 2010, Spatial and temporal patterns of erosion in Western China and Tibet: University of Washington, 158 p.

Hooke, R. L., 1994, On the efficacy of humans as geomorphic agents: GSA Today, v. 4, no. 9, p. 217,224-225.

-, 2000, On the history of humans as geomorphic agents: Geology, v. 28, no. 9, p. 843-846.

Insel, N., Ehlers, T. A., Schaller, M., Barnes, J. B., Tawackoli, S., and Poulsen, C. J., 2010, Spatial and temporal variability in denudation across the Bolivian Andes from multiple geochronometers: 2010, v. 122, p. 65-77.

Ivy-Ochs, S., Kober, F., Alfimov, V., Kubik, P. W., and Synal, H.-A., 2007, Cosmogenic ^{10}Be, ^{21}Ne and ^{36}Cl in sanidine and quartz from Chilean ignimbrites: Nuclear Instruments and Methods in Physics Research B, v. 259, p. 588-594.

Judson, S., 1968, Erosion of the land or what's happening to our continents: American Scientist, v. 56, p. 356-374.

Kirchner, J. W., Finkel, R. C., Riebe, C. S., Granger, D. E., Clayton, J. L., King, J. G., and Megahan, W. F., 2001, Mountain erosion over 10 yr, 10 k.y., and 10 m.y. time scales: Geology, v. 29, no. 7, p. 591-594.

Kober, F., Ivy-Ochs, S., Schlunegger, F., Baur, H., Kubik, P. W., and Wieler, R., 2007, Denudation rates and a topography-driven rainfall threshold in northern Chile: Multiple cosmogenic nuclide data and sediment yield budgets: Geomorphology, v. 83, p. 97-120.

Kober, F., Ivy-Ochs, S., Zeilinger, G., Schlunegger, F., Kubik, P. W., Baur, H., and Wieler, R., 2009, Complex multiple cosmogenic nuclide concentration and histories in the arid Rio Lluta catchment, northern Chile: Earth Surface Processes and Landforms, v. 34, p. 398-412.

Lal, D., 1991, Cosmic ray labeling of erosion surfaces; in situ nuclide production rates and erosion models: Earth and Planetary Science Letters, v. 104, no. 2-4, p. 424-439.

Matmon, A. S., Bierman, P., Larsen, J., Southworth, S., Pavich, M., Finkel, R., and Caffee, M., 2003, Erosion of an ancient mountain range, the Great Smoky Mountains, North Carolina and Tennessee: American Journal of Science, v. 303, p. 817-855.

Monaghan, A. J., Bromwich, D. H., and Wang, S.-H., 2006, Recent trends in Antarctic snow accumulation from Polar MM5 simulations: Philosophical Transactions of the Royal Society London A, v. 364, p. 25.

Montgomery, D. R., and Brandon, M. T., 2002, Topographic controls on erosion rates in tectonically active mountain ranges: Earth and Planetary Science Letters, v. 201, no. 3-4, p. 481-489.

Nishiizumi, K., Klein, J., Middleton, R., and Craig, H., 1990, Cosmogenic [10]Be, [26]Al, and [3]He in olivine from Maui lavas: Earth and Planetary Science Letters, v. 98, no. 3-4, p. 263-265.

Nishiizumi, K., Lal, D., Klein, J., Middleton, R., and Arnold, J. R., 1986, Production of [10]Be and [26]Al by cosmic rays in terrestrial quartz in situ and implications for erosion rates: Nature, v. 319, no. 6049, p. 134-136.

Palumbo, L., Hetzel, R., Tao, M., and Li, X., 2009, Topographic and lithologic control on catchment-wide denudation rates derived from cosmogenic [10]Be in two mountain ranges at the margin of NE Tibet: Geomorphology, v. 117, p. 130-142.

Reuter, J. M., 2005, Erosion rates and patterns inferred from cosmogenic [10]Be in the Susquehanna River basin: University of Vermont, 172 p.

Riebe, C. S., Kirchner, J. W., Granger, D. E., and Finkel, R. C., 2001a, Minimal climatic control on erosion rates in the Sierra Nevada, California: Geology, v. 29, no. 5, p. 447-450.

-, 2001b, Strong tectonic and weak climatic control of long-term chemical weathering rates: Geology, v. 29, no. 6, p. 511–514.

Safran, E. B., Bierman, P. R., Aalto, R., Dunne, T., Whipple, K. X., and Caffee, M., 2005, Erosion rates driven by channel network incision in the Bolivian Andes: Earth Surface Processes and Landforms, v. 30, no. 8, p. 1007-1024.

Saunders, I., and Young, A., 1983, Rates of surface processes on slopes, slope retreat, and denudation: Earth Surface Processes and Landforms, v. 8, p. 473-501.

Schaller, M., von Blanckenburg, F., Hovius, N., and Kubik, P. W., 2001, Large-scale erosion rates from In situ-produced cosmogenic nuclides in European river sediments: Earth and Planetary Science Letters, v. v. 188, p. 441-458.

Small, E. E., Anderson, R. S., Repka, J. L., and Finkel, R., 1997, Erosion rates of alpine bedrock summit surfaces deduced from in situ ^{10}Be and ^{26}Al: Earth and Planetary Science Letters, v. 150, no. 3-4, p. 413-425.

Sullivan, C. L., 2007, ^{10}Be erosion rates and landscape evolution of the Blue Ridge Escarpment, southern Appalachian Mountains: University of Vermont, 76 p.

Syvitski, J. P. M., Vorosmarty, C. J., Kettner, A. J., and Green, P., 2005, Impact of Humans on the Flux of Terrestrial Sediment to the Global Coastal Ocean: Science, v. 308, p. 376-380.

Trimble, S. W., 1977, The fallacy of stream equilibrium in contemporary denudation studies: American Journal of Science, v. 277, p. 876-887.

von Blanckenburg, F., Hewawasam, T., and Kubik, P. W., 2004, Cosmogenic nuclide evidence for low weathering and denudation in the wet, tropical highlands of Sri Lanka: Journal of Geophysical Research, v. 109, no. F3.

Walling, D. E., 1983, The sediment delivery problem: Journal of Hydrology, v. 65, no. 1-3, p. 209-237.

Wilkinson, B.H., 2005, Humans as geologic agents: A deep-time perspective: Geology, v. 33, no. 3, p. 161-164.

Wittmann, H., Blanckenburg, F. v., Guyot, J. L., Maurice, L., and Kubik, P. W., 2009, From source to sink: Preserving the cosmogenic ^{10}Be-derived denudation rate signal of the Bolivian Andes in sediment of the Beni and Mamoré foreland basins: Earth and Planetary Science Letters, v. 288, p. 463-474.

Zeitler, P. K., Meltzer, A. S., Koons, P. O., Craw, D., Hallet, B., Chamberlain, C. P., Kidd, W. S. F., Park, S. K., Seeber, L., Bishop, M., and Shroder, J., 2001, Erosion, Himalayan geodynamics, and the geomorphology of metamorphism: GSA Today, v. 11, no. 1, p. 4-9.

Figure Captions

Figure 1. Geographical distribution of cosmogenic [10]Be erosion rate data (see Tables DR-1, 2, 3 in Appendix B). Location of studies compiled in this paper (A). Distribution of outcrop samples (B) and drainage basin samples (C) are graded by number of samples per study and by relative erosion rate.

Figure 2. Erosion rate data. A. Exceedance probability for compiled erosion rates. B. Histogram of outcrop erosion rates before and after (inset) being log-transformed. Mean erosion rate = 12 ± 1.3 m My^{-1}; median erosion rate = 5.2 m My^{-1}. C. Histogram of drainage basin erosion rates before and after (inset) being log-transformed. Mean erosion rate = 209 ± 33 m My^{-1}; median erosion rate = 53 m My^{-1}.

Figure 3. Analysis of Variance (ANOVA) for the log-transformed CRONUS erosion rates on outcrop and drainage basin samples categorized by rock type, climate zone, and tectonic regime. Letters below each box-plot represent the results from paired Student's t-Tests: categories linked by a similar letter are similar at $p < 0.05$. Green lines are means. Red lines are medians. Box defines 25th and 75th percentiles. Whiskers are data range.

Figure 4. Forward stepwise regressions for outcrop and drainage basin datasets considered globally and by subdivisions of categorical data. Colored boxes indicate variance explained by each statistically significant parameter. R^2 value listed at the bottom of each column represents the total amount of variation in the data that is

explained by the significant parameters. Regressions use log-transformed CRONUS erosion rates. Mean and median values calculated from CRONUS erosion rates.

Figure 5. Mean basin slope and erosion rate co-vary. Correlation is scale dependent and decreases with the area included in the sample. Appalachian Plateau within the Susquehanna River Basin (red squares; Reuter, 2005). Appalachian Mountains crest data (green triangles; Matmon et al., 2003; Reuter, 2005; Sullivan, 2007). Global data set (grey circles; Table DR-1 for references in Appendix B).

Figure 1.

Figure 2.

Figure 3.

Outcrop Erosion Rate (m My⁻¹)

| n = | 230 B | 82 A | 106 A | | 195 C | 108 B | 31 D | 75 A | 11 B,C | | 55 A | 363 A |

Basin Erosion Rate (m My⁻¹)

| n = | 302 B | 298 B | 218 A,B | 292 A | | 224 C | 280 B | 69 A | 465 B | 72 B | | 219 A | 891 B |

Rock Type: Igneous, Meta., Sed., Mixed
Climate Zone: Arid, Cold, Polar, Temp., Tropical
Tectonics: Active, Inactive

34
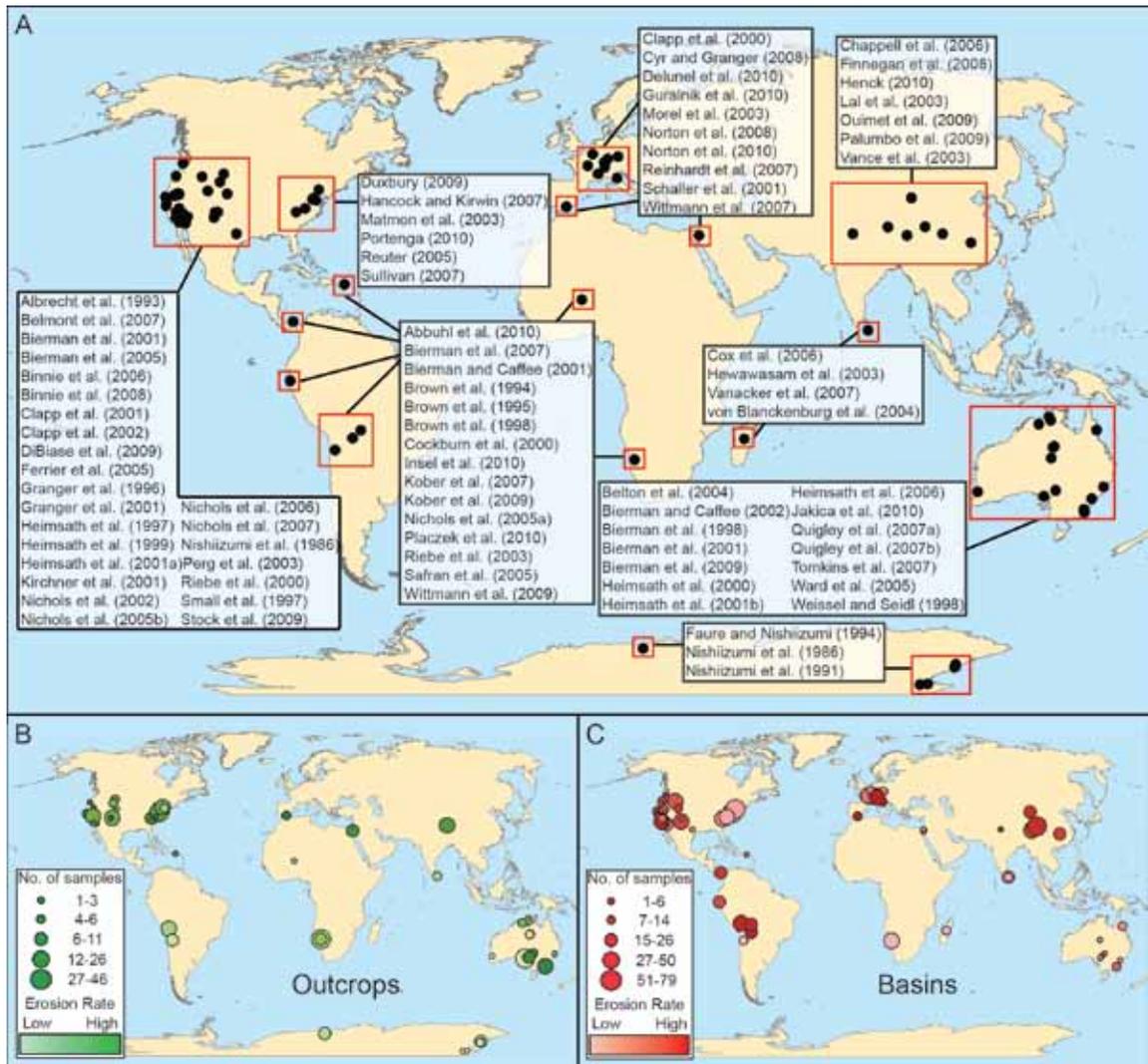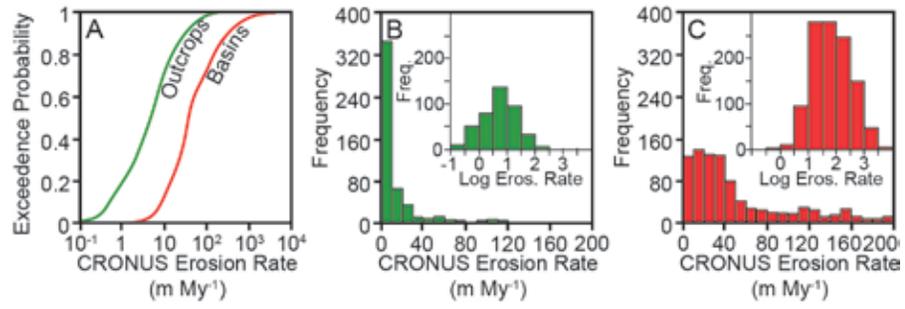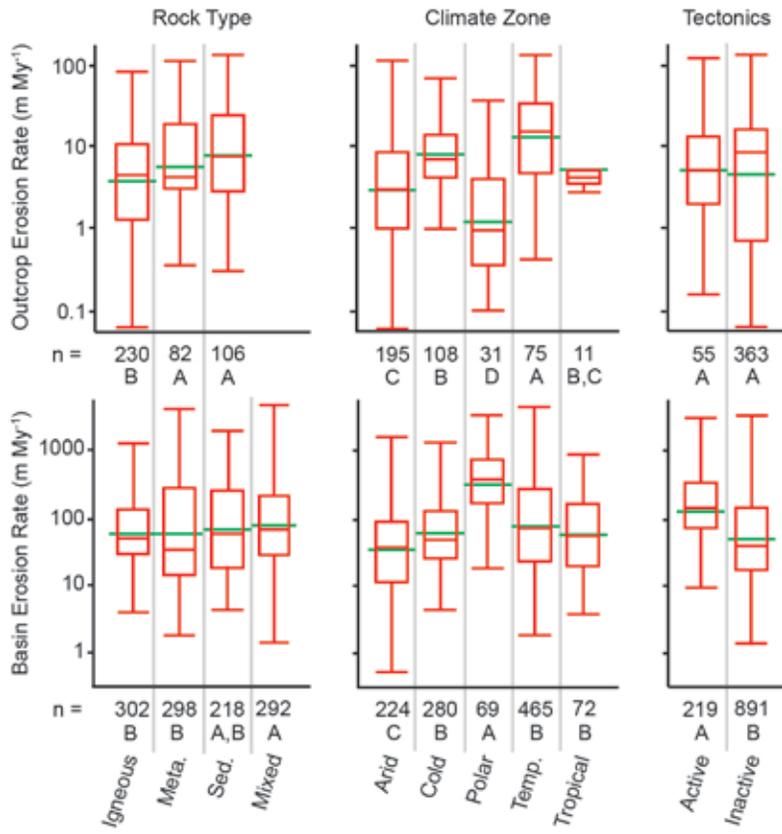
Figure 4.

Forward Stepwise Regression Results

Probability to Enter: 0.250
Probability to Leave: 0.100

Outcrops

	Global Analysis	Igneous	Metamorphic	Sedimentary	Mixed	Arid	Cold	Polar	Temperate	Tropical	Active	Inactive
n =	418	230	82	106	N/A	193	108	31	75	11	55	363
Mean (m My⁻¹) =	12	9	13	19	N/A	8	13	4	26	7	14	12
Median (m My⁻¹) =	5	4	4	8	N/A	3	7	1	14	4	8	5
Latitude (°N/S)	.147	.139			N/A	.046		.484	.071		.379	.031
Elevation (m)	.086	.009		.056	N/A	.093		.034			.094	.066
Basin Relief (m)	.017			.276	N/A	.098						
MAP (mm yr⁻¹)	.060	.082		.059	N/A		.021		.105		.120	.127
MAT (°C)	.017	.102	.115		N/A	.063				.911	.053	.044
Seismicity			.142	.073	N/A			N/A	.127		.050	
R² =	.326	.333	.257	.464	N/A	.299	.021	.518	.331	.911	.626	.268

Basins

	Global Analysis	Igneous	Metamorphic	Sedimentary	Mixed	Arid	Cold	Polar	Temperate	Tropical	Active	Inactive
n =	1110	302	298	218	292	224	280	69	465	72	219	891
Mean (m My⁻¹) =	209	148	288	163	226	103	158	550	254	120	364	171
Median (m My⁻¹) =	53	52	35	60	73	37	49	380	73	54	154	42
Latitude (°N/S)	.043	.036	.077	.022	.072	.207	.001				.089	.045
Elevation (m)			.005	.047	.009	.002			.003	.087		.004
Basin Relief (m)	.102		.088	.009	.138	.013	.471	.035	.158	.091	.152	.052
MAP (mm yr⁻¹)	.011	.075			.008	.186	.010	.006		.006	.008	.013
MAT (°C)	.001	.006	.002	.006	.013	.003		.087	.013	.058		.004
Seismicity	.047	.043	.024	.072	.013	.016	.008		.457	.546	.009	.324
Slope (°)	.342	.450	.481	.355	.349	.298	.172	.864	.045	.032	.377	.119
% Vegetation	.011		.140		.027	.024	.077		.034	.011	.007	.023
Basin Area (km²)	.002		.013		.003			.010	.005	.002	.017	.006
R² =	.557	.610	.831	.512	.631	.747	.749	.796	.712	.849	.642	.588
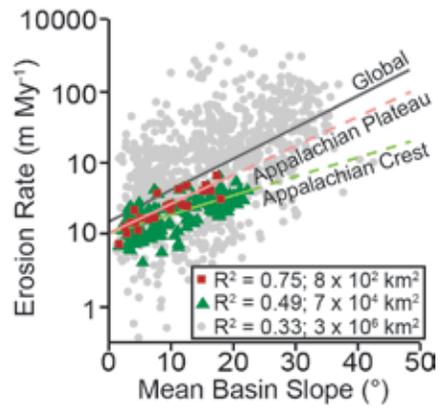
Subdivisions of Categorical Data

Parameters

Relevance: High — Low

Figure 5.

Low rates of bedrock outcrop erosion in the central Appalachian Mountains
inferred from *in situ* [10]Be

Eric W. Portenga*
Department of Geology
University of Vermont
Burlington, VT 05405

Paul R. Bierman
Department of Geology and Rubenstein School of the Environment and Natural
Resources
University of Vermont
Burlington, VT 05405

Dylan H. Rood
Center for Accelerator Mass Spectrometry
Lawrence Livermore National Laboratory
Livermore, CA 94550

*Corresponding Author: contact at eporteng@uvm.edu

Keywords: Geomorphology, Cosmogenic, Landscape evolution, Denudation

Abstract

Bedrock outcrops in the central Appalachian Mountains make up ridgelines that define watershed boundaries and thus influence landscape evolution. The rate at which these ridgelines erode on millennial timescales is poorly constrained. To better understand the rates of bedrock erosion, we collected samples ($n = 72$) from sedimentary and metamorphic rock outcrops in the Susquehanna and Potomac River Basins and measured *in situ* cosmogenic ^{10}Be concentrations. We find that bedrock exposed along ridgelines is eroding on average at 13 m My^{-1} with a median of 7.2 m My^{-1}, which is similar to previously determined erosion rates inferred from ^{10}Be in fluvial sediments. Outcrops erode half as fast as drainage basins in the Susquehanna River Basin but erosion rates of drainage basins are similar to outcrops in the Potomac River Basin. Outcrop erosion rates in the two basins and four different physiographic provinces are statistically similar. Outcrops situated on main ridgelines erode slower than those positioned on spur-ridges lower on the landscape. Relative standard deviations (RSDs) for each sampling site are generally low (<0.50) and those that have higher RSDs indicate the inclusion of a sample which may violate assumptions of the cosmogenic ^{10}Be methodology. The RSD for the entire field area is large (= 1.1), suggesting that multiple samples from one site are similar to each other though the range of erosion rates throughout the field area is large and non-uniform. The range and average of bedrock erosion rates are similar to those previously determined for the region by other means and on other timescales, including from fission track and (U-Th)/He thermochronology. Because ridgelines erode more slowly than other parts of the landscape, calculated erosion rates set the pace of regional

38

landscape evolution on the millennial timescale. Since this rate is consistent with that determined by geochronometers integrating over longer time scales, it appears that the overall pace of landscape evolution in the central Appalachian Mountains has been relatively similar for >100 Ma.

Introduction

The central Appalachian Mountains are a dominant physiographic feature on the Atlantic passive-margin of eastern North America. This linear mountain chain extends 2500 km from the near-polar Canadian Maritime Provinces to humid, subtropical southern Georgia. The range is several hundred kilometers wide and generally steep and forested, except along the highest ridgelines where bedrock outcrops are common. Appalachian Mountain crests are typically 1000 – 1500 meters above sea level (masl), but the highest peaks, Mt. Washington in New Hampshire and Mt. Mitchell in North Carolina, are 1900 and 2000 masl, respectively.

Five physiographic provinces have been defined in and along the Appalachian Mountains (http://tapestry.usgs.gov/physiogr/physio.html). The western margin consists of undeformed sedimentary rock making up the Appalachian Plateau. Further eastward, the highly-deformed Valley and Ridge province consists of a series of plunging sedimentary anticlines and synclines. The Blue Ridge is a resistant unit of quartzite extending from the Blue Ridge Escarpment in the south and terminating just north of the Maryland-Pennsylvania border. The Piedmont is underlain by metamorphic rocks. To the east is the Coastal Plain, which consists of fluvial and shoreline sediments.

Rocks underlying the Appalachian Mountains have been deformed to varying degrees in numerous orogenic events, the most recent event, the Alleghenian Orogeny, occurred throughout the Permian and was followed by Triassic rifting (Pazzaglia and Brandon, 1996; Poag and Sevon, 1989) that led to regional uplift within the region (Pazzaglia and Gardner, 1994). Prior to rifting, Devonian sedimentary sequences were deposited which now underlie the Valley and Ridge province (Roden, 1991). In the Valley and Ridge province, highly deformed, plunging anticlines and synclines trend parallel to the post-Alleghenian rift-margin, exposing sandstones and quartzites along the ridges and limestones and shales beneath the valleys. More recently, increased mid-Miocene uplift rates have been inferred from a combination of heightened sediment fluxes to off-shore basins and erosional unloading of the Appalachian Mountains (Braun, 1989; Pazzaglia and Brandon, 1996; Pazzaglia et al., 2006). Post-Jurassic denudation rates, determined by (U-Th)/He and fission track methods, throughout the region have fluctuated but on average, remain low (~30 m My^{-1}; Braun, 1989; Pazzaglia and Brandon, 1996; Poag and Sevon, 1989; Sevon et al., 1989).

In humid, temperate regions such as the Appalachian Mountains, bedrock outcrops are typically found along ridgelines that define watershed boundaries. The existence of such ridges indicates that, at least for some time in the past, the landscape within the watersheds must have eroded more quickly than the rock ridges defining the watershed boundaries. Erosion rates determined on a drainage-basin scale are not representative of the relatively small area occupied by ridgeline bedrock outcrops. Although understanding the relationship between ridgeline and drainage basin erosion is

critical for determining how landscapes evolve over time, the relationship between watershed-bounding bedrock outcrop erosion rates and those of the drainage basins they contain is poorly understood because, until recently, outcrop erosion rates have been difficult to constrain over millennial timescales. Traditional methods of measuring the tempo of landscape change, such as chemical denudation, sediment flux, and cliff/slope retreat, are difficult to apply or unrepresentative at the outcrop scale (Saunders and Young, 1983).

The advancement of accelerator mass spectrometry (Elmore and Phillips, 1987) has allowed geomorphologists to estimate denudation rates directly by measuring small concentrations of cosmogenic isotopes, such as ^{10}Be, in a variety Earth materials (Bierman and Nichols, 2004; Gosse and Phillips, 2001). *In situ* produced cosmogenic ^{10}Be is found within the uppermost few meters of Earth's surface and is created primarily by spallation nuclear reactions during which high-energy neutrons interact with oxygen. When these reactions occur, ^{10}Be is formed in mineral lattices and starts to radioactively decay ($t_{1/2}$ = 1.36 Ma; Nishiizumi et al., 2007). The production of ^{10}Be decreases exponentially with depth through Earth's surface, such that at ~2m depth, little ^{10}Be is created through spallogenic reactions; muon-induced reactions continue to depths of tens of meters with a much lower production rate. Thus, by sampling the uppermost portion of an outcrop and assuming steady and uniform erosion, the concentration of ^{10}Be reflects the time required for material to pass through the uppermost several meters of rock and regolith (Lal, 1991).

Cosmogenic nuclides were first widely used as erosion rate monitors in the 1980s (Cerling, 1990; Craig and Poreda, 1986; Kurz, 1986; Nishiizumi et al., 2007). [10]Be has been measured in over 400 samples (Portenga et al., in review) from bedrock outcrops, including numerous studies concerning passive-margin and arid-region landscape change (e.g. Bierman and Caffee, 2002; Bierman and Caffee, 2001; Cockburn et al., 2000); however, [10]Be measurements in fluvial sediments has seen far wider use, with over 1100 measurements (Portenga et al., in review) published to date (e.g. Bierman et al., 2005; DiBiase et al., 2009; Safran et al., 2005; Schaller et al., 2001).

During the past decade, hundreds of [10]Be measurements were made on samples collected from various sites near and within the central Appalachian Mountains. Most cosmogenic erosion rate estimates have been made on fluvial sediment collected from drainage basins of different sizes ($n = 264$ Duxbury, 2009; Reuter, 2005; Trodick et al., 2010). Incision rates of the New River in West Virginia and paleo-erosion rates of contributing drainage basins were inferred from [10]Be and [26]Al concentrations of sediments deposited in caves (Granger et al., 1997). Only 20 Appalachian bedrock outcrops had been sampled in the central Appalachian Mountains (Duxbury, 2009; Reuter, 2005; Hancock and Kirwan, 2007), mostly in the Dolly Sods region of West Virginia; thus, bedrock outcrop erosion rates in the Appalachian Mountains are poorly known.

In this study, we present 72 new [10]Be-based bedrock outcrop erosion rates from a variety of locations within the central Appalachian Mountains, specifically the Susquehanna ($n = 26$) and the Potomac River Basins ($n = 46$; Figure 1). By measuring

42

the rate of bedrock outcrop erosion, we can assess the relationship between the lowering rates of ridgelines and the erosion rates of drainage basins, which is prerequisite to understanding large scale landscape change on millennial timescales. The size of the central Appalachian bedrock outcrop [10]Be erosion rate dataset (n = 89) and spatial distribution of these data allow us to test for relationships among erosion rate and climatic and topographic parameters.

Methods

ArcGIS Sampling Strategy

We used ESRI ArcGIS (version 9.3) to develop a sampling strategy. Bedrock geology maps for Maryland, Pennsylvania, Virginia, and West Virginia were downloaded from the USGS Geological Map Database (http://ngmdb.usgs.gov/). We located outcrops of quartz-rich lithologies based upon lithologic descriptions provided by each map. State and National Park and Forest boundaries within the Potomac and Susquehanna River basins were added to the map. We chose to focus on parks and forests because they typically protect and preserve natural landforms and provide easy access to features, including bedrock outcrops, by means of hiking trails and access roads. Internet searches for photos of possible sampling locations helped to assess the suitability and quality of many outcrops for sampling. This pre-fieldwork meta-analysis of possible sampling locations allowed for more efficient field work and resulted in the collection of a large number of high-quality samples, many from remote locations.

Sample Collection and Field Methods

In summer 2009, using a hammer and chisel, we removed the uppermost centimeters (3-10 cm) from exposed bedrock outcrops within our field area (Fig. 1, Table 1). Samples were taken from the center of outcrops, as far from outcrop edges as possible. Seventy-four samples were collected from 27 locations in the central Appalachian Mountains, south of the region that was glaciated during the Last Glacial Maximum (Fig. 1). Multiple samples (two to four) were collected from individual sampling sites to test erosion rate variability at the outcrop scale. While some outcrop samples are only meters apart at the same site (i.e. EPS11 and EPS12), some are hundreds of meters apart (i.e. EPP17 – EPP20).

We group outcrops into three types based on their different geographic positions. Main ridge-line samples ($n = 47$) were taken from the top of bedrock outcrops along the highest ridge in the immediate area. Spur-ridge samples ($n = 10$) were those taken from the top of bedrock outcrops situated along the crest of secondary ridges angling down from the main ridge-line. Near-cliff samples ($n = 15$) were collected from the top of bedrock outcrops near the edge of either a cliff or a zone of high relief; these samples were set back from the edge by a few meters and none were taken from the cliff face.

We sampled from the four physiographic regions of the Potomac and Susquehanna River Basins: 8 samples were taken from the Appalachian Plateau, 31 from the Valley and Ridge, 30 from the Blue Ridge, and 3 from the Piedmont. The three Piedmont samples are all within the Susquehanna River Basin; no suitable bedrock outcrops were found in the Piedmont region of the Potomac River Basin.

44

Laboratory Methods

Samples were returned to the University of Vermont where they were crushed, ground, magnetically separated, and sieved; only the nonmagnetic 250 – 850 µm grain-size fraction was retained. Samples were then etched in a series of dilute HCl, HNO_3, and HF acids (Kohl and Nishiizumi, 1992), and if necessary, mineral grains were separated according to density. Samples were tested for quartz-purity using inductively coupled plasma optical emission spectrometry (ICP-OES) before a final, 10-day long etch in 0.5% HNO_3/HF.

About twenty grams of sample were weighed into digestion bottles and a known amount of SPEX 1000 ppm ^9Be carrier solution (~250 µg) was added to each sample. The sample and carrier were then digested in concentrated HF. Samples were dried down four times in $HClO_4$, treated with HCl and redissolved in 6N HCl. Anion column chromatography primarily removed iron from each sample; subsequent cation column chromatography primarily separated boron, titanium, and aluminum from beryllium. Beryllium hydroxide was precipitated with NH_4OH. Hydroxide gels were dried, flame oxidized, and mixed with niobium in a 1:1 molar ratio before being packed into stainless steel cathodes. Specific quartz-preparation methods can be found at the University of Vermont Cosmogenic Nuclide Laboratory website (http://www.uvm.edu/cosmolab/?Page=methods.html). Samples were analyzed at the Center for Accelerator Mass Spectrometry at the Lawrence Livermore National Laboratory and normalized against the updated Nishiizumi (07KNSTD) standard, with an assumed $^{10}Be/^9Be$ ratio of 2.85 x 10^{-11} (Nishiizumi et al., 2007).

Calculating Erosion Rates

^{10}Be concentrations were derived from measured ratios of ^{10}Be/^{9}Be and used to calculate erosion rates using the CRONUS on-line cosmogenic erosion rate calculator (Balco et al., 2008). The calculator utilizes the samples' geographic coordinates, elevation, thickness, density (2.7 g cm^3), and ^{10}Be concentration to model erosion rates. We used erosion rates corrected for latitude and elevation based on the scaling schemes of Lal (1991) and Stone (2000). Results are normalized to a high-latitude and sea-level ^{10}Be production rate of 4.96 ± 0.43 atoms g^{-1} yr^{-1} (Balco et al., 2008). Errors reported in our analyses are 1σ analytical errors which are propagated through the CRONUS calculations.

Statistical Analyses

The parametric statistical analyses we performed assume a normal distribution of data. Before performing statistical tests, we log-transformed our data to ensure it met this assumption of normality. We analyzed bivariate relationships among sample erosion rates and physical and environmental parameters in the areas surrounding our sample sites for correlation (Table 2). We recognize that our chosen parameters may be correlated to one another and thus carried out a Principle Component Analysis (PCA) to ensure that erosion rates are compared to independent variables. Analyses of Variance (ANOVA) and Student's t-Tests allowed for comparison between erosion rates when samples were grouped into common categories. Spatial autocorrelation of erosion rates is measured

using the Moran's I test in ArcGIS, allowing us to determine how erosion rates relate to all others in our field area.

Results

Bedrock outcrops in the Potomac and Susquehanna River Basins are eroding slowly, on average, at 13 ± 1 m My^{-1} (Table 3). Measured erosion rates range from $1.0 - 66$ m My^{-1} and result in a median rate of 7.2 m My^{-1}, indicating a distribution skewed toward lower erosion rates (Figure 2).

Spatial Variance of Erosion Rates

Rates of bedrock outcrop erosion are similar between the two drainages (Figure 3): The average erosion rate for bedrock outcrops in the Potomac River Basin is 15 ± 1 m My^{-1}; the average erosion rate for bedrock outcrops in the Susquehanna River Basin is 9.7 ± 0.7 m My^{-1}. The distributions are not statistically separable at the 95% confidence interval ($p = 0.32$). The range of bedrock outcrop erosion rates in the Potomac River Basin ($1.0 - 66$ m My^{-1}) includes that of bedrock outcrops in the Susquehanna River Basin ($1.8 - 28$ m My^{-1}). The median outcrop erosion rate for the Potomac River Basin (7.1 m My^{-1}) is similar to that of the Susquehanna River Basin (8.3 m My^{-1}).

When considered by physiographic province, erosion rates are also similar (Figure 4). Bedrock outcrops in the Potomac Blue Ridge erode at an average of 8.3 ± 0.6 m My^{-1} ($n = 25$) while those in the Susquehanna Blue Ridge erode at an average of 8.1 ± 0.6 m My^{-1} ($n = 5$) resulting in an overall Blue Ridge outcrop erosion rate of 8.2 ± 0.6 m

47

My^{-1}. Potomac Valley and Ridge outcrops erode on average at 19 ± 1.4 m My^{-1} ($n = 20$);

those in the Susquehanna Valley and Ridge erode on average at 14 ± 1.0 m My^{-1} ($n = 13$)

resulting in an overall Valley and Ridge erosion rate average of 17 ± 1.2 m My^{-1}. In the

Appalachian Plateau province of the Potomac River Basin, outcrops erode on average at

53 ± 3.8 m My^{-1} (n = 3). In the Susquehanna Basin Appalachian Plateau province,

outcrops erode much more slowly, on average, 2.4 ± 0.2 m My^{-1} ($n = 5$). No comparison

could be made for bedrock outcrops situated in the Piedmont region because all samples

were collected within the Susquehanna River Basin; these outcrops erode at an average of

6.2 ± 0.5 m My^{-1} ($n = 3$). An ANOVA indicates that there are statistically significant

differences at the 95% confidence level in the mean erosion rates from each province ($p = $

0.02) and paired Student's t-Tests show that bedrock outcrop erosion rates from the

Valley and Ridge are significantly higher than those from the Blue Ridge ($p < 0.01$);

otherwise, all pairs of erosion rates are similar.

Erosion rates varied depending on where an outcrop was situated on the

landscape, whether on the crest of a main ridgeline, the crest of a spur-ridge, or near a

cliff, (Figure 5). Bedrock outcrops along main ridgelines within the Potomac River Basin

erode on average at 16 ± 1.2 m My^{-1} ($n = 29$) and outcrops situated on main ridgelines

within the Susquehanna River Basins erode on average at 8.9 ± 0.7 m My^{-1} ($n = 18$); this

yields an average main ridgeline erosion rate of 13 ± 1.0 m My^{-1} with a median of 6.0 ±

0.48 m My^{-1}. Samples collected along the crest of spur-ridges, or ridgelines coming down

off of a main ridgeline, within the Potomac River Basin average at 47 ± 3.4 m My^{-1} ($n = $

6); those within the Susquehanna River Basin erode on average at 18 ± 1.3 m My^{-1} ($n = $

4); spur-ridges erode on average at 35 ± 2.5 m My^{-1} for the entire field area with a median of 28 ± 2.0 m My^{-1}. Near-cliff samples, or those from outcrops at or near the top of a large, immediate change in relief, within the Potomac River Basin erode on average at 15 ± 1.1 m My^{-1} ($n = 11$); those within the Susquehanna River Basin erode on average at 14 ± 1.0 m My^{-1} ($n = 4$); near-cliff samples from both river basins thus erode at an average of 15 ± 1.1 m My^{-1} with a median of 12 ± 1.0 m My^{-1}. An ANOVA indicates that there is a difference between average erosion rates of different location types ($p < 0.01$) and paired Student's t-Tests show that main ridgeline and near-cliff outcrops erode similarly, whereas those situated on spur-ridges erode significantly faster ($p < 0.01$).

Relative standard deviations (RSDs) from each sampling site cover a wide range (0.03 – 0.98; Table 5) with an average of 0.39 for 30 sampling sites suggesting significant variability of erosion rates at the scale of meters to tens of meters. This observation is consistent with a hypothesis put forward by Hancock and Kirwan (2007) that the erosion rate from one bedrock outcrop may not be representative of the average outcrop erosion rate in the area. Sites with high relative standard deviations (>0.50) suggest sites that may have violated crucial assumptions as mentioned above. Erosion rates are even more variable throughout our entire field area (108,000 km^2), indicated by a large relative standard deviation (RSD = 1.1). RSDs for each physiographic province are moderate (0.4 – 0.8), although erosion rates are more variable in the Blue Ridge province (RSD = 1.2).

Erosion rates from each site are more similar to each other than they are to erosion rates from a different site. Results from the Moran's I test support this

observation and indicate that there is less than a one percent chance that clustering of erosion rates is random ($p < 0.01$).

Parameter Control on Erosion Rates

Regression analyses of environmental and physical parameters show that just a few variables significantly describe the observed variance of erosion rates. We observe a significant inverse correlation between erosion rate and latitude ($p < 0.01$); positive correlations exist among erosion rate and elevation and relief, where relief is measured in meters of elevation change within a 5 km radius of the sample ($p < 0.01$; Figure 6a-c). Erosion rates do not vary between different climate zones (Fig. 6d) as defined by temperature and precipitation, neither of which show any significant correlation to erosion rates alone (Fig. 6e-f). Erosion rates have no relationship with seismicity (Fig. 6g). An ANOVA shows that erosion rates of individual outcrops do not vary by lithology, with the exception that sandstone outcrops erode significantly faster than all lithologies other than quartz veins (Fig. 6h).

PCA suggests that our six numeric variables considered above (latitude, elevation, relief, mean annual temperature, mean annual precipitation, and seismicity) are correlated to each other and one is thus dependent on others. PCA calculated three principle components, or new variables, that account for 91% of this dependent correlation (Tables 4 and 5). Elevation, relief, and seismicity account for 46% of this dependent correlation and are combined to create a new variable, which we term "seismic-physiographogy." Only a part of the variability of relief and seismicity data are taken up by the new

seismic-physiographogy variable. Residuals of relief are correlated to latitude and mean

annual temperature, the combination of which accounts for 28% of dependent correlation

between all parameters, thus creating a new "latitude-temperature" variable. Residuals of

seismicity are correlated to mean annual precipitation and account for 16% of dependent

correlation. Since mean annual temperature is not correlated to other variables, we refer

to this principle component as the "precipitation" variable. When combined in a

multivariate standard least squares analysis, these new independent components —

seismic-physiology, latitude-temperature, and precipitation — describe about 25% of the

variability of erosion rates throughout our field site ($R^2 = 0.242$, $p < 0.01$).

Discussion

^{10}Be concentrations from bedrock outcrops in the central Appalachian Mountains

indicate low rates of erosion, on the order of meters to a few tens of meters per million

years. These erosion rates, assuming steady state, suggest that ^{10}Be measurements

integrate over tens of thousands to many hundreds of thousands of years of erosion

history, the time it takes to remove several meters of rock from the outcrops we sampled.

Although rapid erosion rates exist within our dataset, the majority of outcrops suggest

ridgelines within our study area are eroding slowly, as represented by the median erosion

rate of 7.2 m My^{-1}. The outcrops we sampled are the most stable features of the central

Appalachian landscape and thus set the pace for ridgeline lowering.

Effects of Violated Assumptions of the Cosmogenic Methodology

Though most outcrops we sampled appear to follow the assumptions inherent to inferring erosion rates from cosmogenic isotope abundances, the history of some outlying samples may violate these assumptions, thus inflating calculated erosion rates. The data reduction method we employed requires continuous exposure of the sampled outcrop; soil cover attenuates the cosmic-rays (decreases the production rate used to estimate erosion, Lal 1998) and increases the apparent rate at which bedrock outcrops erode (Heimsath et al., 1997, 1999). For example, sample EPP20 may overestimate the true outcrop erosion rate. This sample comes from a poorly consolidated sandstone outcrop situated on a spur-ridge north of Massanutten Ridge in northern Virginia and sits only ~50 cm above the hillslope. The model erosion rate for EPP20 is 66 m My^{-1} which is at least 10 times more rapid than nearby samples EPP17 – EPP19. The fissile nature of the outcrop and its low position above surrounding soil cover is consistent with recent burial, thus increasing the inferred erosion rate. Its position on a spur-ridge raises the possibility that the outcrop is being affected by erosional processes different from those on main ridgelines.

Samples taken from the top of an outcrop receive maximum cosmic ray bombardment, whereas those taken from sites shielded or obstructed by other objects must be corrected for shielding geometry (Dunne et al., 1999; Lal, 1991). Samples EPP43 and EPP44 were collected from a horizontal surface, ~1 m away from a ~3 m high vertical slab of rock. We used the methods of Dunne (1999) to obtain an estimated shielding factor of ~ 0.575 for these two samples, yielding geometry-corrected erosion

rates of 40 and 18 m My^{-1}, respectively. These rates are still higher than the study-average erosion rate by at least a factor of 1.5. It is possible these rates could be increased due to block-removal of mass from the outcrop (Lal, 1991).

Comogenic erosion rates assume that mass is lost from an outcrop through granular disintegration or thin sheeting rather than thick sheeting failures (i.e. Bierman and Caffee, 2002) or block removal (i.e. Lal, 1991; Small et al., 1997). Samples EPP43, EPP44, and EPS17 may violate this assumption. Sample EPS17 was taken from a heavily-fractured outcrop along the Appalachian Trail near Duncannon, PA. Its erosion rate (28 m My^{-1}) is nearly twice as high as two samples collected from the same area (14 and 15 m My^{-1}, samples EPS16 and EPS18, respectively). Though sample EPS16 is taken from a main ridgeline and sample EPS18 is taken from a near-cliff location, the agreement between these two samples is consistent with results from the ANOVA of outcrop positions (Fig. 5). The apparently high erosion rate of sample EPS17 is most likely due to its extremely fractured nature and loss of mass in slabs.

Spatial Variability of Erosion Rates

Erosion rates are similar within different physiographic provinces in both the Susquehanna and Potomac Basins (Fig. 4), suggesting that mechanisms controlling erosion rates in both the Susquehanna and Potomac Basins are similar. Exceptions are the erosion rates from the Appalachian Plateau region of the Potomac River. Samples EPP28 – EPP30 were taken from outcrops standing at least one meter above the soil-line of a spur-ridge coming down off of the Appalachian Plateau. The elevated rates of erosion

53

could be due to numerous cycles of freeze-thaw action (Delunel et al., 2010; Hales and Roering, 2007), extended periods of minimal soil cover (Heimsath et al., 1997, 1999), or block removal (Lal, 1991; Small et al., 1997).

Erosion rates inferred from outcrops above the top of the Appalachian Plateau situated in the nearby Dolly Sods region (averaging 6.7 m My^{-1}, n = 8; Hancock and Kirwan, 2007), just outside of the boundaries of the Potomac River Basin, better represent the true rate of erosion for the Potomac portions of the Appalachian Plateau. These samples suggest significantly lower erosion rates than EPP28 – EPP30 and are more similar to erosion rates determined for the Appalachian Plateau within the Susquehanna River Basin determined from this study (2.4 m My^{-1}) and from a previous study (3.8 m My^{-1}; Reuter, 2005).

The higher erosion rates of spur-ridge outcrops compared to those on main ridgelines suggests that erosional processes on spur-ridges are either different or that they occur more rapidly than along the highest main ridgelines. Small amounts of soil cover increase the rate of bedrock outcrop erosion by retention of water (Heimsath et al., 1997, 1999) and are more likely on topographically lower spur ridges than on high-standing main ridgelines. Whereas water falling on main ridgelines flows away from outcrops, groundwater may seep out at or near lower spur-ridge outcrops. In the central Appalachian, additional water may speed rates of rock weathering and exacerbate frost-cracking where temperatures fluctuate around freezing (Hales and Roering, 2007). The Potomac and Susquehanna River Basins are located in the temperate and cold climate zones where such freeze-thaw activity is frequent (Peel et al., 2007).

Inferred erosion rates from four previous studies strengthens the argument that the landscape of the central Appalachian Mountains is held up by stable and slowly eroding bedrock outcrops along ridgelines. Erosion rates of bedrock outcrops in the central Appalachian Mountains agree well across the region, including Shenandoah, VA (Duxbury, 2009); Dolly Sods, WV (Hancock and Kirwan, 2007); and the Susquehanna River Basin (Reuter, 2005; Figure 7). An ANOVA reveals that there is minimal variance between the means of sample populations from these studies ($p = 0.20$) and paired Student's t-Tests indicate equality between each sample population ($p > 0.08$; Figure 8).

Average bedrock outcrop erosion rates in the central Appalachian Mountains are similar to the global bedrock outcrop average erosion rate. A global compilation of bedrock outcrop erosion rates in quiescent tectonic settings ($n = 269$) inferred from cosmogenic ^{10}Be (Portenga et al., in review), yields an average erosion rate of 12 m My^{-1}. The Appalachian bedrock outcrop average erosion rate is slightly higher than the global average; a Student's t-Test indicates they are significantly different ($p < 0.01$, Figure 9a). In the central Appalachian Mountains, the median erosion rate is slightly above and the distribution is narrower (i.e. we measured neither extremely slow nor fast erosion rates — those <1 m My^{-1} or >100 m My^{-1}) than that of the global data (Fig. 9b). The distribution within each sample population, however, is similar (Fig. 9c) and both are heavily skewed toward lower erosion rates.

Cosmogenic Outcrop Erosion Rates in the Central Appalachian Mountains Compared to

Other Erosion Rate Estimates

In the Potomac and Susquehanna Rivers of the central Appalachian Mountains, the average erosion rate estimated from bare bedrock outcrops (13 m My^{-1}) is in the same range as the average erosion rates measured on a basin scale using ^{10}Be concentrations in fluvial sediment (15 My^{-1}; n = 178 from Duxbury, 2009; Reuter, 2005; Trodick et al., 2010). Within the Susquehanna River basin, the average erosion rate of basins (20 ± 1.6 m My^{-1}, n = 79; Reuter, 2005) is twice as fast as those of bedrock outcrops (8.9 ± 0.7 m My^{-1}; n = 30; p < 0.01) determined from samples in multiple studies (Reuter, 2005; this study). Conversely, in the Potomac River Basin, outcrop erosion rates (15 ± 1 m My^{-1}; n = 46) are statistically inseparable from those of river basins (10 ± 0.8 m My^{-1}; n = 99; p = 0.58) determined from multiple studies (Duxbury, 2009; Trodick et al., 2010; this study). Only basins draining westward from Shenandoah National Park were used for this statistical comparison (Duxbury, 2009).

In the central Appalachians, rates of erosion inferred from ^{10}Be in bedrock outcrops are comparable to, but slightly lower than, those determined from apatite fission track thermochronology (AFTT) and (U-Th)/He methods. AFTT indicates denudation rates of 16 m My^{-1} (Valley and Ridge, Blue Ridge, Piedmont and Coastal Plain of Tennessee, N. Carolina, Virginia, and Maryland, Naeser et al., 2001), 17 m My^{-1} (Appalachian Plateau of Pennsylvania, Blackmer et al., 1994), 20 m My^{-1} (Blue Ridge of Virginia, Naeser et al., 2005; Blue Ridge of Virginia, Naeser et al., 2004), 21 – 29 m My^{-1} (Spotila et al., 2003), 29 m My^{-1} (Valley and Ridge, eastern Kentucky, Boettcher and

Milliken, 1994), and 14 – 33 m My[-1] (Appalachian Plateau and Valley and Ridge of W. Virginia, Virginia, and Maryland, Roden, 1991). (U-Th)/He dating suggests denudation rates of 25 m My[-1] (Appalachian Plateau and Valley and Ridge of W. Virginia, Reed et al., 2005) and 7 – 23 m My[-1] (Valley and Ridge, Blue Ridge, and Piedmont of southern Virginia, Spotila et al., 2003). The similarity of thermochronologically and cosmogenically determined erosion rates confirms the slow denudational history for the central Appalachian Mountains since post-Alleghenian rifting events and most likely reflects isostatically driven rebound responding to mass loss by erosion. Such similarity between erosion rates on cosmogenic and thermochronologic time scales is not uncommon in steady-state landscapes (i.e. Cockburn et al., 2000; Granger et al., 2001; von Blanckenburg et al., 2004).

Our data have significant implications for landscape erosion histories of the central Appalachian Mountains in time and space. Outcrop and basin-scale rates of erosion in the Potomac River Basin suggest that ridges and valleys are lowering at a similar rate and that relief is thus steady, similar to the Great Smoky Mountains (Matmon et al., 2003). In contrast, the two-fold difference in the Susquehanna River Basin between basin scale and outcrop erosion rates suggests that relief is increasing. In the central Appalachians, erosion rates inferred from fluvial sediments on millennial timescales are similar to denudation rates determined for the $>10^6$-year timescale, suggesting an overall steady lowering of the central Appalachian Mountains.

Conclusions

Erosion rates of bedrock outcrops in the central Appalachian Mountains are similar to those in tectonically inactive settings around the world (average = 13 m My^{-1}; median = 7.2 m My^{-1}). Outcrops in the Potomac River Basin erode at a rate similar to those in the Susquehanna River Basin. These bedrock outcrop erosion rates are comparable to others measured previously in the central Appalachian Mountains including those determined in the Susquehanna River, Dolly Sods, and Shenandoah National Park (Duxbury, 2009; Hancock and Kirwan, 2007; Reuter, 2005). Cosmogenically determined bedrock outcrop erosion rates in the central Appalachian Mountains are within range of longer-term denudation rates determined from AFTT and (U-Th)/He methods. Together, these datasets imply that while there may have been short-term perturbations in erosion rates, over the past tens of millions of years and the past tens to hundreds of thousands of years, erosion rates in the Appalachian Mountains have averaged just tens to a few tens of meters per million years.

The position occupied by a bedrock outcrop on a landscape affects the rate at which it erodes. Outcrops situated on main ridgelines erode more slowly than those situated on the crest of spur-ridges. Outcrops seated near a zone of large local relief, such as a cliff or very steep hill slope, have erosion rates similar to ridgelines and erode significantly slower than outcrops on spur-ridges. Outcrops within the four physiographic provinces of the Potomac and Susquehanna River Basins generally agree well. Such similar erosion rates of bedrock outcrops across different physiographic regions suggest a uniform lowering of the highest points within the central Appalachian Mountains.

58

Acknowledgements

References Cited

Balco, G., Stone, J. O., Lifton, N. A., and Dunai, T. J., 2008, A complete and easily accessible means of calculating surface exposure ages or erosion rates from ^{10}Be and ^{26}Al measurements: Quaternary Geochronology, v. 3, p. 174-195.

Bierman, P. R., and Caffee, M., 2002, Cosmogenic exposure and erosion history of ancient Australian bedrock landforms: Geological Society of America Bulletin, v. 114, no. 7, p. 787-803.

Bierman, P. R., and Caffee, M. W., 2001, Slow rates of rock surface erosion and sediment production across the Namib Desert and escarpment, Southern Africa: American Journal of Science, v. 301, no. 4-5, p. 326-358.

Bierman, P., and Nichols, K., 2004, Rock to sediment – Slope to sea with 10-Be – Rates of landscape change: Annual review of Earth and Planetary Sciences, v. 32, p. 215-255.

Bierman, P. R., and Steig, E., 1996, Estimating rates of denudation and sediment transport using cosmogenic isotope abundances in sediment: Earth Surface Processes and Landforms, v. 21, p. 125-139.

Bierman, P. R., Reuter, J. M., Pavich, M., Gellis, A. C., Caffee, M. W., and Larsen, J., 2005, Using cosmogenic nuclides to contrast rates of erosion and sediment yield in a semi-arid, arroyo-dominated landscape, Rio Puerco Basin, New Mexico: Earth Surface Processes and Landforms, v. 30, no. 8, p. 935-953.

Blackmer, G. C., Omar, G. I., and Gold, D. P., 1994, Post-Alleghanian unroofing history of the Appalachian Basin, Pennsylvania, from apatite fission track analysis and thermal models: Tectonics, v. 13, no. 5, p. 1259-1276.

Boettcher, S. S., and Milliken, K. L., 1994, Mesozoic-Cenozoic unroofing of the southern Appalachian Basin: apatite fission track evidence from Middle Pennsylvanian Sandstones: The Journal of Geology, v. 102, p. 655-663.

Braun, D. D., 1989, Glacial and Periglacial Erosion of the Appalachians: Geomorphology, v. 2, p. 233-256.

Cerling, T. E., 1990, Dating geomorphologic surfaces using cosmogenic (super 3) He: Quaternary Research (New York), v. 33, no. 2, p. 148-156.

Cockburn, H. A. P., Brown, R. W., Summerfield, M. A., and Seidl, M. A., 2000, Quantifying passive margin denudation and landscape development using a combined fission-track thermochronology and cosmogenic isotope analysis approach: Earth and Planetary Science Letters, v. 179, no. 3-4, p. 429-435.

Craig, H., and Poreda, R. J., 1986, Cosmogenic 3He and model erosion rates in terrestrial rocks: AGU 1986 spring meeting Eos, Transactions, American Geophysical Union, v. 67, no. 16, p. 414.

Delunel, R., Beek, P. A. v. d., Carcaillet, J., Bourlès, D. L., and Valla, P. G., 2010, Frost-cracking control on catchment denudation rates: Insights from in situ produced [10]Be concentrations in stream sediments (Ecrins–Pelvoux massif, French Western Alps): Earth and Planetary Science Letters, v. 293, p. 72-83.

DiBiase, R. A., Whipple, K. X., Heimsath, A. M., and Ouimet, W. B., 2009, Landscape form and millennial erosion rates in the San Gabriel Mountains, CA: Earth and Planetary Science Letters, v. 289, p. 134-144.

Dunne, A., Elmore, D., and Muzikar, P., 1999, Scaling factors for the rates of production of cosmogenic nuclides for geometric shielding and attenuation at depth on sloped surfaces, *in* Harbor, J., ed., Cosmogenic isotopes in geomorphology Geomorphology 27, no. 1-2 (199902), Elsevier, Amsterdam, Netherlands, p. 3-11.

Duxbury, J., 2009, Erosion rates in and around Shenandoah National Park, VA, determined using analysis of cosmogenic [10]Be: University of Vermont, 134 p.

Elmore, D., and Phillips, F., 1987, Accelerator mass spectrometry for measurement of long-lived radioisotopes: Science, v. 236, p. 543-550.

Giardini, D., Grunthal, G., Shedlock, K. M., and Zhang, P., 1999, The GSHAP Global Seismic Hazard Map: Annali Di Geofisica, v. 42, no. 6, p. 1225-1230.

Gosse, J. C., and Phillips, F. M., 2001, Terrestrial in situ cosmogenic nuclides: theory and application: Quaternary Science Reviews, v. 20, no. 14, p. 1475-1560.

Granger, D. E., Kirchner, J. W., and Finkel, R. C., 1997, Quaternary downcutting rate of the New River, Virginia, measured from differential decay of cosmogenic ^{26}Al and ^{10}Be in cave-deposited alluvium: Geology, v. 25, no. 2, p. 107-110.

Granger, D. E., Riebe, C. S., Kirchner, J. W., and Finkel, R. C., 2001, Modulation of erosion on steep granitic slopes by boulder armoring, as revealed by cosmogenic ^{26}Al and ^{10}Be: Earth and Planetary Science Letters, v. 186, no. 2, p. 269-281.

Hales, T. C., and Roering, J. J., 2007, Climatic controls on frost cracking and implications for the evolution of bedrock landscapes: Journal of Geophysical Research, v. 112.

Hancock, G., and Kirwan, M., 2007, Summit erosion rates deduced from ^{10}Be: Implications for relief production in the central Appalachians: Geology, v. 35, no. 1, p. 89-92.

Heimsath, A. M., Dietrich, W. E., Nishiizumi, K., and Finkel, R. C., 1997, The soil production function and landscape equilibrium: Nature (London), v. 388, no. 6640, p. 358-361.

-, 1999, Cosmogenic nuclides, topography, and the spatial variation of soil depth: Geomorphology, v. 27, no. 1-2, p. 151-172.

Kohl, C. P., and Nishiizumi, K., 1992, Chemical isolation of quartz for measurement of *in-situ* –produced cosmogenic nuclides: Geochimica et Cosmochimica Acta, v. 56, p. 3583-3587.

Kurz, M. M., 1986, In situ production of terrestrial cosmogenic helium and some applications to geochronology: Geochimica et Cosmochimica Acta, v. 50, no. 12, p. 2855-2862.

Lal, D., 1988, In situ-produced cosmogenic isotopes in terrestrial rocks: Annual Reviews of Earth and Planetary Science, v. 16, p. 355-388.

Lal, D., 1991, Cosmic ray labeling of erosion surfaces; in situ nuclide production rates and erosion models: Earth and Planetary Science Letters, v. 104, no. 2-4, p. 424-439.

Matmon, A., Bierman, P. R., Larsen, J., Southworth, S., Pavich, M., and Caffee, M., 2003, Temporally and spatially uniform rates of erosion in the southern Appalachian Great Smoky Mountains: Geology, v. 31, no. 2, p. 155–158.

Naeser, C. W., Naeser, N. D., Kunk, M. J., Morgan Iii, B. A., Schultz, A. P., Southworth, C. S., and Weems, R. E., 2001, Paleozoic through Cenozoic uplift, erosion, stream capture, and deposition history in the Valley and Ridge, Blue Ridge, Piedmont, and Coastal Plain provinces of Tennessee, North Carolina, Virginia, Maryland, and District of Columbia, *in* GSA Annual Meeting, November 5-8, 2001.

Naeser, C. W., Naeser, N. D., and Southworth, C. S., 2005, Tracking Across the southern Appalachians *in* Blue Ridge Geology Geotraverse East of the Great Smoky Mountains National Park, Western North Carolina: Carolina Geological Society.

Naeser, N. D., Naeser, C. W., Southworth, C. S., Morgan Iii, B. A., and Schultz, A. P., 2004, Paleozoic to recent tectonic and denudation history of rocks in the Blue Ridge Province, central and southern Appalachians – Evidence from fission-track thermochronology, *in* Geological Society of America Abstracts with Programs, p. 114.

Nishiizumi, K., Imamura, M., Caffee, M. W., Southon, J. R., Finkel, R. C., and McAninch, J., 2007, Absolute calibration of ^{10}Be AMS standards: Nuclear Inst. and Methods in Physics Research, B, v. 258, no. 2, p. 403-413.

Nishiizumi, K., Kohl, C. P., Arnold, J. R., Klein, J., Fink, D., and Middleton, R., 1991, Cosmic ray produced ^{10}Be and ^{26}Al in Antarctic rocks; exposure and erosion history: Earth and Planetary Science Letters, v. 104, no. 2-4, p. 440-454.

Pazzaglia, F. J., and Brandon, M. T., 1996, Macrogeomorphic evolution of the post-Triassic Appalachian mountians determined by deconvolution of the offshore basin sedimentary record: Basin Research, v. 8, no. 255-278.

Pazzaglia, F. J., Braun, D. D., Pavich, M., Bierman, P., Potter Jr, N., Merritts, D., Walter, R., and Germanoski, D., 2006, Rivers, glaciers, landscape evolution, and active tectonics of the central Appalachians, Pennsylvania and Maryland, *in* Pazzaglia, F. J., ed., Excursions in Geology and History: Field Trips in the Middle Atlantic States: Geological Society of America Field Guide 8: Denver, GSA, p. 169-197.

Pazzaglia, F. J., and Gardner, T. W., 1994, Late Cenozoic flexural deformation of the middle U. S. Atlantic passive margin: Journal of Geophysical Research, B, Solid Earth and Planets, v. 99, no. 6, p. 12,143-12,157.

Peel, M. C., Finlayson, B. L., and McMahon, T. A., 2007, Updated world map of the Köppen-Geiger climate classification: Hydrology and Earth System Sciences, v. 11, p. 1633-1644.

Poag, C. W., and Sevon, W. D., 1989, A record of Appalachian denudation in postrift Mesozoic and Cenozoic sedimentary deposits of the U.S. middle Atlantic continental margin: Geomorphology, v. 2, p. 119-157.

Reed, J. S., Spotila, J. A., Eriksson, K. A., and Bodnar, R. J., 2005, Burial and exhumation history of Pennsylvanian strata, central Appalachian basin: an integrated study: Basin Research, v. 17, p. 259-268.

Reuter, J. M., 2005, Erosion rates and patterns inferred from cosmogenic [10]Be in the Susquehanna River basin: University of Vermont, 172 p.

Roden, M. K., 1991, Apatite fission-track thermochronology of the southern Appalachian basin: Maryland, West Virginia, and Virginia: Journal of Geology, v. 99, no. 1, p. 41–53.

Saunders, I., and Young, A., 1983, Rates of surface processes on slopes, slope retreat, and denudation: Earth Surface Processes and Landforms, v. 8, p. 473-501.

Safran, E. B., Bierman, P. R., Aalto, R., Dunne, T., Whipple, K. X., and Caffee, M., 2005, Erosion rates driven by channel network incision in the Bolivian Andes: Earth Surface Processes and Landforms, v. 30, no. 8, p. 1007-1024.

Schaller, M., von Blanckenburg, F., Hovius, N., and Kubik, P. W., 2001, Large-scale erosion rates from In situ-produced cosmogenic nuclides in European river sediments: Earth and Planetary Science Letters, v. v. 188, p. 441-458.

Sevon, W. D., Braun, D. D., and Ciolkosz, E. R., 1989, The Rivers and Valleys of Pennsylvania Then and Now: Guidebook for the 20th Annual Geomorphology Symposium: Harrisburg, PA, Pennsylvania Geological Survey, 69 p.

Small, E. E., Anderson, R. S., Repka, J. L., and Finkel, R., 1997, Erosion rates of alpine bedrock summit surfaces deduced from in situ [10]Be and [26]Al: Earth and Planetary Science Letters, v. 150, no. 3-4, p. 413-425.

Spotila, J. A., Bank, G. C., Reiners, P. W., Naeser, C. W., Naeser, N. D., and Henika, B. S., 2003, Origin of the Blue Ridge escarpment along the passive margin of Eastern North America: Basin Research, v. 16, p. 41-63.

Sullivan, C. L., 2007, [10]Be erosion rates and landscape evolution of the Blue Ridge Escarpment, southern Appalachian Mountains: University of Vermont, 76 p.

Trodick, C. D. J., Bierman, P., Pavich, M. J., Reusser, L. J., Portenga, E. W., and Rood, D., 2010, Basin scale erosion rates from the Potomac River basin using *In situ* and meteoric [10]Be, *in* 2010 GSA Denver Annual Meeting, Denver, Colorado.

von Blanckenburg, F., Hewawasam, T., and Kubik, P. W., 2004, Cosmogenic nuclide evidence for low weathering and denudation in the wet, tropical highlands of Sri Lanka: Journal of Geophysical Research, v. 109, no. F3.

Figure Captions

Figure 1. Bedrock outcrop sampling sites in the Potomac (n = 46) and Susquehanna (n = 26) River Basins. White circles represent individual outcrop sites. Samples from the Potomac River Basin are labeled EPPxx and those from the Susquehanna River Basin are labeled EPSxx, where xx refers to the numbers in the figure. All samples were collected south of the Wisconsinan glacial maximum. Samples come from four physiographic provinces: Blue Ridge (EPP01 – EPP27 and EPS19 – EPS23), Valley and Ridge (EPP31 – EPP48, EPP01 – EPP10, and EPP16 – EPP18), the Appalachian Plateau (EPP28 – EPP30 and EPS11 – EPS15), and the Piedmont (EPS24 – EPS26).

Figure 2. Frequency distribution of outcrop erosion rates calculated using the CRONUS on-line calculator (Balco et al., 2008). After a log-transformation, erosion rates form a normal distribution (inset).

Figure 3. Boxplot diagrams of outcrop erosion rates for the Susquehanna and Potomac River Basins. A Student's t-Test indicates similarity between the two sample populations (p = 0.39). Whiskers cover the range of erosion rates for each category while the top, middle, and bottom bars of the box represent the 75th, 50th, and 25th percentile, respectively. Grey dots represent each erosion rate values.

Figure 4. ANOVA of upper boxplot diagrams from the four physiographic provinces of the central Appalachian Mountains from which samples were collected show unequal

means ($p = 0.02$). Individual p-values of Student's t-Test comparisons of means of upper

boxplots are displayed in the inset chart. Lower boxplot diagrams from samples in the

same region are compared between the Potomac and Susquehanna River Basins. Only

sample means from the Appalachian Plateau are separable.

Figure 5. Boxplot diagrams and ANOVA results comparing averages of groups of

outcrops based on their geographic position on the landscape.

Figure 6. Bivariate relationships between outcrop erosion rate and physical and

environmental parameters representative of the area surrounding each outcrop. A:

Latitude (°N); B: Elevation (m above sea level); C: Relief (m, within a 5 km radius of

outcrop); D: Climate zone, as classified by the Köppen-Geiger Classification system

(Peel et al., 2007): Cfa = Temperate: hot summer without dry season; Dfa = Cold: Hot

summer without dry season; Dfb = Cold: warm summer without dry season; E: Mean

annual temperature (°C); F: Mean annual precipitation(mm yr^{-1}); G: Seismicity (Seismic

Hazard; Giardini et al., 1999); H: Lithology (based off of USGS state geologic maps).

Figure 7. Location map of all sites in the central Appalachian Mountains where outcrop

erosion rates have been inferred from concentrations of ^{10}Be.

Figure 8. Boxplot diagrams and ANOVA results comparing average erosion rates from

bedrock outcrops in the central Appalachian region (Duxbury, 2009; Hancock and

Kirwan, 2007; Matmon et al., 2003; Reuter, 2005; this study).

Figure 9. A: Results of a Student's t-Test indicating significant separability between the

global average erosion rate of global outcrops in tectonically quiescent regimes (n = 269)

and the average of outcrops in the central Appalachian Mountains ($p < 0.01$). B:

Exceedence probability of global ^{10}Be erosion rates (light grey line) shows a wider

distribution than samples from this study (dark grey line). C: Histograms of cosmogenic

^{10}Be erosion rates around the world (light grey bars) and this study (inset dark grey bars).

Figures

Figure 1.

Figure 2.

Mean: 13 ± 1 m My⁻¹
Median: 7.2 m My⁻¹
Min.: 1 ± 0.1 m My⁻¹
Max.: 66 ± 4.8 m My⁻¹
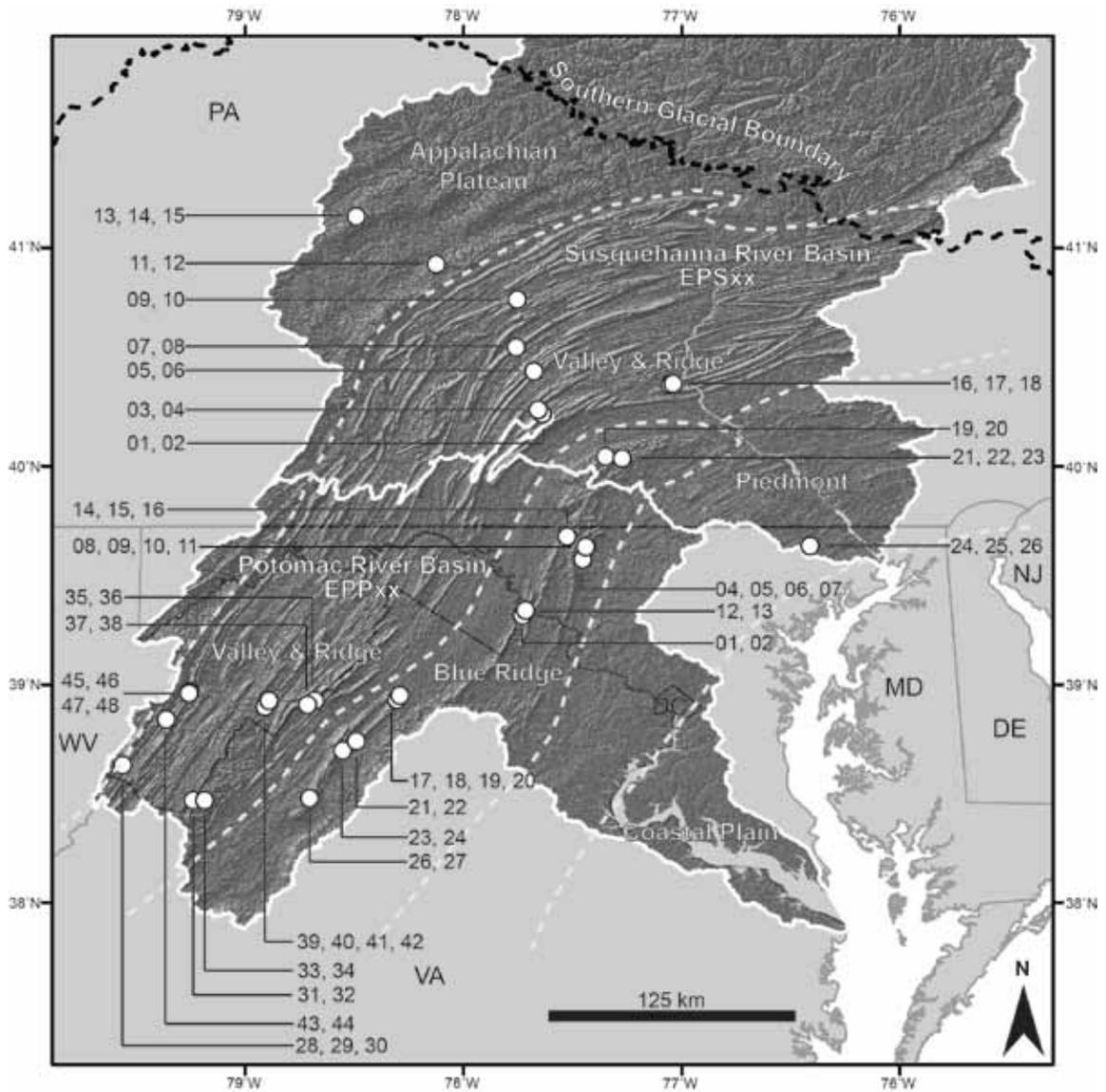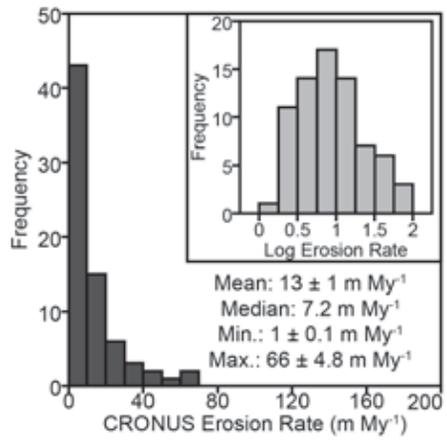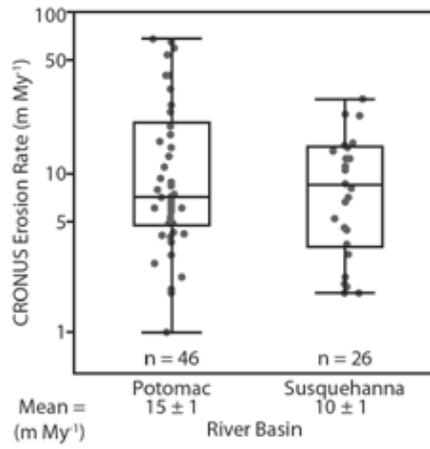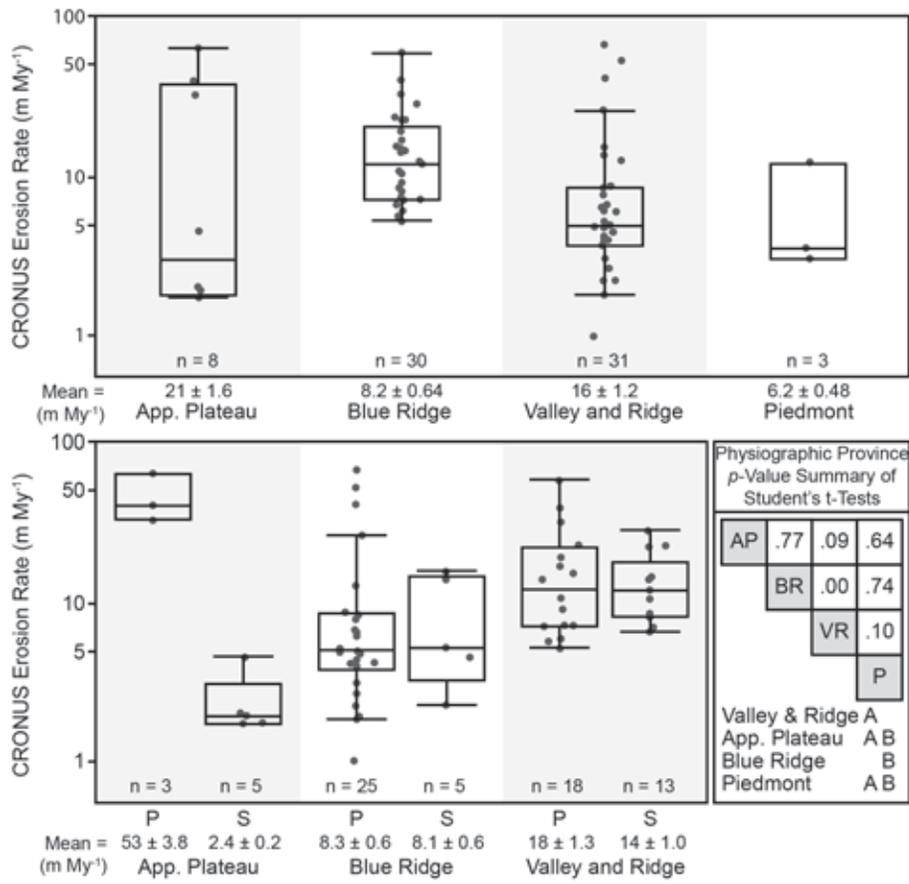
Figure 3.

Figure 4.

Figure 5.
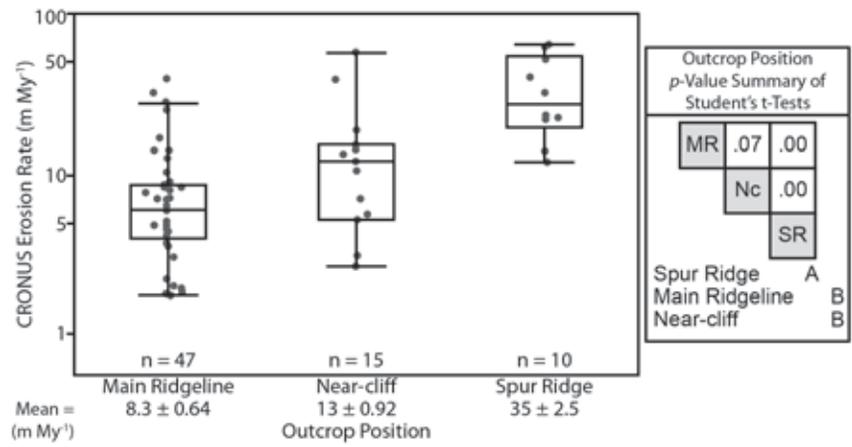
Figure 6.
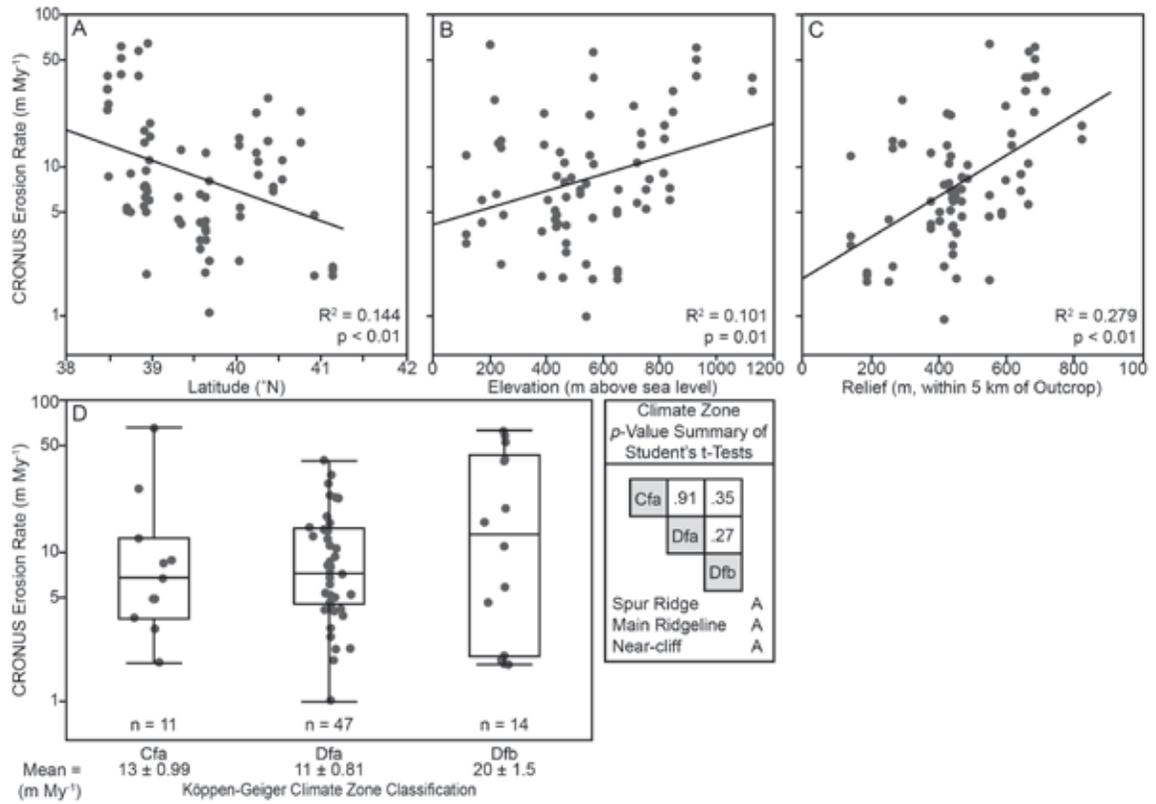
Figure 6 (continued).
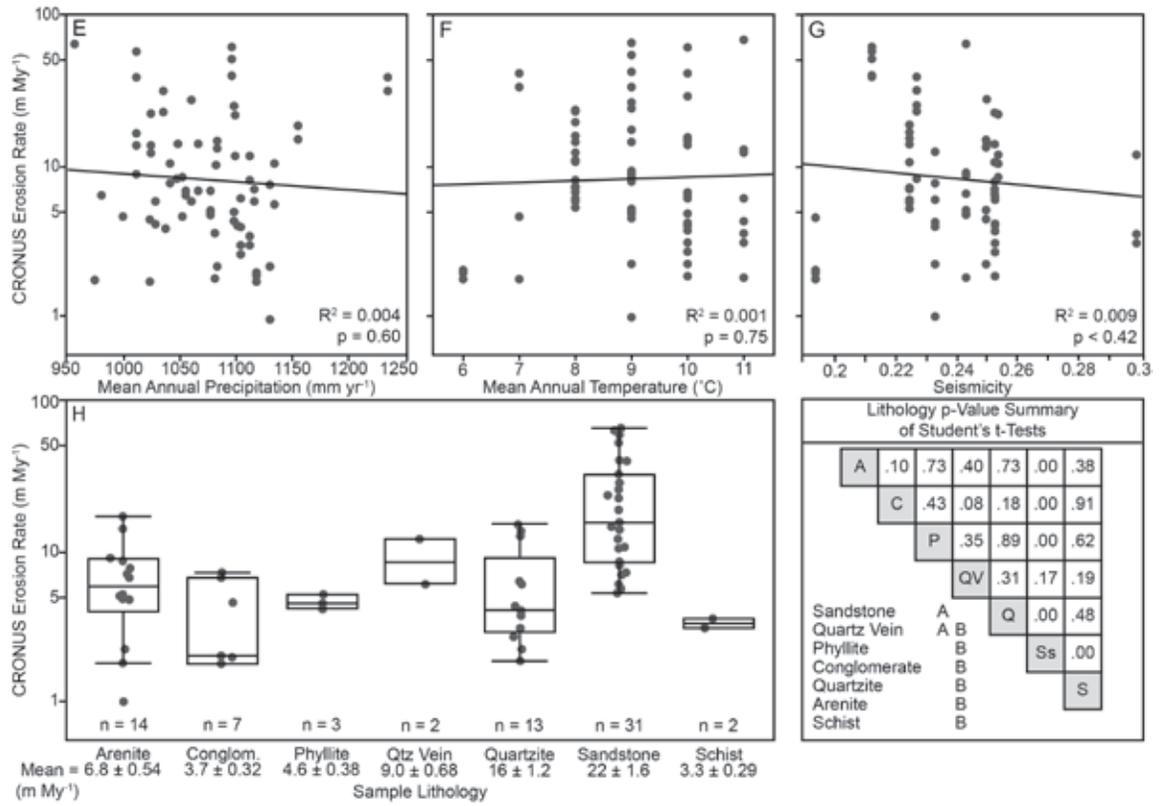
Figure 7.
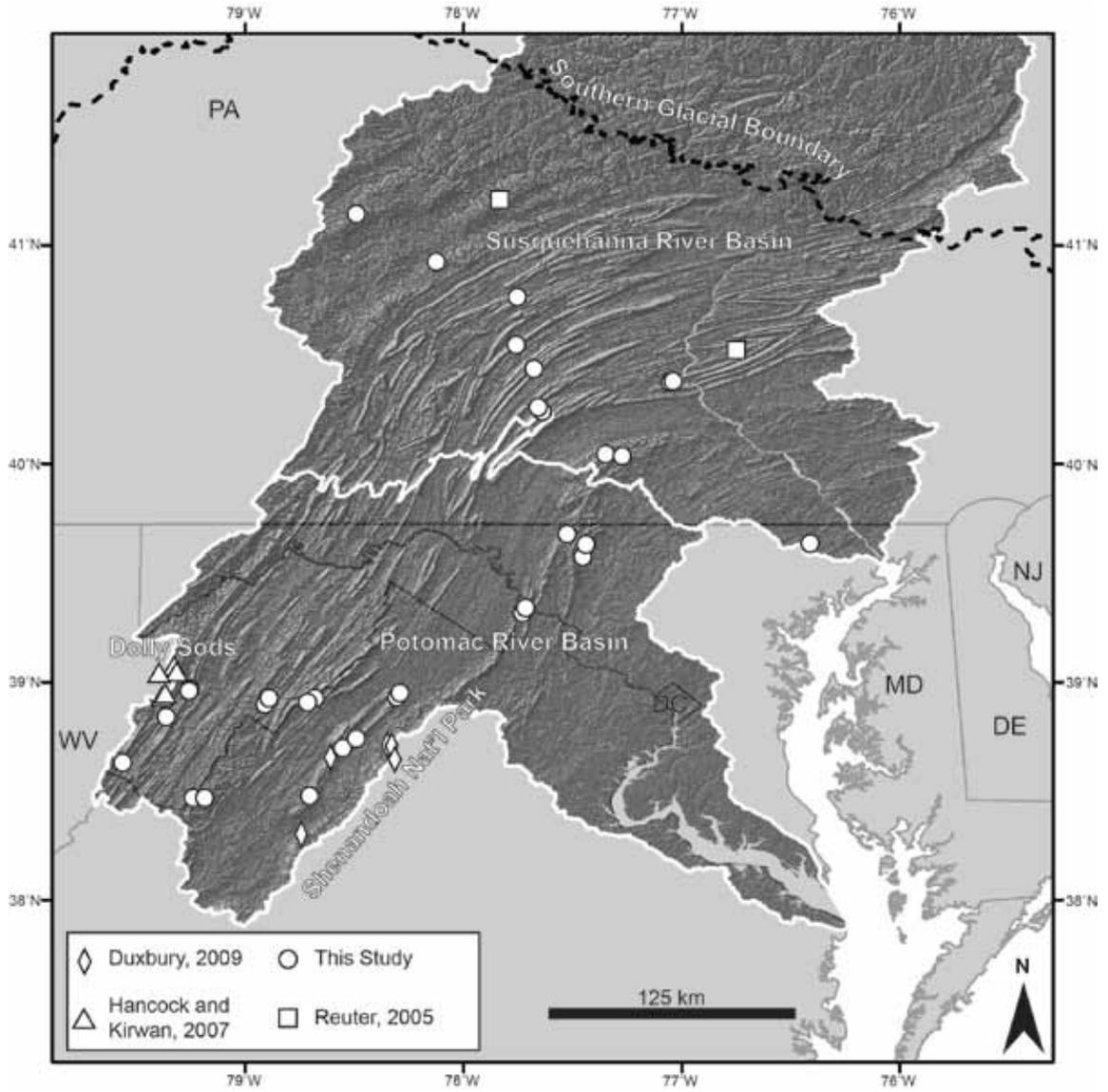
Figure 8.
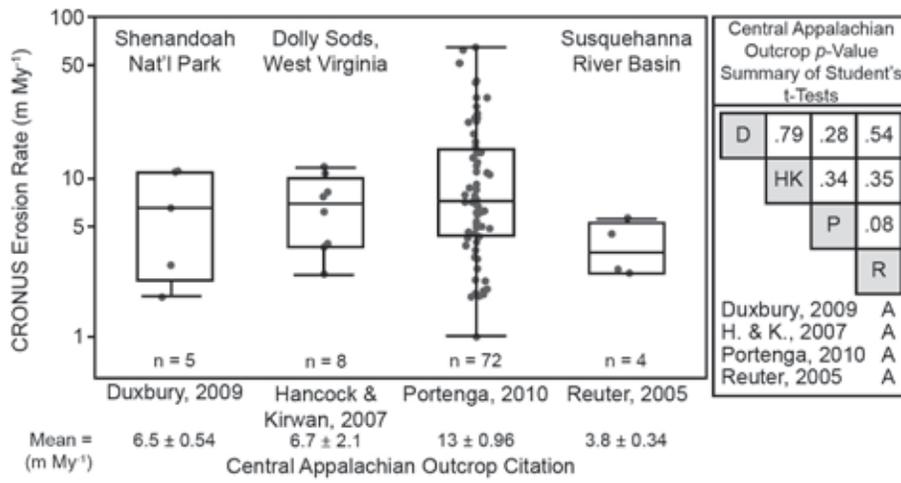
Figure 8.

Figure 9.

Tables

Table 1.
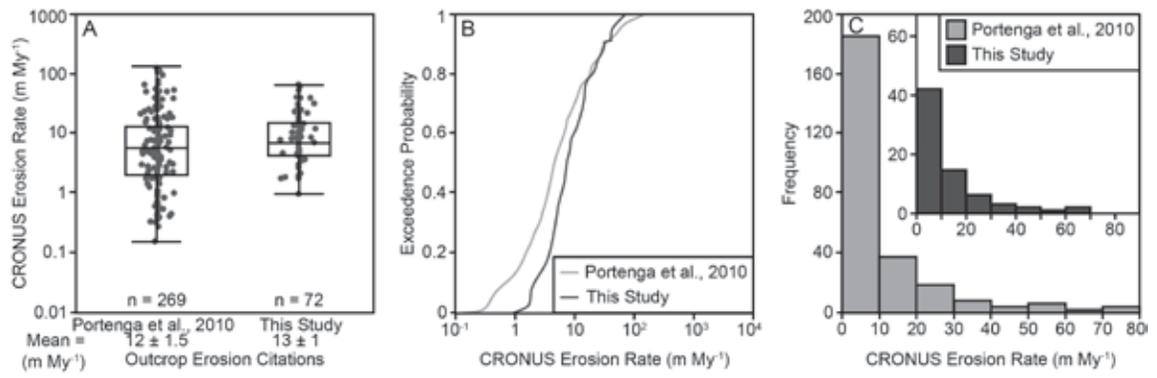
Sample ID	Location Name	Latitude (degrees)	Longitude (degrees)	LLNL Be Identifier*
	Table 1: Sample Locations			
EPP01	Loudoun Heights, Harpers Ferry National Historic Park, VA	-77.7364	39.31041	BE28738
EPP02		-77.73652	39.31003	BE28739
EPP04	White Rocks, Cunningham Falls State Park, MD	-77.45293	39.56918	BE28740
EPP05		-77.45421	39.5681	BE28741
EPP06		-77.45427	39.56794	BE28742
EPP07		-77.45306	39.56895	BE28743
EPP08	Chimney Rock, Catoctin Mountain Park, MD	-77.43211	39.62942	BE28744
EPP09		-77.43271	39.62911	BE28745
EPP10	Wolf Rocks, Catoctin Mountain Park, MD	-77.43777	39.6334	BE28746
EPP11		-77.43788	39.63204	BE28747
EPP12	Maryland Heights, Harpers Ferry National Historical Park, MD	-77.7163	39.34103	BE28749
EPP13		-77.71601	39.34185	BE28750
EPP14	Raven Rock, South Mountain State Park, MD	-77.5241	39.67564	BE28751
EPP15		-77.5235	39.67712	BE28752
EPP16		-77.52499	39.67506	BE28753
EPP17	Buzzards Rock, George Washington National Forest, VA	-78.30852	38.92642	BE28754
EPP18		-78.30779	38.93028	BE28755
EPP19		-78.30289	38.94021	BE28756
EPP20		-78.29897	38.94517	BE28757
EPP21	Kennedy Peak, George Washington National Forest, VA	-78.48763	38.74201	BE28758
EPP22		-78.48698	38.74238	BE28760
EPP23	Duncan Knob, George Washington National Forest, VA	-78.55121	38.6981	BE28761
EPP24		-78.55103	38.6983	BE28762
EPP26	Cub Run, George Washington National Forest, VA	-78.70035	38.47895	BE28763
EPP27		-78.69967	38.48009	BE28764
EPP28	Sawmill Run Rd., Monongahela National Forest, WV	-79.56098	38.62863	BE28765
EPP29		-79.56072	38.62846	BE28766
EPP30		-79.56027	38.62862	BE28767
EPP31	Reddish Knob, George Washington National Forest, VA/WV	-79.24008	38.46995	BE28768
EPP32		-79.24036	38.46958	BE28769
EPP33	Hone Quarry Ridge, George Washington National Forest, VA	-79.19068	38.46645	BE28771
EPP34		-79.18474	38.46374	BE28772
EPP35	Big Schloss Mountain, George Washington National Forest, VA/WV	-78.68158	38.92576	BE28773
EPP36		-78.67994	38.92479	BE28774
EPP37	Devil's Hole Mountain, George Washington National Forest, VA/WV	-78.71337	38.90656	BE28775
EPP38		-78.71312	38.90709	BE28776
EPP39	Crannys Crow, Lost River State Park, WV	-78.90575	38.90126	BE28777
EPP40		-78.90549	38.9017	BE28778
EPP41	Miller Rock, Lost River State Park, WV	-78.89387	38.91569	BE28779
EPP42		-78.89413	38.91539	BE28780
EPP43	Seneca Rocks, Monongahela National Forest, WV	-79.3656	38.83581	BE28782
EPP44		-79.36555	38.83591	BE28783
EPP45	Chimney Rocks, Monongahela National Forest, WV	-79.25528	38.97292	BE28784
EPP46		-79.25539	38.97279	BE28785

EPP47		-79.25916	38.96392	BE28786
EPP48		-79.2593	38.96333	BE28787
EPS01	Rim Trail, Tuscarora State Forest, PA	-77.64166	40.23536	BE28788
EPS02		-77.64129	40.2352	BE28789
EPS03	Round Top Trail, Tuscarora State Forest, PA	-77.65526	40.25835	BE28790
EPS04		-77.65564	40.25779	BE28791
EPS05	Pine Ridge Trail, Tuscarora State Forest, PA	-77.6777	40.43601	BE28793
EPS06		-77.67752	40.43613	BE28794
EPS07	Prayer Rock, PA	-77.75675	40.54408	BE28795
EPS08		-77.75827	40.54309	BE28796
EPS09	Spring Creek, Rothrock State Forest, PA	-77.75514	40.76299	BE28797
EPS10		-77.75477	40.76294	BE28798
EPS11	Turtle Rocks, Moshannon State Forest, PA	-78.12403	40.9237	BE28799
EPS12		-78.12404	40.92369	BE28800
EPS13	Panther Rocks, Moshannon State Forest, PA	-78.49061	41.14231	BE28801
EPS14		-78.49048	41.14241	BE28802
EPS15		-78.49029	41.14255	BE28804
EPS16	Hawk Rock, Duncannon, PA	-77.05495	40.37026	BE28805
EPS17		-77.04499	40.37362	BE28806
EPS18		-77.0411	40.37573	BE28807
EPS19	Michaux Oaks Rd., Michaux State Forest, PA	-77.34778	40.04329	BE28808
EPS20		-77.34759	40.04349	BE28809
EPS21	Pole Steeple, Michaux State Forest, PA	-77.26745	40.03235	BE28810
EPS22		-77.26721	40.03252	BE28811
EPS23		-77.2673	40.03252	BE28812
EPS24	Rock Ridge, Rocks State Park, MD	-76.41276	39.63543	BE28813
EPS25		-76.4126	39.63556	BE28815
EPS26		-76.41283	39.63546	BE28816

*Identification reference number for each sample within the sample database at the Center for Mass Spectrometry at Lawrence Livermore National Laboratory, Livermore, CA.

Table 2.

			Table 2: Sample Parameter Data				
Sample ID	Thickness (cm)	Sample Geometry	Elevation (m asl)	Relief (m)*	MAP (mm yr^{-1})	MAT (°C)	Seismicity†	Climate Zone§
EPP01	3	Main Ridge	170	376	1028	11	0.23270	Dfa
EPP02	2	Main Ridge	170	376	1028	11	0.23270	Dfa
EPP04	5	Near-Cliff	468	441	1104	10	0.25229	Dfa
EPP05	5	Main Ridge	468	439	1104	10	0.25229	Dfa
EPP06	7	Main Ridge	468	439	1104	10	0.25229	Dfa
EPP07	6	Near-Cliff	468	441	1104	10	0.25229	Dfa
EPP08	2	Main Ridge	382	452	1081	10	0.25229	Dfa
EPP09	2	Main Ridge	382	452	1081	10	0.25229	Dfa
EPP10	5	Main Ridge	439	442	1101	10	0.25229	Dfa
EPP11	3	Main Ridge	403	442	1060	10	0.25229	Dfa
EPP12	3	Main Ridge	446	376	1024	11	0.23270	Dfa
EPP13	2	Main Ridge	433	376	1037	10	0.23270	Dfa
EPP14	4	Near-Cliff	539	415	1130	9	0.23270	Dfa
EPP15	4	Main Ridge	539	415	1130	9	0.23270	Dfa
EPP16	4	Main Ridge	539	415	1130	9	0.23270	Dfa
EPP17	6	Main Ridge	246	549	999	10	0.24280	Cfa
EPP18	3	Main Ridge	456	550	974	11	0.24280	Cfa
EPP19	6	Main Ridge	221	550	980	10	0.24280	Cfa
EPP20	2	Spur Ridge	199	550	956	11	0.24280	Cfa
EPP21	2	Main Ridge	435	468	1052	9	0.24280	Cfa
EPP22	3	Main Ridge	435	468	1052	9	0.24280	Cfa
EPP23	7	Main Ridge	648	586	1077	9	0.24280	Dfa
EPP24	6	Main Ridge	648	586	1077	9	0.24280	Dfa
EPP26	3	Main Ridge	707	598	1098	9	0.22669	Cfa
EPP27	5	Main Ridge	763	598	1112	9	0.22669	Cfa
EPP28	2	Spur Ridge	929	685	1096	9	0.21203	Dfb
EPP29	2	Spur Ridge	929	685	1096	9	0.21203	Dfb
EPP30	2	Spur Ridge	929	685	1096	9	0.21203	Dfb
EPP31	2	Main Ridge	1127	657	1235	7	0.22669	Dfa
EPP32	4	Main Ridge	1127	657	1235	7	0.22669	Dfa
EPP33	2	Spur Ridge	846	682	1035	9	0.22669	Dfa
EPP34	3	Spur Ridge	846	717	1035	9	0.22669	Dfa
EPP35	2	Main Ridge	653	643	1066	8	0.22433	Dfa
EPP36	4	Main Ridge	813	643	1011	9	0.24280	Dfa
EPP37	2	Main Ridge	734	616	1011	9	0.22433	Dfa
EPP38	4	Main Ridge	734	616	1011	9	0.22433	Dfa
EPP39	3	Near-Cliff	751	434	1077	8	0.22433	Dfa
EPP40	5	Near-Cliff	751	434	1077	8	0.22433	Dfa
EPP41	8	Main Ridge	835	467	1116	8	0.22433	Dfa
EPP42	2	Main Ridge	835	467	1116	8	0.22433	Dfa
EPP43	3	Near-Cliff	564	667	1011	10	0.21203	Dfb
EPP44	4	Near-Cliff	564	667	1011	10	0.21203	Dfb
EPP45	3	Near-Cliff	816	824	1155	8	0.22433	Dfb
EPP46	4	Near-Cliff	816	824	1155	8	0.22433	Dfb
EPP47	1	Near-Cliff	719	665	1134	8	0.22433	Dfb
EPP48	1	Near-Cliff	719	665	1134	8	0.22433	Dfb
EPS01	6	Spur Ridge	552	435	1099	8	0.25331	Dfa

EPS02	4	Spur Ridge	552	435	1099	8	0.25331	Dfa
EPS03	3	Main Ridge	486	485	1047	9	0.25331	Dfa
EPS04	1	Main Ridge	565	485	1082	8	0.25331	Dfa
EPS05	1	Main Ridge	518	449	1055	8	0.25216	Dfa
EPS06	1	Main Ridge	518	449	1055	8	0.25216	Dfa
EPS07	3	Main Ridge	462	430	1041	8	0.25216	Dfa
EPS08	2	Main Ridge	462	430	1041	8	0.25216	Dfa
EPS09	7	Spur Ridge	390	424	1024	8	0.25216	Dfa
EPS10	2	Spur Ridge	390	424	1024	8	0.25216	Dfa
EPS11	2	Main Ridge	562	251	1023	7	0.19364	Dfb
EPS12	4	Main Ridge	562	251	1023	7	0.19364	Dfb
EPS13	2	Main Ridge	650	186	1118	6	0.19364	Dfb
EPS14	2	Main Ridge	650	186	1118	6	0.19364	Dfb
EPS15	1	Main Ridge	650	186	1118	6	0.19364	Dfb
EPS16	2	Main Ridge	233	291	1066	10	0.24958	Dfa
EPS17	7	Main Ridge	215	291	1060	10	0.24958	Dfa
EPS18	3	Near-Cliff	228	291	1048	10	0.24958	Dfa
EPS19	2	Main Ridge	429	402	1098	9	0.24935	Dfa
EPS20	4	Main Ridge	429	402	1098	9	0.24935	Dfa
EPS21	4	Near-Cliff	238	263	1083	10	0.24935	Dfa
EPS22	5	Main Ridge	238	263	1083	10	0.24935	Dfa
EPS23	5	Near-Cliff	238	263	1083	10	0.24935	Dfa
EPS24	4	Main Ridge	114	138	1112	11	0.29851	Cfa
EPS25	2	Main Ridge	114	138	1112	11	0.29851	Cfa
EPS26	5	Near-Cliff	114	138	1112	11	0.29851	Cfa

*Relief is measured in change in elevation, given in meters, within a 5 km radius of the sampled outcrop

†Seismicity is a proxy for Seismic Hazard (Giardini et al., 1999)

§Climate zone as designated by the Köppen-Geiger climate classification system (Peel et al., 2005). Cfa = Temperate with hot summers without a dry season. Dfa = Cold with hot summers without a dry season. Dfb = Cold with warm summers without a dry season.

Table 3.

	Table 3: Erosion Rate Data			
Sample ID	^{10}Be (atom g^{-1})*	^{10}Be Error (atom g^{-1})*	Erosion Rate (m My^{-1})†	Erosion Rate Error (m My^{-1})†
EPP01	7.62E+05	1.04E+04	4.30	0.36
EPP02	5.82E+05	1.09E+04	5.96	0.48
EPP04	1.24E+06	1.65E+04	3.11	0.27
EPP05	6.78E+05	9.18E+03	6.29	0.5
EPP06	9.76E+05	1.48E+04	4.06	0.35
EPP07	1.39E+06	1.96E+04	2.70	0.24
EPP08	1.02E+06	1.38E+04	3.71	0.32
EPP09	1.81E+06	2.41E+04	1.86	0.18
EPP10	9.50E+05	1.32E+04	4.16	0.35
EPP11	6.87E+05	9.57E+03	5.97	0.48
EPP12	3.62E+05	5.13E+03	12.65	0.94
EPP13	9.95E+05	1.34E+04	4.00	0.34
EPP14	3.23E+06	3.61E+04	1.00	0.11
EPP15	1.72E+06	1.93E+04	2.25	0.21
EPP16	5.97E+05	1.05E+04	7.77	0.62
EPP17	7.19E+05	8.34E+03	4.79	0.39
EPP18	1.89E+06	1.60E+04	1.84	0.18
EPP19	5.37E+05	6.76E+03	6.59	0.52
EPP20	6.69E+04	2.37E+03	66.10	4.81
EPP21	8.44E+05	9.03E+03	4.80	0.4
EPP22	5.00E+05	5.41E+03	8.66	0.66
EPP23	9.23E+05	1.43E+04	4.95	0.41
EPP24	8.95E+05	1.52E+04	5.17	0.43
EPP26	2.23E+05	3.41E+03	25.52	1.83
EPP27	6.36E+05	7.88E+03	8.34	0.66
EPP28	1.29E+05	2.25E+03	53.03	3.77
EPP29	1.65E+05	3.03E+03	41.18	2.97
EPP30	1.09E+05	2.53E+03	63.21	4.57
EPP31	2.37E+05	4.00E+03	32.00	2.37
EPP32	1.89E+05	2.87E+03	39.94	2.9
EPP33	2.64E+05	4.29E+03	23.58	1.73
EPP34	1.95E+05	3.45E+03	32.24	2.33
EPP35	7.00E+05	9.99E+03	7.10	0.57
EPP36	6.20E+05	8.69E+03	9.06	0.71
EPP37	3.38E+05	5.66E+03	16.83	1.26
EPP38	3.94E+05	5.59E+03	14.06	1.06
EPP39	9.65E+05	1.34E+04*	5.30	0.44
EPP40	7.44E+05	1.04E+04	7.00	0.56
EPP41	8.89E+05	1.49E+04	5.97	0.49
EPP42	7.76E+05	1.68E+04	7.29	0.6
EPP43§	9.36E+04	1.72E+03	40.04	2.58
EPP44§	1.83E+05	2.75E+03	18.94	1.27
EPP45	2.53E+05	3.19E+03	24.16	1.75
EPP46	3.78E+05	6.12E+03	15.60	1.18
EPP47	5.09E+05	1.05E+04	10.73	0.84
EPP48	8.87E+05	1.03E+04	5.78	0.47
EPS01	2.31E+05	3.46E+03	22.19	1.59

EPS02	4.11E+05	5.97E+03	11.99	0.9
EPS03	5.33E+05	7.67E+03	8.60	0.67
EPS04	4.74E+05	6.84E+03	10.58	0.81
EPS05	6.55E+05	9.35E+03	7.12	0.57
EPS06	6.92E+05	1.69E+04	6.68	0.56
EPS07	4.27E+05	7.29E+03	10.83	0.83
EPS08	5.70E+05	1.24E+04	7.90	0.64
EPS09	2.00E+05	2.91E+03	23.10	1.62
EPS10	3.24E+05	4.46E+03	14.09	1.03
EPS11	2.18E+06	2.30E+04	1.79	0.17
EPS12	9.82E+05	1.05E+04	4.57	0.38
EPS13	2.11E+06	2.24E+04	2.03	0.19
EPS14	2.35E+06	3.24E+04	1.78	0.17
EPS15	2.21E+06	2.99E+04	1.94	0.19
EPS16	2.85E+05	4.04E+03	14.32	1.04
EPS17	1.48E+05	2.20E+03	28.13	1.92
EPS18	2.77E+05	3.95E+03	14.62	1.06
EPS19	8.07E+05	1.12E+04	5.14	0.42
EPS20	9.00E+05	1.33E+04	4.46	0.38
EPS21	2.96E+05	4.14E+03	13.52	0.98
EPS22	1.36E+06	1.66E+04	2.25	0.21
EPS23	2.64E+05	3.70E+03	15.27	1.1
EPS24	9.50E+05	1.05E+04	3.12	0.27
EPS25	8.72E+05	9.60E+03	3.52	0.3
EPS26	2.97E+05	4.14E+03	12.09	0.88

*Normalized using the ICN standard solution, 07KNSTD (Nishiizumi et al., 2007)

†Erosion rates estimated using the CRONUS on-line cosmogenic calculator (Balco et al., 2008)

§EPP43 and EPP44 were collected from a site with horizon blocking of incoming cosmic-rays. Erosion rates in table are corrected for this shielding (Dunne, 1999). Pre-correction erosion rates are 58.43 ± 4.00 and 28.43 ± 2.00 m My^{-1}, respectively.

Table 4.

Table 4. Principle Component Analysis Results						
	Eigenvectors§					
Parameter	pc1	pc2	pc3	pc4	pc5	pc6
Latitude (°N)	-0.296173	-0.623759	-0.1526423	0.3080451	0.4788233	0.4192172
Elevation (masl)	0.58071	-0.035209	0.0626853	0.1124461	-0.3652329	0.7152395
Relief (m)*	0.4385142	0.4428472	-0.0709503	0.4888088	0.5981095	-0.0994424
Mean Annual Precipitation (mm yr^{-1})	0.2439762	-0.2580719	0.8300836	-0.2743057	0.3222362	-0.0758683
Mean Annual Temperature (°C)	-0.375257	0.5512475	0.0804003	-0.4072187	0.2993723	0.541658
Seismicity†	-0.4271072	0.2075972	0.5217605	0.64223	-0.2934932	0.0604251
Percent	46	28	16	7	2	1

*Relief is measured in change in elevation, given in meters, within a 5 km radius of the sampled outcrop

†Seismicity is a proxy for Seismic Hazard (Giardini et al., 1999)

§Parameters with absolute values of Eigenvectors ≥0.4 are correlated. Correlations observed in pc4-pc6 are only of residual data not utilized in the creation of pc1-pc3. pc1 is renamed "Seismic-Physiography;" pc2 is renamed "Latitude-Temperature;" pc3 is renamed "Precipitation." Values determined for these new variables are found in Table 5.

Table 5.

	Table 5: Statistical Data				
Sample ID	Average Location Erosion Rate (m My^{-1})*	RSD†	Seismic-Physiography§	Latitude-Temperature§	Precipitation§
EPP01	5.13	0.23	1.04225	-0.77265	-1.07039
EPP02			1.04255	-0.77257	-1.07055
EPP04	4.04	0.40	0.34114	0.85821	-0.11874
EPP05			0.33655	0.85930	-0.12519
EPP06			0.33668	0.85933	-0.12525
EPP07			0.34132	0.85826	-0.11883
EPP08	2.79	0.47	0.44980	0.45087	0.01941
EPP09			0.45005	0.45093	0.01929
EPP10	5.07	0.25	0.31140	0.78950	-0.08801
EPP11			0.52180	0.12417	0.11130
EPP12	8.33	0.73	0.99678	-0.77016	-0.90698
EPP13			0.49445	-0.62971	-0.65730
EPP14	3.67	0.98	-0.58501	0.73969	-0.52491
EPP15			-0.58620	0.73940	-0.52432
EPP16			-0.58454	0.73981	-0.52514
EPP17	19.83	1.56	1.61557	-1.03347	0.11563
EPP18			2.14748	-1.31556	0.02714
EPP19			1.70542	-1.34726	0.21281
EPP20			2.26299	-1.67408	0.00711
EPP21	6.73	0.41	0.81254	-0.12793	-0.06845
EPP22			0.81224	-0.12801	-0.06830
EPP23	5.06	0.03	1.01385	0.28521	0.23750
EPP24			1.01369	0.28517	0.23758
EPP26	16.93	0.72	0.95275	0.28021	-0.38227
EPP27			0.87391	0.51875	-0.42945
EPP28	52.47	0.21	0.90388	-0.12007	-0.38772
EPP29			0.90402	-0.12003	-0.38779
EPP30			0.90389	-0.12006	-0.38772
EPP31	35.97	0.16	-0.50054	2.43102	-0.08633
EPP32			-0.50024	2.43109	-0.08647
EPP33	27.91	0.22	1.48483	-0.72573	0.26432
EPP34			1.58246	-0.74049	0.36860
EPP35	8.08	0.17	0.42130	-0.47546	0.32769
EPP36			1.29094	-0.79720	0.92597
EPP37	15.45	0.13	1.06371	-1.25478	0.24360
EPP38			1.06328	-1.25488	0.24381
EPP39	6.15	0.20	-0.19816	-0.17753	-0.32317
EPP40			-0.19852	-0.17761	-0.32299
EPP41	6.63	0.14	-0.32622	0.45142	-0.38475
EPP42			-0.32598	0.45148	-0.38487
EPP43	29.49	0.51	1.60379	-1.54519	-0.40634
EPP44			1.60371	-1.54521	-0.40630
EPP45	19.88	0.30	0.41010	0.90331	0.49744
EPP46			0.41021	0.90334	0.49739
EPP47	8.26	0.42	0.10252	0.61299	0.08057
EPP48			0.10300	0.61311	0.08034
EPS01	17.09	0.42	-1.06655	0.56881	0.87330

EPS02			-1.06642	0.56884	0.87323
EPS03	9.59	0.15	-0.24132	-0.24308	0.95261
EPS04			-0.86557	0.27390	1.12875
EPS05	6.90	0.05	-0.97706	-0.21803	1.17721
EPS06			-0.97715	-0.21805	1.17726
EPS07	9.37	0.22	-1.03790	-0.46977	1.21060
EPS08			-1.03710	-0.46958	1.21020
EPS09	18.60	0.34	-1.13518	-0.80123	1.33548
EPS10			-1.13514	-0.80122	1.33546
EPS11	3.18	0.62	-2.76586	-2.22535	-0.47501
EPS12			-2.76585	-2.22535	-0.47501
EPS13	1.92	0.07	-4.04357	-0.76055	-0.72051
EPS14			-4.04365	-0.76057	-0.72047
EPS15			-4.04376	-0.76060	-0.72041
EPS16	19.02	0.41	-0.51515	0.02971	-0.24355
EPS17			-0.48534	-0.07170	-0.21897
EPS18			-0.42925	-0.26074	-0.14854
EPS19	4.80	0.10	-0.57860	0.53967	0.20126
EPS20			-0.57876	0.53964	0.20134
EPS21	10.35	0.68	-0.40715	0.37633	-0.55644
EPS22			-0.40729	0.37630	-0.55637
EPS23			-0.40729	0.37630	-0.55637
EPS24	6.24	0.81	0.36319	2.20845	-0.14470
EPS25			0.36309	2.20843	-0.14465
EPS26			0.36317	2.20845	-0.14469

*Values are for each sampling location, listed in Table 1.

†Relative standard deviation

§Values for new variables derived from Principle Component Analysis

CHAPTER 4: CONCLUSIONS

Summary of Findings from Global Data Compilations

Compilation and recalculation of 418 bedrock outcrop erosion rates and 1110 drainage basin erosion rates inferred from concentrations of cosmogenic [10]Be produced *in situ* in quartz provides the first true comparison of erosion rate studies and confirms the notion that outcrops erode more slowly than their surrounding landscape. Average global erosion rates of drainage basins (209 ± 33 m My^{-1}) are more than twice as rapid as average erosion rates of outcrops (12 ± 1.3 m My^{-1}); median erosion rates are similarly separated by two orders of magnitude. Locations where both drainage basin and outcrop erosion rates have been estimated show that landscapes are either wearing down evenly or that relief is increasing due to higher drainage basin erosion rates.

Though combinations of latitude, elevation, relief, mean annual temperature, mean annual precipitation, seismicity, basin slope, basin area, and percent vegetation account for 33% and 56% of erosion rate variability for outcrops and drainage basins, respectively, a large portion of variability is controlled by unknown parameters and variables. Basin slope is the only parameter that repeatedly shows significant influence over erosion rates and is only applicable to drainage basin erosion. Other parameters show significant influence on erosion rates for drainage basins and outcrops in various climate zones, lithologies, and seismic zones, but no parameter is as consistent in asserting is influence over erosion rates as basin slope.

87

This compilation sets the groundwork for future study as large geographic regions exist where few to no bedrock outcrop or drainage basins have been analyzed for erosion. Details missing from individual studies such as outcrop fracture density and the specific lithology of outcrops make it difficult to generalize erosion rates for unsampled regions. As future work is carried out using cosmogenic [10]Be to study erosion rates, importance must be placed on sample-site detail. Once these sampling gaps have been filled and sufficient detail provided for study-sites, erosion rate prediction will be more feasible.

Summary of Findings from the Central Appalachian Mountains

Erosion rates of bedrock outcrops along ridgelines in the central Appalachian Mountains are now numerous enough that inferences about their relationship to erosion rates of the drainage basins they surround can be made. Slowly eroding outcrops of the Potomac (15 ± 1 m My^{-1}) and Susquehanna (9.7 ± 0.7 m My^{-1}) River Basins are similar throughout the region (average $= 13 \pm 1$ m My^{-1}). New data presented here are similar to outcrop erosion rates inferred from previous studies in the immediate region. Relief is being created in the Susquehanna River Basin as outcrops erode more slowly than drainage basins. In the Potomac River Basin outcrops and drainage basins are eroding similarly, indicating the landscape is lowering at a continuous rate and landforms are being preserved.

Erosion rates within physiographic regions show cross-basin agreement and outcrops at different positions on the landscape also show similar erosional patterns in both basins, though variables influencing outcrop erosion rates have not been identified.

Latitude, elevation, relief, mean annual temperature, mean annual precipitation, and seismicity only account for 24% of variability of outcrop erosion rates in the central Appalachian Mountains.

The range of modeled ^{10}Be erosion rates for the Potomac and Susquehanna River Basins are consistent with longer-term denudation rates determined by apatite fission track thermochronology and (U-Th)/He dating method for the study area. Integration of landscape evolution rates over millennial and longer-term timescales for the central Appalachian Mountains results in a relative consistent slow lowering of the landscape on the order of ten to tens of meters per million years.

COMPREHENSIVE BIBLIOGRAPHY

Abbühl, L. M., Norton, K. P., Schlunegger, F., Kracht, O., Aldahan, A., and Possnert, G., 2010, El Niño forcing on ^{10}Be-based surface denudation rates in the northwestern Peruvian Andes?: Geomorphology, v. 123, p. 257-268.

Albrecht, A., Herzog, G. F., Klein, J., Dezfouly-Arjomandy, B., and Goff, F., 1993, Quaternary erosion and cosmic-ray-exposure history derived from ^{10}Be and ^{26}Al produced in situ; an example from Pajarito Plateau, Valles Caldera region: Geology, v. 21, no. 6, p. 551-554.

Balco, G., Stone, J. O., Lifton, N. A., and Dunai, T. J., 2008, A complete and easily accessible means of calculating surface exposure ages or erosion rates from ^{10}Be and ^{26}Al measurements: Quaternary Geochronology, v. 3, p. 174-195.

Belmont, P., Pazzaglia, F. J., and Gosse, J. C., 2007, Cosmogenic ^{10}Be as a tracer for hillslope and channel sediment dynamics in the Clearwater River, western Washington State: Earth and Planetary Science Letters.

Belton, D. X., Brown, R. W., Kohn, B. P., Fink, D., and Farley, K. A., 2004, Quantitative resolution of the debate over antiquity of the central Australian landscape: implications for the tectonic and geomorphic stability of cratonic interiors: Earth and Planetary Science Letters, v. 219, no. 1-2, p. 21-34.

Bierman, P. R., 1994, Using in situ produced cosmogenic isotopes to estimate rates of landscape evolution; a review from the geomorphic perspective: Journal of Geophysical Research, B, Solid Earth and Planets, v. 99, no. 7, p. 13885-13896.

Bierman, P. R., Albrecht, A., Bothner, M., Brown, E., Bullen, T., Gray, L., and Turpin, L., 1998, Weathering, erosion and sedimentation, *in* Kendall, C., and McDonnell, J. J., eds., Isotope Tracers in Catchment Hydrology, Elsevier, p. 647-678.

Bierman, P. R., and Caffee, M. W., 2001, Slow rates of rock surface erosion and sediment production across the Namib Desert and escarpment, Southern Africa: American Journal of Science, v. 301, no. 4-5, p. 326-358.

Bierman, P. R., and Caffee, M., 2002, Cosmogenic exposure and erosion history of ancient Australian bedrock landforms: Geological Society of America Bulletin, v. 114, no. 7, p. 787-803.

Bierman, P. R., and Steig, E., 1996, Estimating rates of denudation and sediment transport using cosmogenic isotope abundances in sediment: Earth Surface Processes and Landforms, v. 21, p. 125-139.

Bierman, P. R., Clapp, E. M., Nichols, K. K., Gillespie, A. R., and Caffee, M., 2001, Using cosmogenic nuclide measurements in sediments to understand background rates of erosion and sediment transport,, *in* Harmon, R. S., and Doe, W. M., eds., Landscape Erosion and Evolution Modelling: New York, Kluwer, p. 89-116.

Bierman, P. R., Nichols, K. K., Matmon, A., Enzel, Y., Larsen, J., and Finkel, R., 2007, 10-Be shows that Namibian drainage basins are slowly, steadily and uniformly eroding: Quaternary International v. 167–168 no. 3, p. 33.

Bierman, P. R., Reusser, L. J., Nichols, K. K., Matmon, A., and Rood, D., 2009, Where is the sediment coming from and where is it going - A 10Be examination of the northern Queensland escarpment, Australia, 2009 Portland GSA Annual Meeting: Portland, Or.

Bierman, P. R., Reuter, J. M., Pavich, M., Gellis, A. C., Caffee, M. W., and Larsen, J., 2005, Using cosmogenic nuclides to contrast rates of erosion and sediment yield in a semi-arid, arroyo-dominated landscape, Rio Puerco Basin, New Mexico: Earth Surface Processes and Landforms, v. 30, no. 8, p. 935-953.

Bierman, P., and Nichols, K., 2004, Rock to sediment - Slope to sea with 10-Be - Rates of landscape change: Annual review of Earth and Planetary Sciences, v. 32, p. 215-255.

Binnie, S. A., Phillips, W. M., Summerfield, M. A., and Fifield, L. K., 2006, Sediment mixing and basin-wide cosmogenic nuclide analysis in rapidly eroding mountainous environments: Quaternary Geochronology v. 1, p. 4-14.

Binnie, S. A., Phillips, W. M., Summerfield, M. A., Fifield, L. K., and Spotila, J. A., 2008, Patterns of denudation through time in the San Bernardino Mountains, California: Implications for early-stage orogenesis Earth and Planetary Science Letters, v. In Press.

Blackmer, G. C., Omar, G. I., and Gold, D. P., 1994, Post-Alleghanian unroofing history of the Appalachian Basin, Pennsylvania, from apatite fission track analysis and thermal models: Tectonics, v. 13, no. 5, p. 1259-1276.

Boettcher, S. S., and Milliken, K. L., 1994, Mesozoic-Cenozoic unroofing of the southern Appalachian Basin: apatite fission track evidence from Middle Pennsylvanian Sandstones: The Journal of Geology, v. 102, p. 655-663.

Braun, D. D., 1989, Glacial and Periglacial Erosion of the Appalachians: Geomorphology, v. 2, p. 233-256.

Brown, E. T., Bourles, D. L., Colin, F., Sanfo, Z., Raisbeck, G. M., and Yiou, F., 1994, The development of iron crust lateritic systems in Burkina Faso, West Africa examined with in-situ-produced cosmogenic nuclides: Earth and Planetary Science Letters, v. 124, p. 19-33.

Brown, E. T., Stallard, R. F., Larsen, M. C., Bourles, D. L., Raisbeck, G. M., and Yiou, F., 1998, Determination of predevelopment denudation rates of an agricultural watershed (Cayaguas River, Puerto Rico) using in-situ-produced ^{10}Be in river-borne quartz: Earth and Planetary Science Letters, v. 160, no. 3-4, p. 723-728.

Brown, E. T., Stallard, R. F., Larsen, M. C., Raisbeck, G. M., and Yiou, F., 1995, Denudation rates determined from the accumulation of in situ-produced ^{10}Be in the Luquillo Experimental Forest, Puerto Rico: Earth and Planetary Science Letters, v. 129, p. 193-202.

Cerling, T. E., 1990, Dating geomorphologic surfaces using cosmogenic (super 3) He: Quaternary Research (New York), v. 33, no. 2, p. 148-156.

Chappell, J., Zheng, H., and Fifield, K., 2006, Yangtse River sediments and erosion rates from source to sink traced with cosmogenic ^{10}Be: Sediments from major rivers: Palaeogeography, Palaeoclimatology, Palaeoecology, v. 241, no. 1, p. 79-94.

Clapp, E. M., Bierman, P. R., Nichols, K. K., Pavich, M., and Caffee, M., 2001, Rates of sediment supply to arroyos from upland erosion determined using in situ produced cosmogenic ^{10}Be and ^{26}Al: Quaternary Research (New York), v. 55, no. 2, p. 235-245.

Clapp, E. M., Bierman, P. R., Schick, A. P., Lekach, J., Enzel, Y., and Caffee, M., 2000, Sediment yield exceeds sediment production in arid region drainage basins: Geology, v. 28, no. 11, p. 995-998.

Clapp, E., Bierman, P. R., and Caffee, M., 2002, Using ^{10}Be and ^{26}Al to determine sediment generation rates and identify sediment source areas in an arid region drainage basin: Geomorphology, v. 45, no. 1,2, p. 89-104.

Cockburn, H. A. P., Brown, R. W., Summerfield, M. A., and Seidl, M. A., 2000, Quantifying passive margin denudation and landscape development using a combined fission-track thermochronology and cosmogenic isotope analysis approach: Earth and Planetary Science Letters, v. 179, no. 3-4, p. 429-435.

Cox, R., Bierman, P. R., Jungers, M., Rakotondrazafy, A. F. M., and Finkel, R. C., 2006, Just how fast does Madagascar erode? Evidence from ^{10}Be analysis of lavaka, slope, and river sediment: Geological Society of America *Abstracts with Programs*, v. 38, no. 7, p. 278.

Craig, H., and Poreda, R. J., 1986, Cosmogenic ^{3}He and model erosion rates in terrestrial rocks: AGU 1986 spring meeting Eos, Transactions, American Geophysical Union, v. 67, no. 16, p. 414.

Cyr, A. J., and granger, D. E., 2008, Dynamic equilibrium among erosion, river incision, and coastal uplift in the northern and central Apennines, Italy: Geology, v. 36, no. 2, p. 103-106.

Defries, R. S., Hansen, M. C., Townshend, J. R. G., Janetos, A. C., and Loveland, T. R., 2000, A new global 1-km dataset of percentage tree cover drived from remote sensing: Global Change Biology, v. 6, p. 247-254.

Delunel, R., Beek, P. A. v. d., Carcaillet, J., Bourlès, D. L., and Valla, P. G., 2010, Frost-cracking control on catchment denudation rates: Insights from in situ produced ^{10}Be concentrations in stream sediments (Ecrins–Pelvoux massif, French Western Alps): Earth and Planetary Science Letters, v. 293, p. 72-83.

DiBiase, R. A., Whipple, K. X., Heimsath, A. M., and Ouimet, W. B., 2009, Landscape form and millennial erosion rates in the San Gabriel Mountains, CA: Earth and Planetary Science Letters, v. 289, p. 134-144.

Dole, R. B., and Stabler, H., 1909, Denudation: USGS Water Supply Paper, v. 234, p. 78-93.

Dunai, T. J., 2001, Influence of secular variation of the geomagnetic field on production rates of in situ produced cosmogenic nuclides: Earth and Planetary Science Letters, v. 193, no. 1-2, p. 197-212.

Dunne, A., Elmore, D., and Muzikar, P., 1999, Scaling factors for the rates of production of cosmogenic nuclides for geometric shielding and attenuation at depth on sloped surfaces, *in* Harbor, J., ed., Cosmogenic isotopes in geomorphology Geomorphology 27, no. 1-2 (199902), Elsevier, Amsterdam, Netherlands, p. 3-11.

Duxbury, J., 2009, Erosion rates in and around Shenandoah National Park, VA, determined using analysis of cosmogenic 10Be: University of Vermont, 134 p.

Ehlers, T. A., and Farley, K. A., 2003, Apatite (U-Th)/He thermochronometry: methods and applications to problems in tectonic and surface processes: Earth and Planetary Science Letters, v. 206, p. 1-14.

Elmore, D., and Phillips, F., 1987, Accelerator mass spectrometry for measurement of long-lived radioisotopes: Science, v. 236, p. 543-550.

Faure, G., and Nishiizumi, K., 1994, Exposure dating of quartz sandstone in the Transantarctic Mountains by cosmogenic [10]Be and [26]Al, *in* Harte, B., ed., V. M. Goldschmidt Conference; extended abstracts Mineralogical Magazine 58A, no. A-K (199408), Mineralogical Society, London, United Kingdom, p. 268-269.

Ferrier, K. L., Kirchner, J. W., and Finkel, R. C., 2005, Erosion rates over millennial and decadal timescales at Caspar Creek and Redwood Creek, Northern California Coast Ranges: Earth Surface Processes and Landforms, v. 30, no. 8, p. 1025-1038.

Finnegan, N. J., Hallet, B., Montgomery, D. R., Zeitler, P., Stone, J., Anders, A. M., and Yuping, L., 2008, coupling of rock uplift and river incision in the Namche Barwa-Gyala peri massif, Tibet: 2007 GSA Denver Annual Meeting.

Giardini, D., Grunthal, G., Shedlock, K. M., and Zhang, P., 1999, The GSHAP Global Seismic Hazard Map: Annali Di Geofisica, v. 42, no. 6, p. 1225-1230.

Gosse, J. C., and Phillips, F. M., 2001, Terrestrial in situ cosmogenic nuclides: theory and application: Quaternary Science Reviews, v. 20, no. 14, p. 1475-1560.

Granger, D. E., and Riebe, C. S., 2007, Cosmogenic Nuclides in Weathering and Erosion, *in* Holland, H. D., and Turekian, K. K., eds., Treatise on Geochemistry: Oxford, Pergamon, p. 1-42.

Granger, D. E., Kirchner, J. W., and Finkel, R. C., 1997, Quaternary downcutting rate of the New River, Virginia, measured from differential decay of cosmogenic [26]Al and [10]Be in cave-deposited alluvium: Geology, v. 25, no. 2, p. 107-110.

Granger, D. E., Kirchner, J. W., and Finkel, R., 1996, Spatially averaged long-term erosion rates measured from in situ-produced cosmogenic nuclides in alluvial sediments: Journal of Geology, v. 104, no. 3, p. 249-257.

Granger, D. E., Riebe, C. S., Kirchner, J. W., and Finkel, R. C., 2001, Modulation of erosion on steep granitic slopes by boulder armoring, as revealed by cosmogenic [26]Al and [10]Be: Earth and Planetary Science Letters, v. 186, no. 2, p. 269-281.

Guralnik, B., Matmon, A., Avni, Y., and Fink, D., 2010, [10]Be exposure ages of ancient desert pavements reveal Quaternary evolution of the Dead Sea drainage basin and rift margin tilting: Earth and Planetary Science Letters, v. 290, p. 132-141.

Hack, J. T., 1975, Dynamic equilibrium and landscape evoluion, *in* Melhorn, W. N., and Flemal, R. C., eds., Theories of landform development: Binghamton, N.Y., SUNY Binghamton,, p. 87-102.

-, 1979, Rock control and tectonism, their importance in shaping the Appalachian highlands: U.S. Geological Survey professional paper, v. 1126-B, p. 17.

Hales, T. C., and Roering, J. J., 2007, Climatic controls on frost cracking and implications for the evolution of bedrock landscapes: Journal of Geophysical Research, v. 112.

Hancock, G., and Kirwan, M., 2007, Summit erosion rates deduced from [10]Be: Implications for relief production in the central Appalachians: Geology, v. 35, no. 1, p. 89-92.

Heimsath, A. M., Chappell, J., Dietrich, W. E., Nishiizumi, K., and Finkel, R. C., 2000, Soil production on a retreating escarpment in southeastern Australia: Geology, v. 28, no. 9, p. 787-790.
-, 2001, Late Quaternary erosion in southeastern Australia: a field example using cosmogenic nuclides: Quaternary International, v. 83-85, p. 169-185.

Heimsath, A. M., Dietrich, W. E., Nishiizumi, K., and Finkel, R. C., 1997, The soil production function and landscape equilibrium: Nature (London), v. 388, no. 6640, p. 358-361.

-, 1999, Cosmogenic nuclides, topography, and the spatial variation of soil depth: Geomorphology, v. 27, no. 1-2, p. 151-172.

-, 2001, Stochastic processes of soil production and transport; erosion rates, topographic variation and cosmogenic nuclides in the Oregon Coast Range: Earth Surface Processes and Landforms, v. 26, no. 5, p. 531-552.

Heimsath, A., Chappel, J., Finkel, R. C., Fifield, K., and Alimanovic, A., 2006, Escarpment Erosion and Landscape Evolution in Southeastern Australia: Special Papers-Geological Society of America, v. 398, p. 173.

Henck, A. C., 2010, Spatial and temporal patterns of erosion in Western China and Tibet: University of Washington, 158 p.

Hewawasam, T., von Blackenburg, F., Schaller, M., and Kubik, P., 2003, Increase of human over natural erosion rates in tropical highlands constrained by cosmogenic nuclides: Geology, v. 31, no. 7, p. 597-600.

Hijmans, R. J., Cameron, S. E., Parra, J. L., Jones, P. G., and Jarvis, A., 2005, Very High Resolution Interpolates Climate Surfaces for Global Land Areas: International Journal of Climatology, v. 25, p. 1965-1978.

Hooke, R. L., 1994, On the efficacy of humans as geomorphic agents: GSA Today, v. 4, no. 9, p. 217,224-225.

-, 2000, On the history of humans as geomorphic agents: Geology, v. 28, no. 9, p. 843-846.

Insel, N., Ehlers, T. A., Schaller, M., Barnes, J. B., Tawackoli, S., and Poulsen, C. J., 2010, Spatial and temporal variability in denudation across the Bolivian Andes from multiple geochronometers: 2010, v. 122, p. 65-77.

Ivy-Ochs, S., Kober, F., Alfimov, V., Kubik, P. W., and Synal, H.-A., 2007, Cosmogenic [10]Be, [21]Ne and [36]Cl in sanidine and quartz from Chilean ignimbrites: Nuclear Instruments and Methods in Physics Research B, v. 259, p. 588-594.

Jakica, S., Quigley, M. C., Sandiford, M., Clark, D., Fifield, K., and Alimanovic, A., 2010, Geomorphic and cosmogenic nuclide constraings on escarpment evolution in an intraplate setting, Darling Escarpment, Western Australia: Earth Surface Processes and Landforms.

Judson, S., 1968, Erosion of the land or what's happening to our continents: American Scientist, v. 56, p. 356-374.

Kirchner, J. W., Finkel, R. C., Riebe, C. S., Granger, D. E., Clayton, J. L., King, J. G., and Megahan, W. F., 2001, Mountain erosion over 10 yr, 10 k.y., and 10 m.y. time scales: Geology, v. 29, no. 7, p. 591-594.

Kober, F., Ivy-Ochs, S., Schlunegger, F., Baur, H., Kubik, P. W., and Wieler, R., 2007, Denudation rates and a topography-driven rainfall threshold in northern Chile: Multiple cosmogenic nuclide data and sediment yield budgets: Geomorphology, v. 83, p. 97-120.

Kober, F., Ivy-Ochs, S., Zeilinger, G., Schlunegger, F., Kubik, P. W., Baur, H., and Wieler, R., 2009, Complex multiple cosmogenic nuclide concentration and histories in the arid Rio Lluta catchment, northern Chile: Earth Surface Processes and Landforms, v. 34, p. 398-412.

Kohl, C. P., and Nishiizumi, K., 1992, Chemical isolation of quartz for measurement of *in-situ* –produced cosmogenic nuclides: Geochimica et Cosmochimica Acta, v. 56, p. 3583-3587.

Kurz, M. M., 1986, In situ production of terrestrial cosmogenic helium and some applications to geochronology: Geochimica et Cosmochimica Acta, v. 50, no. 12, p. 2855-2862.

Lal, D., 1988, In situ-produced cosmogenic isotopes in terrestrial rocks: Annual Reviews of Earth and Planetary Science, v. 16, p. 355-388.

Lal, D., 1991, Cosmic ray labeling of erosion surfaces; in situ nuclide production rates and erosion models: Earth and Planetary Science Letters, v. 104, no. 2-4, p. 424-439.

Lal, D., and Peters, B., 1967, Cosmic ray produced radioactivity on the earth, *in* Sitte, K., ed., Handbuch der Physik: New York, Springer-Verlag, p. 551-612.

Lal, D., Harris, N. B. W., Sharma, K. K., Gu, Z., Ding, L., Liu, T., Dong, W., Caffee, M. W., and Jull, A. J. T., 2003, Erosion history of the Tibetan Plateau since the last interglacial: constraints from the ¢rst studies of cosmogenic [10]Be from Tibetan bedrock: Earth and Planetary Science Letters, v. 217, p. 33-42.

Matmon, A. S., Bierman, P., Larsen, J., Southworth, S., Pavich, M., Finkel, R., and Caffee, M., 2003, Erosion of an ancient mountain range, the Great Smoky Mountains, North Carolina and Tennessee: American Journal of Science, v. 303, p. 817-855.

Matthias, G. F., 1967, Weathering rates of Portland arkose tombstones: Journal of Geological Education, v. 15, p. 140-144.

Monaghan, A. J., Bromwich, D. H., and Wang, S.-H., 2006, Recent trends in Antarctic snow accumulation from Polar MM5 simulations: Philosophical Transactions of the Royal Society London A, v. 364, p. 25.

Montgomery, D. R., and Brandon, M. T., 2002, Topographic controls on erosion rates in tectonically active mountain ranges: Earth and Planetary Science Letters, v. 201, no. 3-4, p. 481-489.

Morel, P., von Blackenburg, F., Schaller, M., Kubik, P. W., and Hinderer, M., 2003, Lithology, landscape dissection and glaciation controls on catchment erosion as determined by cosmogenic nuclides in river sediment (the Wutach Gorge, Black Forest): Terra Nova, v. 15, no. 6, p. 398-404.

Naeser, C. W., Naeser, N. D., and Southworth, C. S., 2005, Tracking Across the southern Appalachians *in* Blue Ridge Geology Geotraverse East of the Great Smoky Mountains National Park, Western North Carolina: Carolina Geological Society.

Naeser, C. W., Naeser, N. D., Kunk, M. J., Morgan Iii, B. A., Schultz, A. P., Southworth, C. S., and Weems, R. E., 2001, Paleozoic through Cenozoic uplift, erosion, stream capture, and deposition history in the Valley and Ridge, Blue Ridge, Piedmont,

and Coastal Plain provinces of Tennessee, North Carolina, Virginia, Maryland, and District of Columbia, *in* GSA Annual Meeting, November 5-8, 2001.

Naeser, N. D., Naeser, C. W., Southworth, C. S., Morgan Iii, B. A., and Schultz, A. P., 2004, Paleozoic to recent tectonic and denudation history of rocks in the Blue Ridge Province, central and southern Appalachians – Evidence from fission-track thermochronology, *in* Geological Society of America Abstracts with Programs, p. 114.

Nichols, K. K., Bierman, P. R., Eppes, M. C., Caffee, M., Finkel, R., and Larsen, J., 2005, Late Quaternary history of the Chemehuevi Mountain piedmont, Mojave Desert, deciphered using ^{10}Be and ^{26}Al: American Journal of Science, v. 305, no. 5, p. 345-368.

-, 2007, Timing of surficial process changes down a Mojave Desert piedmont: Quaternary Research, v. 68, no. 1, p. 151-161.

Nichols, K. K., Bierman, P. R., Foniri, W. R., Gillespie, A. R., Caffee, M., and Finkel, R., 2006, Dates and rates of arid region geomorphic processes: GSA Today, v. 16, no. 8, p. 4-11.

Nichols, K. K., Bierman, P. R., Hooke, R. L., Clapp, E., and Caffee, M., 2002, Quantifying sediment transport on desert piedmonts using ^{10}Be and ^{26}Al: Geomorphology, v. 45, no. 1,2, p. 89-104.

Nichols, K., Bierman, P., Finkel, R., and Larsen, J., 2005, Long-Term (10 to 20 kyr) Sediment Generation Rates for the Upper Rio Chagres Basin Based on Cosmogenic ^{10}Be, *in* Harmon, R. S., ed., The Rio Chagres: A Multidisciplinary Profile of a Tropical Watershed, Kluwer Academic Publishers.

Nishiizumi, K., Imamura, M., Caffee, M. W., Southon, J. R., Finkel, R. C., and McAninch, J., 2007, Absolute calibration of 10Be AMS standards: Nuclear Inst. and Methods in Physics Research, B, v. 258, no. 2, p. 403-413.

Nishiizumi, K., Klein, J., Middleton, R., and Craig, H., 1990, Cosmogenic ^{10}Be, ^{26}Al, and ^{3}He in olivine from Maui lavas: Earth and Planetary Science Letters, v. 98, no. 3-4, p. 263-265.

Nishiizumi, K., Kohl, C. P., Arnold, J. R., Klein, J., Fink, D., and Middleton, R., 1991, Cosmic ray produced ^{10}Be and ^{26}Al in Antarctic rocks; exposure and erosion history: Earth and Planetary Science Letters, v. 104, no. 2-4, p. 440-454.

Nishiizumi, K., Lal, D., Klein, J., Middleton, R., and Arnold, J. R., 1986, Production of [10]Be and [26]Al by cosmic rays in terrestrial quartz in situ and implications for erosion rates: Nature, v. 319, no. 6049, p. 134-136.

Norton, K. P., Blanckenburg, F. v., and Kubik, P. W., 2010, Cosmogenic nuclide-derived rates of diffusive and episodic erosion in the glacially sculpted upper Rhone Valley, Swiss Alps: Earth Surface Processes and Landforms, v. 35, p. 651-662.

Norton, K. P., Blanckenburg, F. v., Schlunegger, F., Schwab, M., and Kubik, P. W., 2008, Cosmogenic nuclide-based investigation of spatial erosion and hillslope channel coupling in the transient foreland of the Swiss Alps: Geomorphology, v. 95, p. 474-486.

Ouimet, W. B., Whipple, K. X., and Granger, D. E., 2009, Beyond threshold hillslopes: Channel adjustment to base-level fall in tectonically active mountain ranges: Geology, v. 37, no. 7, p. 579-582.

Palumbo, L., Hetzel, R., Tao, M., and Li, X., 2009, Topographic and lithologic control on catchment-wide denudation rates derived from cosmogenic [10]Be in two mountain ranges at the margin of NE Tibet: Geomorphology, v. 117, p. 130-142.

Pazzaglia, F. J., and Brandon, M. T., 1996, Macrogeomorphic evolution of the post-Triassic Appalachian mountians determined by deconvolution of the offshore basin sedimentary record: Basin Research, v. 8, no. 255-278.

Pazzaglia, F. J., and Gardner, T. W., 1994, Late Cenozoic flexural deformation of the middle U. S. Atlantic passive margin: Journal of Geophysical Research, B, Solid Earth and Planets, v. 99, no. 6, p. 12,143-12,157.

Pazzaglia, F. J., Braun, D. D., Pavich, M., Bierman, P., Potter Jr, N., Merritts, D., Walter, R., and Germanoski, D., 2006, Rivers, glaciers, landscape evolution, and active tectonics of the central Appalachians, Pennsylvania and Maryland, *in* Pazzaglia, F. J., ed., Excursions in Geology and History: Field Trips in the Middle Atlantic States: Geological Society of America Field Guide 8: Denver, GSA, p. 169-197.

Peel, M. C., Finlayson, B. L., and McMahon, T. A., 2007, Updated world map of the Köppen-Geiger climate classification: Hydrology and Earth System Sciences, v. 11, p. 1633-1644.

Perg, L., Anderson, R., and Finkel, R., 2003, Use of cosmogenic radionuclides as a sediment tracer in the Santa Cruz littoral cell, California, USA: Geology, v. 31, p. 299-302.

Placzek, C. J., Matmon, A., Granger, D. E., Quade, J., and Niedermann, S., 2010, Evidence for active landscape evolution in the hyperarid Atacama from multiple terrestrial cosmogenic nuclides: Earth and Planetary Science Letters, v. 295, p. 12-20.

Poag, C. W., and Sevon, W. D., 1989, A record of Appalachian denudation in postrift Mesozoic and Cenozoic sedimentary deposits of the U.S. middle Atlantic continental margin: Geomorphology, v. 2, p. 119-157.

Portenga, E. W., Bierman, P. R., Trodick, C. D. J., and Rood, D. H., 2010, Low rates of bedrock outcrop erosion in the central Appalachian Mountains inferred from *In Situ* [10]Be concentrations, *in* 2010 GSA Denver Annual Meeting, Denver, Colorado.

Quigley, M., Sandiford, M., Fifield, K., and Alimanovic, A., 2007a, Bedrock erosion and relief production in the northern Flinders Ranges, Australia: Earth Surface Processes and Landforms, v. 32, no. 6, p. 929.

Quigley, M., Sandiford, M., Fifield, L. K., and Alimanovic, A., 2007b, Landscape responses to intraplate tectonism: Quantitative constraints from [10]Be nuclide abundances: Earth and Planetary Science Letters, v. 261, no. 1-2, p. 120-133.

Rahn, P. H., 1971, The Weathering of tombstones and its relationship to the topography of New England: Journal of Geologic Education, v. 19, p. 112-118.

Reed, J. S., Spotila, J. A., Eriksson, K. A., and Bodnar, R. J., 2005, Burial and exhumation history of Pennsylvanian strata, central Appalachian basin: an integrated study: Basin Research, v. 17, p. 259-268.

Reiners, P. W., and Brandon, M. T., 2006, Using Thermochronology to Understand Orogenic Erosion: Annu. Rev. Earth Planet. Sci, v. 34, p. 419-66.

Reinhardt, L. J., Bishop, P., Hoey, T. B., Dempster, T. J., and Sanderson, D. C. W., 2007, Quantification of the transient response to base-level fall in a small mountain catchment: Sierra Nevada, southern Spain Journal of Geophysical Research, v. 112, no. F03S05, p. 20.

Reuter, J. M., 2005, Erosion rates and patterns inferred from cosmogenic [10]Be in the Susquehanna River basin: University of Vermont, 172 p.

Riebe, C. S., Kirchner, J. W., and Finkel, R. C., 2003, Long-term rates of chemical weathering and physical erosion from cosmogenic nuclides and geochemical mass balance: Geochimica et Cosmochimica Acta, v. 67, no. 22, p. 4411-4427.

Riebe, C. S., Kirchner, J. W., Granger, D. E., and Finkel, R. C., 2000, Erosional equilibrium and disequilibrium in the Sierra Nevada, inferred from cosmogenic ^{26}Al and ^{10}Be in alluvial sediment: Geology, v. 28, no. 9, p. 803-806.

-, 2001a, Minimal climatic control on erosion rates in the Sierra Nevada, California: Geology, v. 29, no. 5, p. 447-450.

-, 2001b, Strong tectonic and weak climatic control of long-term chemical weathering rates: Geology, v. 29, no. 6, p. 511–514.

Roden, M. K., 1991, Apatite fission-track thermochronology of the southern Appalachian basin: Maryland, West Virginia, and Virginia: Journal of Geology, v. 99, no. 1, p. 41–53.

Safran, E. B., Bierman, P. R., Aalto, R., Dunne, T., Whipple, K. X., and Caffee, M., 2005, Erosion rates driven by channel network incision in the Bolivian Andes: Earth Surface Processes and Landforms, v. 30, no. 8, p. 1007-1024.

Saunders, I., and Young, A., 1983, Rates of surface processes on slopes, slope retreat, and denudation: Earth Surface Processes and Landforms, v. 8, p. 473-501.

Schaller, M., von Blanckenburg, F., Hovius, N., and Kubik, P. W., 2001, Large-scale erosion rates from In situ-produced cosmogenic nuclides in European river sediments: Earth and Planetary Science Letters, v. v. 188, p. 441-458.

Sevon, W. D., Braun, D. D., and Ciolkosz, E. R., 1989, The Rivers and Valleys of Pennsylvania Then and Now: Guidebook for the 20th Annual Geomorphology Symposium: Harrisburg, PA, Pennsylvania Geological Survey, 69 p.

Small, E. E., Anderson, R. S., Repka, J. L., and Finkel, R., 1997, Erosion rates of alpine bedrock summit surfaces deduced from in situ ^{10}Be and ^{26}Al: Earth and Planetary Science Letters, v. 150, no. 3-4, p. 413-425.

Spotila, J. A., Bank, G. C., Reiners, P. W., Naeser, C. W., Naeser, N. D., and Henika, B. S., 2003, Origin of the Blue Ridge escarpment along the passive margin of Eastern North America: Basin Research, v. 16, p. 41-63.

Stock, G. M., Frankel, K. L., Ehlers, T. A., Schaller, M., Briggs, S. M., and Finkel, R. C., 2009, Spatial and temporal variations in denudation of the Wasatch Mountains, Utah, USA: Lithosphere, v. 1, no. 1, p. 34-40.

Stone, J., 2000, Air pressure and cosmogenic isotope production: Journal of Geophysical Research, v. 105, no. b10, p. 23753-23759.

Sullivan, C. L., 2007, [10]Be erosion rates and landscape evolution of the Blue Ridge Escarpment, southern Appalachian Mountains: University of Vermont, 76 p.

Syvitski, J. P. M., Vorosmarty, C. J., Kettner, A. J., and Green, P., 2005, Impact of Humans on the Flux of Terrestrial Sediment to the Global Coastal Ocean: Science, v. 308, p. 376-380.

Tomkins, K. M., Humphreys, G. S., Wilkinson, M. T., Fink, D., Hesse, P. P., Doerr, S. H., Shakesby, R. A., Wallbrink, P. J., and Blake, W. H., 2007, Contemporary versus long-term denudation along a passive plate margin: the role of extreme events: Earth Surface Processes and Landforms, v. 32, no. 7, p. 1013.

Trimble, S. W., 1977, The fallacy of stream equilibrium in contemporary denudation studies: American Journal of Science, v. 277, p. 876-887.

Trodick, C. D. J., Bierman, P., Pavich, M. J., Reusser, L. J., Portenga, E. W., and Rood, D., 2010, Basin scale erosion rates from the Potomac River basin using *In situ* and meteoric [10]Be, *in* 2010 GSA Denver Annual Meeting, Denver, Colorado.

Vanacker, V., von Blanckenburg, F., Hewawasam, T., and Kubik, P. W., 2007, Constraining landscape development of the Sri Lankan escarpment with cosmogenic nuclides in river sediment: Earth and Planetary Science Letters, v. 253, no. 3-4, p. 402-414.

Vance, D., Bickle, M., Ivy-Ochs, S., and Kubik, P. W., 2003, Erosion and exhumation in the Himalaya from cosmogenic isotope inventories of river sediments: Earth and Planetary Science Letters, v. 206, p. 273-288.

von Blanckenburg, F., Hewawasam, T., and Kubik, P. W., 2004, Cosmogenic nuclide evidence for low weathering and denudation in the wet, tropical highlands of Sri Lanka: Journal of Geophysical Research, v. 109, no. F3.

Walling, D. E., 1983, The sediment delivery problem: Journal of Hydrology, v. 65, no. 1-3, p. 209-237.

Ward, I. A. K., Nanson, G. C., Head, L. M., Fullagar, R. L. K., Price, D. M., and Fink, D., 2005, Late Quaternary landscape evolution in the Keep River region, northwestern Australia: Quaternary Science Reviews, v. 24, no. 16-17, p. 1906-1922.

Weissel, J. K., and Seidl, M. A., 1998, Inland propagation of erosional escarpments and river profile evolution across the southeast Australian passive continental margin: Geophysical Monograph, v. 107, p. 189-206.

Wilkinson, B.H., 2005, Humans as geologic agents: A deep-time perspective: Geology, v. 33, no. 3, p. 161-164.

Wittmann, H., Blanckenburg, F. v., Guyot, J. L., Maurice, L., and Kubik, P. W., 2009, From source to sink: Preserving the cosmogenic ^{10}Be-derived denudation rate signal of the Bolivian Andes in sediment of the Beni and Mamoré foreland basins: Earth and Planetary Science Letters, v. 288, p. 463-474.

Wittmann, H., Blanckenburg, F. v., Kruesmann, T., Norton, K. P., and Kubik, P. W., 2007, Relation between rock uplift and denudation from cosmogenic nuclides in river sediment in the Central Alps of Switzerland: Journal of Geophysical Research, v. 112, no. F04010.

Zeitler, P. K., Meltzer, A. S., Koons, P. O., Craw, D., Hallet, B., Chamberlain, C. P., Kidd, W. S. F., Park, S. K., Seeber, L., Bishop, M., and Shroder, J., 2001, Erosion, Himalayan geodynamics, and the geomorphology of metamorphism: GSA Today, v. 11, no. 1, p. 4-9.

Global [10]Be Erosion Rate Data Compilation

Beryllium-10, erosion rate, and site-specific data were compiled from bedrock outcrop and drainage basin studies done around the world and were standardized in order to perform a global erosion analysis. The specific location coordinates, elevation, lithology, measured [10]Be concentration with errors, AMS standard material, density, reported half-life, production rate, and neutron attenuation coefficient of each sample were catalogued from each publication (Table DR-1 in Appendix B). In most publications, all of the necessary information was provided in the sample table; however, latitude and longitude were sometimes estimated from study-area maps and elevations from topographic maps. Other data, including standards and the standard values used for normalization, half-life, mass attenuation depth, and the [10]Be production rate were not included in many publications. We requested these data from authors.

By excluding certain samples from our study we are able to look at general trends in erosion rates from a completely normalized global dataset. The value for nuclide concentration is influenced by horizon shielding for samples taken from non-horizontal surfaces (i.e. cliff or quarry faces), latitude, elevation, and sample thickness. We filtered through published data and only included those samples which are horizontally and sub-horizonally positioned (i.e. ridge crests, tops of tors, bornhardts, etc.) to ensure samples in our datasets are treated as similarly as possible since samples from knickpoints,

retreating cliffs, and basins with heavy anthropogenic alteration may erode through different processes.

Recalculating Outcrop and Drainage Basin Erosion Rates

Published erosion rates are most often calculated from the equation provided in Lal (1991) and frequently consider only neutron spallation. The erosion rate (ε), a function of the density (ρ) of the target material, the absorption mean free path (Λ) the production rate of the radionuclide at sea level at high latitudes (P) and the nuclide concentration (N) is given by the following equation:

$$e = \frac{\mathsf{L}}{r} \overset{\acute{e}}{\underset{\hat{e}}{\mathsf{e}}} \frac{P}{N} - l \overset{\grave{u}}{\underset{\mathsf{u}}{\acute{u}}}.$$

Since ^{10}Be decays over time, its decay constant (λ) is included.

Samples in this data compilation require recalculation for two reasons: (1) constraints on constants such as production rate, mass attenuation depths, and half-lives have been redefined through time and values used in individual studies vary; and (2) some publications amend the erosion rate equation to correct for location-dependent anomalies such as geometric shielding, glacial history, and muon production, making it difficult to observe general global patterns from published results.

Though the general purpose of using ^{10}Be to calculate erosion rates has remained the same, studies we reviewed use a variety of calculation methods, applied corrections, and inclusion of standardization information. Because of this, results from direct comparisons of multi-study results become less meaningful. It is therefore crucial for

[10]Be data to be normalized to the same type of calculations, correcting for any changes in half-life, production rate, and attenuation depth before further analytical or statistical interpretations can be made.

The CRONUS on-line erosion rate calculator was established so that geoscientists using cosmogenic radionuclides could "compare previously published…erosion rate measurements on a common basis" (Balco et al., 2008). In compiling data from all bedrock outcrop and basin-averaged studies, we amalgamated the necessary input parameters for the CRONUS calculator such that results from all erosion rate studies could be compared and analyzed as one large set of data. We also used CRONUS because it is a method which is accessible to everyone working with cosmogenic nuclides and changes to its methods and procedures are well documented (http://hess.ess.washington.edu/math/docs/al_be_v22/al_be_docs.html).

Of the 14 data entries the CRONUS calculator requires of each sample, 4 were not provided by most published studies: sample thickness, geometric shielding factors, density, and Be standard material used during AMS analysis. Unless otherwise specified through personal communication or in-text data, sample thicknesses were assigned a value of 3 cm for outcrops and 1 cm for basins; geometric shielding factors were interpreted from site descriptions (i.e. samples come from top of flat lying outcrop); densities were assigned average crustal density of 2.7 g cm^{-3} if not otherwise noted.

Beryllium standard material used for normalization and its presumed value were more difficult to ascertain because many published studies do not explicitly state the AMS Be standard or standard ratio used to normalize measured isotopic ratios. Each

AMS laboratory facility uses a specific Be standard material. These standard materials do not originate from the same source and their assumed ratios have changed through time (see Nishiizumi et al., 2007). The standard used is an input into the CRONUS calculator in order to correct for any changes in the constants used to calculate erosion rates; thus, assigning the correct standard is important.

The absorption mean free path and production rate are two parameters crucial for calculating erosion rates from ^{10}Be concentrations, yet are not inputs into the CRONUS calculator. Values for mean free path used in published studies ranged from 145-172 g cm^{-2} and publications utilize various half-lives of ^{10}Be, ranging from 1.32-1.53 Ma. The CRONUS calculator utilizes the most recent and widely accepted values for these parameters: 160 g cm^{-2} and 1.36 Ma, respectively (Balco et al., 2008; Nishiizumi et al., 2007). Though multiple scaling schemes are provided, we used erosion rates determined using the scaling methods of Lal (1991) and Stone (2000).

Once all data required for CRONUS were collected, we used the on-line calculator to calculate erosion rates for every sample. A total of 1110 basin samples and 418 bedrock outcrop erosion rates were recalculated.

We compared erosion rates calculated with CRONUS to published erosion rates (Figs. DR-1A and DR-1B). Recalculated erosion rates which were more than 30% different than original published values were carefully examined and we communicated directly with the study's authors. Some erosion rates from early cosmogenic publications change significantly once recalculated due to the compounded effects of changes in half-life, production rate, and attenuation length; when densities and thicknesses were filled in

107

with assumed values, small discrepancies may have been introduced, thus producing

CRONUS erosion rates slightly different than those published. The greatest change

usually comes from the inclusion of muon-specific production in the CRONUS code.

Global Coverages and Data Extraction

Gridded and spatially-interpolated precipitation and temperature datasets

continuously cover the Earth, with the exception of Antarctica, at a 1 km resolution

(Hijmans et al., 2005). The WorldClim coverages do not provide data for Antarctica.

Mean annual precipitation and temperature were taken from the Polar Meteorology

Group's Antarctic Hindcast Project, part of the Byrd Polar Research Center at the Ohio

State University (Monaghan et al., 2006).

We used the Global Seismic Hazard Assessment Program map of peak ground

acceleration (Giardini et al., 1999) as a proxy for global seismicity to test the hypothesis

that erosion rates may be related to seismic activity. Seismicity is defined here as a

magnitude of ground motion with a 10% chance of being exceeded within 50 years. Data

points are available from the GSHAP and were interpolated to a raster grid with a

resolution of about 60 km.

The Köppen-Geiger climate classification system has been recently updated by

Peel et al. (2007). We used digital data to group our data into non-numeric categories.

The Köppen-Geiger methods define five major climate zones: tropical, arid, temperate,

cold, and polar. Each major climate zone is divided into sub-zones; however, our data are

not numerous enough to make use of these sub-zones. The updated climate classification

data was calculated for each continent has a resolution of ~10km^2. Some basins cover more than one type of climate zone, in which case the dominant climate zone within the basin was used for categorization.

Digital elevation models were used to analyze elevation, basin relief, relief within a 5 km radius around bedrock samples, and mean basin slope. Stream catchment boundaries were regenerated from DEMs based off of the area upslope from where the channel sediment was collected. SRTM data of the United States has a resolution of 1 arc-second, while global data is provided at a resolution of 3 arc-seconds. SRTM data do not cover Antarctica, in which case, the GTopo 30 arc-second digital elevation model was used (provided by the ESRI corporation, through the University of Vermont). SRTM data tiles contain holes in which no data is present. We filled these holes with elevation data from the GTopo 30 DEM; this typically only affected basins and sample points in mountainous terrain. The GTopo 30 DEM was also used to calculate elevation-based parameters for large basins (i.e. Yangtze and Amazon River basins) as the ArcGIS computational power required for these analyses greatly exceeded that of the machines being used for the computations.

The mean percentage of vegetation within a basin was also generated for all basin samples. This dataset was created by Defries et al. (2000) and has a 1 km resolution. Values for cells range from 10-80%, where those with a value of 10% representing 0-10% tree coverage and those with a value of 80% represent 80-100% tree coverage. Some grid cells contained a specific assigned value indicating it had between 0-10% tree

coverage; cells with this value were given a reassigned value of 5% - the average of its range.

Data from global coverages were extracted from each grid to the corresponding overlying sample point using the 'Extract Values to Points' tool from the 'Spatial Analyst' toolbox in ArcGIS. For basins, the "Zonal Statistics as Table" tool was used to calculate the average parameter value for each basin. These methods allowed us to use the fewest possible sources to acquire the data necessary to complete our global analysis of exposed bedrock erosion rates.

We analyzed erosion rates compared to the lithology of the outcrop or drainage basin from which they were collected. Because some studies are very specific in their definition of the sample's lithology (e.g. graphitic mica-schist, metagraywacke, arkosic sandstone) while others are not (e.g. granite, schist, sandstone), we generalized the lithology to three basic groupings: igneous, metamorphic, and sedimentary. A fourth category, "Mixed," was introduced for basins underlain by lithologies of multiple types.

A complete set of data used in our multivariate analyses can be found in Table DR-2 for bedrock outcrop samples and Table DR-3 for drainage basin samples. Both tables can be found in Appendix B.

Statistical Methods

The JMP Statistical Software package was used for all statistical analyses. We determined correlations between erosion rates and the numeric local parameters (i.e. mean annual precipitation, latitude, etc.) using the "Fit Y by X" bivariate analysis tool.

The y-variable was the erosion rate and the x-variable were any of the local parameters. For bedrock outcrop samples, this bivariate analysis was performed for latitude, elevation, relief, mean annual precipitation, mean annual temperature, and peak ground acceleration; for basin samples, analyses on basin area, mean basin slope, and percent tree coverage were also run. A strong global regression was determined for drainage basins using a seasonal precipitation parameter (Reuter, 2005) using the sum of the precipitation for the three driest months for each basin and dividing that sum by the mean annual precipitation. We repeated this analysis as well, though it was not included in the global drainage basin multivariate regression because it showed no statistical power in explaining erosion rates and is in some way duplicative of other climate parameters such as mean annual precipitation.

Analyses of variance were performed in order to summarize erosion rates according to categorical variables. Samples were categorized by general lithology (i.e. igneous, metamorphic, and sedimentary), into specific climate zones (i.e. tropical, arid, temperate, cold, and polar), and also into zones of either seismically active or inactive zones – with the separation being locations expected to feel a magnitude 2 earthquake within 50 years and those that are not. Student's t-Tests were applied to determine if average erosion rates from these categories were significantly higher, lower, or similar than others at a 95% confidence interval.

No one parameter dictates the rate of erosion at any given site so we use forward stepwise regressions to determine which numeric variables are significant in determining erosion rates globally and at what level. This was done at the global scale as well as for

categorical subsets of the database (i.e. for each climate zone, lithology, or seismic activity). It was necessary to split the global dataset into these subsets of data because categorical data cannot be entered into a multivariate analysis of this type. We can see which parameters are more likely to affect erosion rates in specific lithologies, climate zones, and seismic zones by performing the forward stepwise regressions on each category.

Two criteria must be met in order for a parameter to be considered for the regression: the Probability to Enter and the Probability to Leave. If the p-value is less than the Probability to Enter, the variable is entered into the analysis. Parameters are entered into the analysis one at a time and a new p-value is generated for those which make it into the analysis based on how well it helps the multivariate regression. If the new p-value is less than the Probability to Leave, the variable remains in the analysis; however, if it is greater than the Probability to Leave, the parameter is removed. This step-by-step analysis considers all variables but only fits a regression through those that are most statistically important. For our analyses, we set the Probability to Enter as 0.250 and the Probability to Leave as 0.100.

A Standard Least Squares regression was also computed for the global outcrop and drainage basin datasets. The R^2 value for the least squares regression is equal to that of the forward stepwise regressions, the only difference being that the regression for the least squares regression is forced through every parameter, not just the ones that significantly improve it. Equations and parameter coefficients are provided in Table DR-

5 in Appendix B. These equations could be used to predict the erosion rate of unsampled basins and outcrops.

Data Preparation for CRONUS Erosion Rate Calculations of Drainage Basins

We recalculated all erosion rates with the CRONUS-Earth online calculator using [10]Be concentrations published in the 58 drainage basin studies complied here in order to normalize all measurements to one comparable format (http://hess.ess.washington.edu/math/al_be_v22/al_be_erosion_multiple_v22.php). The calculator considers erosion at single points on Earth's surface, and by itself is not capable of weighting elevation and latitude scaling factors for the distribution of elevations represented within a given drainage basin. We addressed this complication by generating several tools designed to find the hypsometerically-weighted effective elevation required by the CRONUS calculator to calculate an erosion rate.

Part 1: We developed a model in ArcGIS that exports cell-by-cell elevation, longitude, and latitude ASCII grid files for any sized drainage basin and elevation datasets of any resolution.

Part 2: The grid files are fed directly into a Matlab script to find the effective elevation and latitude needed by the CRONUS calculator. In essence, the script reduces the distribution of elevation and latitude across any drainage basin of any shape or size to a single point representing the basin as a whole. The elevation and latitude grids are used to calculate the ELD scaling factor for each cell. The average scaling factor for all cells, or the effective ELD, is used in conjunction with the actual effective latitude for the basin

113

to back calculate the corresponding effective elevation. The effective elevation and latitude, along with the concentration of ^{10}Be, are fed to the CRONUS calculator to produce an erosion rate for the basin.

Results of Statistical Analyses

Outcrop Erosion Rates

Biviariate analyses between log-transformed CRONUS erosion rates for outcropping bedrock sites do not show strong correlations with any one parameter on the global-scale (Fig. DR-2). Combinations of parameters provide much stronger regressions as seen in Figure 4 of the main text. The strongest bivariate regression was with mean annual precipitation (Fig. DR-2e); outcrop erosion rates are also seen to increase with an increase in relief (Fig. DR-2c). Analyses of variance were carried out for subdivisions of categorical data. Lithology is not a strong indicator of outcrop erodability: Student's t-Tests show that metamorphic and sedimentary outcrops are inseparable, but both are higher than igneous outcrops (Fig. DR-2g). There is no difference between erosion rates in active tectonic settings from those in inactive settings (Fig. DR-2h). We see that outcrops in temperate climate zones erode the fastest, that those in cold and tropical zones are indistinguishable from each other, as are those in tropical and arid climates, and outcrops in polar settings erode significantly slower than those in any other setting (Fig. DR-2i). Though the forward stepwise regression only fits a line through significant parameters, a standard least squares regression produces the same R^2 value, though it

forces each parameter into the regression. The global regression equation and parameter coefficients are presented in Table DR-5 in Appendix B.

Basin Erosion Rates

Bivariate analyses show few relationships between log-transformed CRONUS erosion rates and drainage basin parameters. The strongest correlation is found with mean basin slope (Fig. DR-3d), though mean basin elevation, basin relief, and average seismicity for each basin provide significant, albeit weak, regressions (Figs. DR-3b, DR-3c, DR-3f). Though correlations between drainage basin erosion rates and seasonal precipitation have been found before (Reuter, 2005), we could not reproduce those results (Fig. DR-3j) using this much larger and more geographically varied data set and the parameter was not included in subsequent multivariate analyses. Analysis of variation was determined for categorical data. An ANOVA of basin lithology shows that mixed-lithology basins erode faster than metamorphic and igneous basins, but not sedimentary basins (Fig. DR-3k). Basins in active tectonic settings erode significantly faster than those in inactive settings (Fig. DR-3l). Basins in polar settings erode the fastest while those in arid settings erode the slowest (Fig. DR-3m); basins in temperate, cold, and tropical settings are indistinguishable. Multiviarite global regressions provide very strong regressions as seen in Figure 4 of the main text. A standard least squares regression was carried out for global drainage basins and provided an R^2 value the same as that from the forward stepwise regression. The global regression equation and parameter coefficients for drainage basins are found in Table DR-5 in Appendix B.

References Cited

Abbühl, L. M., Norton, K. P., Schlunegger, F., Kracht, O., Aldahan, A., and Possnert, G., 2010, El Niño forcing on [10]Be-based surface denudation rates in the northwestern Peruvian Andes?: Geomorphology, v. 123, p. 257-268.

Albrecht, A., Herzog, G. F., Klein, J., Dezfouly-Arjomandy, B., and Goff, F., 1993, Quaternary erosion and cosmic-ray-exposure history derived from [10]Be and [26]Al produced in situ; an example from Pajarito Plateau, Valles Caldera region: Geology, v. 21, no. 6, p. 551-554.

Balco, G., Stone, J. O., Lifton, N. A., and Dunai, T. J., 2008, A complete and easily accessible means of calculating surface exposure ages or erosion rates from 10Be and 26Al measurements: Quaternary Geochronology, v. 3, p. 174-195.

Belmont, P., Pazzaglia, F. J., and Gosse, J. C., 2007, Cosmogenic [10]Be as a tracer for hillslope and channel sediment dynamics in the Clearwater River, western Washington State: Earth and Planetary Science Letters.

Belton, D. X., Brown, R. W., Kohn, B. P., Fink, D., and Farley, K. A., 2004, Quantitative resolution of the debate over antiquity of the central Australian landscape: implications for the tectonic and geomorphic stability of cratonic interiors: Earth and Planetary Science Letters, v. 219, no. 1-2, p. 21-34.

Bierman, P., and Nichols, K., 2004, Rock to sediment - Slope to sea with 10-Be - Rates of landscape change: Annual review of Earth and Planetary Sciences, v. 32, p. 215-255.

Bierman, P. R., Albrecht, A., Bothner, M., Brown, E., Bullen, T., Gray, L., and Turpin, L., 1998, Weathering, erosion and sedimentation, *in* Kendall, C., and McDonnell, J. J., eds., Isotope Tracers in Catchment Hydrology, Elsevier, p. 647-678.

Bierman, P. R., and Caffee, M., 2002, Cosmogenic exposure and erosion history of ancient Australian bedrock landforms: Geological Society of America Bulletin, v. 114, no. 7, p. 787-803.

Bierman, P. R., and Caffee, M. W., 2001, Slow rates of rock surface erosion and sediment production across the Namib Desert and escarpment, Southern Africa: American Journal of Science, v. 301, no. 4-5, p. 326-358.

Bierman, P. R., Clapp, E. M., Nichols, K. K., Gillespie, A. R., and Caffee, M., 2001, Using cosmogenic nuclide measurements in sediments to understand background rates of erosion and sediment transport,, *in* Harmon, R. S., and Doe, W. M., eds., Landscape Erosion and Evolution Modelling: New York, Kluwer, p. 89-116.

Bierman, P. R., Nichols, K. K., Matmon, A., Enzel, Y., Larsen, J., and Finkel, R., 2007, 10-Be shows that Namibian drainage basins are slowly, steadily and uniformly eroding: Quaternary International v. 167–168 no. 3, p. 33.

Bierman, P. R., Reusser, L. J., Nichols, K. K., Matmon, A., and Rood, D., 2009, Where is the sediment coming from and where is it going - A 10Be examination of the northern Queensland escarpment, Australia, 2009 Portland GSA Annual Meeting: Portland, Or.

Bierman, P. R., Reuter, J. M., Pavich, M., Gellis, A. C., Caffee, M. W., and Larsen, J., 2005, Using cosmogenic nuclides to contrast rates of erosion and sediment yield in a semi-arid, arroyo-dominated landscape, Rio Puerco Basin, New Mexico: Earth Surface Processes and Landforms, v. 30, no. 8, p. 935-953.

Bierman, P. R., and Steig, E., 1996, Estimating rates of denudation and sediment transport using cosmogenic isotope abundances in sediment: Earth Surface Processes and Landforms, v. 21, p. 125-139.

Binnie, S. A., Phillips, W. M., Summerfield, M. A., and Fifield, L. K., 2006, Sediment mixing and basin-wide cosmogenic nuclide analysis in rapidly eroding mountainous environments: Quaternary Geochronology v. 1, p. 4-14.

Binnie, S. A., Phillips, W. M., Summerfield, M. A., Fifield, L. K., and Spotila, J. A., 2008, Patterns of denudation through time in the San Bernardino Mountains, California: Implications for early-stage orogenesis Earth and Planetary Science Letters, v. In Press.

Brown, E. T., Bourles, D. L., Colin, F., Sanfo, Z., Raisbeck, G. M., and Yiou, F., 1994, The development of iron crust lateritic systems in Burkina Faso, West Africa examined with in-situ-produced cosmogenic nuclides: Earth and Planetary Science Letters, v. 124, p. 19-33.

Brown, E. T., Stallard, R. F., Larsen, M. C., Bourles, D. L., Raisbeck, G. M., and Yiou, F., 1998, Determination of predevelopment denudation rates of an agricultural watershed (Cayaguas River, Puerto Rico) using in-situ-produced [10]Be in river-borne quartz: Earth and Planetary Science Letters, v. 160, no. 3-4, p. 723-728.

Brown, E. T., Stallard, R. F., Larsen, M. C., Raisbeck, G. M., and Yiou, F., 1995, Denudation rates determined from the accumulation of in situ-produced [10]Be in the Luquillo Experimental Forest, Puerto Rico: Earth and Planetary Science Letters, v. 129, p. 193-202.

Chappell, J., Zheng, H., and Fifield, K., 2006, Yangtse River sediments and erosion rates from source to sink traced with cosmogenic [10]Be: Sediments from major rivers: Palaeogeography, Palaeoclimatology, Palaeoecology, v. 241, no. 1, p. 79-94.

Clapp, E., Bierman, P. R., and Caffee, M., 2002, Using [10]Be and [26]Al to determine sediment generation rates and identify sediment source areas in an arid region drainage basin: Geomorphology, v. 45, no. 1,2, p. 89-104.

Clapp, E. M., Bierman, P. R., Nichols, K. K., Pavich, M., and Caffee, M., 2001, Rates of sediment supply to arroyos from upland erosion determined using in situ produced cosmogenic [10]Be and [26]Al: Quaternary Research (New York), v. 55, no. 2, p. 235-245.

Clapp, E. M., Bierman, P. R., Schick, A. P., Lekach, J., Enzel, Y., and Caffee, M., 2000, Sediment yield exceeds sediment production in arid region drainage basins: Geology, v. 28, no. 11, p. 995-998.

Cockburn, H. A. P., Brown, R. W., Summerfield, M. A., and Seidl, M. A., 2000, Quantifying passive margin denudation and landscape development using a combined fission-track thermochronology and cosmogenic isotope analysis approach: Earth and Planetary Science Letters, v. 179, no. 3-4, p. 429-435.

Cox, R., Bierman, P. R., Jungers, M., Rakotondrazafy, A. F. M., and Finkel, R. C., 2006, Just how fast does Madagascar erode? Evidence from [10]Be analysis of lavaka, slope, and river sediment: Geological Society of America *Abstracts with Programs*, v. 38, no. 7, p. 278.

Cyr, A. J., and granger, D. E., 2008, Dynamic equilibrium among erosion, river incision, and coastal uplift in the northern and central Apennines, Italy: Geology, v. 36, no. 2, p. 103-106.

Defries, R. S., Hansen, M. C., Townshend, J. R. G., Janetos, A. C., and Loveland, T. R., 2000, A new global 1-km dataset of percentage tree cover drived from remote sensing: Global Change Biology, v. 6, p. 247-254.

Delunel, R., Beek, P. A. v. d., Carcaillet, J., Bourlès, D. L., and Valla, P. G., 2010, Frost-cracking control on catchment denudation rates: Insights from in situ produced [10]Be concentrations in stream sediments (Ecrins–Pelvoux massif, French Western Alps): Earth and Planetary Science Letters, v. 293, p. 72-83.

DiBiase, R. A., Whipple, K. X., Heimsath, A. M., and Ouimet, W. B., 2009, Landscape form and millennial erosion rates in the San Gabriel Mountains, CA: Earth and Planetary Science Letters, v. 289, p. 134-144.

Dole, R. B., and Stabler, H., 1909, Denudation: USGS Water Supply Paper, v. 234, p. 78-93.

Duxbury, J., 2009, Erosion rates in and around Shenandoah National Park, VA, determined using analysis of cosmogenic 10Be: University of Vermont, 134 p.

Elmore, D., and Phillips, F., 1987, Accelerator mass spectrometry for measurement of long-lived radioisotopes: Science, v. 236, p. 543-550.

Faure, G., and Nishiizumi, K., 1994, Exposure dating of quartz sandstone in the Transantarctic Mountains by cosmogenic ^{10}Be and ^{26}Al, *in* Harte, B., ed., V. M. Goldschmidt Conference; extended abstracts Mineralogical Magazine 58A, no. A-K (199408), Mineralogical Society, London, United Kingdom, p. 268-269.

Ferrier, K. L., Kirchner, J. W., and Finkel, R. C., 2005, Erosion rates over millennial and decadal timescales at Caspar Creek and Redwood Creek, Northern California Coast Ranges: Earth Surface Processes and Landforms, v. 30, no. 8, p. 1025-1038.

Finnegan, N. J., Hallet, B., Montgomery, D. R., Zeitler, P., Stone, J., Anders, A. M., and Yuping, L., 2008, coupling of rock uplift and river incision in the Namche Barwa-Gyala peri massif, Tibet: 2007 GSA Denver Annual Meeting.

Giardini, D., Grunthal, G., Shedlock, K. M., and Zhang, P., 1999, The GSHAP Global Seismic Hazard Map: Annali Di Geofisica, v. 42, no. 6, p. 1225-1230.

Granger, D. E., Kirchner, J. W., and Finkel, R., 1996, Spatially averaged long-term erosion rates measured from in situ-produced cosmogenic nuclides in alluvial sediments: Journal of Geology, v. 104, no. 3, p. 249-257.

Granger, D. E., Riebe, C. S., Kirchner, J. W., and Finkel, R. C., 2001, Modulation of erosion on steep granitic slopes by boulder armoring, as revealed by cosmogenic ^{26}Al and ^{10}Be: Earth and Planetary Science Letters, v. 186, no. 2, p. 269-281.

Guralnik, B., Matmon, A., Avni, Y., and Fink, D., 2010, ^{10}Be exposure ages of ancient desert pavements reveal Quaternary evolution of the Dead Sea drainage basin and rift margin tilting: Earth and Planetary Science Letters, v. 290, p. 132-141.

Hack, J. T., 1975, Dynamic equilibrium and landscape evoluion, *in* Melhorn, W. N., and Flemal, R. C., eds., Theories of landform development: Binghamton, N.Y., SUNY Binghamton,, p. 87-102.

-, 1979, Rock control and tectonism, their importance in shaping the Appalachian highlands: U.S. Geological Survey professional paper, v. 1126-B, p. 17.

Hales, T. C., and Roering, J. J., 2007, Climatic controls on frost cracking and implications for the evolution of bedrock landscapes: Journal of Geophysical Research, v. 112.

Hancock, G., and Kirwan, M., 2007, Summit erosion rates deduced from [10]Be: Implications for relief production in the central Appalachians: Geology, v. 35, no. 1, p. 89-92.

Heimsath, A., Chappel, J., Finkel, R. C., Fifield, K., and Alimanovic, A., 2006, Escarpment Erosion and Landscape Evolution in Southeastern Australia: Special Papers-Geological Society of America, v. 398, p. 173.

Heimsath, A. M., Chappell, J., Dietrich, W. E., Nishiizumi, K., and Finkel, R. C., 2000, Soil production on a retreating escarpment in southeastern Australia: Geology, v. 28, no. 9, p. 787-790.

-, 2001a, Late Quaternary erosion in southeastern Australia: a field example using cosmogenic nuclides: Quaternary International, v. 83-85, p. 169-185.

Heimsath, A. M., Dietrich, W. E., Nishiizumi, K., and Finkel, R. C., 1997, The soil production function and landscape equilibrium: Nature (London), v. 388, no. 6640, p. 358-361.

-, 1999, Cosmogenic nuclides, topography, and the spatial variation of soil depth: Geomorphology, v. 27, no. 1-2, p. 151-172.

-, 2001b, Stochastic processes of soil production and transport; erosion rates, topographic variation and cosmogenic nuclides in the Oregon Coast Range: Earth Surface Processes and Landforms, v. 26, no. 5, p. 531-552.

Henck, A. C., 2010, Spatial and temporal patterns of erosion in Western China and Tibet: University of Washington, 158 p.

Hewawasam, T., von Blackenburg, F., Schaller, M., and Kubik, P., 2003, Increase of human over natural erosion rates in tropical highlands constrained by cosmogenic nuclides: Geology, v. 31, no. 7, p. 597-600.

Hijmans, R. J., Cameron, S. E., Parra, J. L., Jones, P. G., and Jarvis, A., 2005, Very High Resolution Interpolates Climate Surfaces for Global Land Areas: International Journal of Climatology, v. 25, p. 1965-1978.

Hooke, R. L., 1994, On the efficacy of humans as geomorphic agents: GSA Today, v. 4, no. 9, p. 217,224-225.

-, 2000, On the history of humans as geomorphic agents: Geology, v. 28, no. 9, p. 843-846.

Insel, N., Ehlers, T. A., Schaller, M., Barnes, J. B., Tawackoli, S., and Poulsen, C. J., 2010, Spatial and temporal variability in denudation across the Bolivian Andes from multiple geochronometers: 2010, v. 122, p. 65-77.

Ivy-Ochs, S., Kober, F., Alfimov, V., Kubik, P. W., and Synal, H.-A., 2007, Cosmogenic ^{10}Be, ^{21}Ne and ^{36}Cl in sanidine and quartz from Chilean ignimbrites: Nuclear Instruments and Methods in Physics Research B, v. 259, p. 588-594.

Jakica, S., Quigley, M. C., Sandiford, M., Clark, D., Fifield, K., and Alimanovic, A., 2010, Geomorphic and cosmogenic nuclide constraings on escarpment evolution in an intraplate setting, Darling Escarpment, Western Australia: Earth Surface Processes and Landforms.

Judson, S., 1968, Erosion of the land or what's happening to our continents: American Scientist, v. 56, p. 356-374.

Kirchner, J. W., Finkel, R. C., Riebe, C. S., Granger, D. E., Clayton, J. L., King, J. G., and Megahan, W. F., 2001, Mountain erosion over 10 yr, 10 k.y., and 10 m.y. time scales: Geology, v. 29, no. 7, p. 591-594.

Kober, F., Ivy-Ochs, S., Schlunegger, F., Baur, H., Kubik, P. W., and Wieler, R., 2007, Denudation rates and a topography-driven rainfall threshold in northern Chile: Multiple cosmogenic nuclide data and sediment yield budgets: Geomorphology, v. 83, p. 97-120.

Kober, F., Ivy-Ochs, S., Zeilinger, G., Schlunegger, F., Kubik, P. W., Baur, H., and Wieler, R., 2009, Complex multiple cosmogenic nuclide concentration and histories in the arid Rio Lluta catchment, northern Chile: Earth Surface Processes and Landforms, v. 34, p. 398-412.

Lal, D., 1991, Cosmic ray labeling of erosion surfaces; in situ nuclide production rates and erosion models: Earth and Planetary Science Letters, v. 104, no. 2-4, p. 424-439.

Lal, D., Harris, N. B. W., Sharma, K. K., Gu, Z., Ding, L., Liu, T., Dong, W., Caffee, M. W., and Jull, A. J. T., 2003, Erosion history of the Tibetan Plateau since the last interglacial: constraints from the ¢rst studies of cosmogenic ^{10}Be from Tibetan bedrock: Earth and Planetary Science Letters, v. 217, p. 33-42.

Matmon, A. S., Bierman, P., Larsen, J., Southworth, S., Pavich, M., Finkel, R., and Caffee, M., 2003, Erosion of an ancient mountain range, the Great Smoky

Mountains, North Carolina and Tennessee: American Journal of Science, v. 303, p. 817-855.

Monaghan, A. J., Bromwich, D. H., and Wang, S.-H., 2006, Recent trends in Antarctic snow accumulation from Polar MM5 simulations: Philosophical Transactions of the Royal Society London A, v. 364, p. 25.

Montgomery, D. R., and Brandon, M. T., 2002, Topographic controls on erosion rates in tectonically active mountain ranges: Earth and Planetary Science Letters, v. 201, no. 3-4, p. 481-489.

Morel, P., von Blackenburg, F., Schaller, M., Kubik, P. W., and Hinderer, M., 2003, Lithology, landscape dissection and glaciation controls on catchment erosion as determined by cosmogenic nuclides in river sediment (the Wutach Gorge, Black Forest): Terra Nova, v. 15, no. 6, p. 398-404.

Nichols, K., Bierman, P., Finkel, R., and Larsen, J., 2005a, Long-Term (10 to 20 kyr) Sediment Generation Rates for the Upper Rio Chagres Basin Based on Cosmogenic ^{10}Be, *in* Harmon, R. S., ed., The Rio Chagres: A Multidisciplinary Profile of a Tropical Watershed, Kluwer Academic Publishers.

Nichols, K. K., Bierman, P. R., Eppes, M. C., Caffee, M., Finkel, R., and Larsen, J., 2005b, Late Quaternary history of the Chemehuevi Mountain piedmont, Mojave Desert, deciphered using ^{10}Be and ^{26}Al: American Journal of Science, v. 305, no. 5, p. 345-368.

-, 2007, Timing of surficial process changes down a Mojave Desert piedmont: Quaternary Research, v. 68, no. 1, p. 151-161.

Nichols, K. K., Bierman, P. R., Foniri, W. R., Gillespie, A. R., Caffee, M., and Finkel, R., 2006, Dates and rates of arid region geomorphic processes: GSA Today, v. 16, no. 8, p. 4-11.

Nichols, K. K., Bierman, P. R., Hooke, R. L., Clapp, E., and Caffee, M., 2002, Quantifying sediment transport on desert piedmonts using ^{10}Be and ^{26}Al: Geomorphology, v. 45, no. 1,2, p. 89-104.

Nishiizumi, K., Imamura, M., Caffee, M. W., Southon, J. R., Finkel, R. C., and McAninch, J., 2007, Absolute calibration of 10Be AMS standards: Nuclear Inst. and Methods in Physics Research, B, v. 258, no. 2, p. 403-413.

Nishiizumi, K., Klein, J., Middleton, R., and Craig, H., 1990, Cosmogenic ^{10}Be, ^{26}Al, and ^{3}He in olivine from Maui lavas: Earth and Planetary Science Letters, v. 98, no. 3-4, p. 263-265.

Nishiizumi, K., Kohl, C. P., Arnold, J. R., Klein, J., Fink, D., and Middleton, R., 1991, Cosmic ray produced ^{10}Be and ^{26}Al in Antarctic rocks; exposure and erosion history: Earth and Planetary Science Letters, v. 104, no. 2-4, p. 440-454.

Nishiizumi, K., Lal, D., Klein, J., Middleton, R., and Arnold, J. R., 1986, Production of ^{10}Be and ^{26}Al by cosmic rays in terrestrial quartz in situ and implications for erosion rates: Nature, v. 319, no. 6049, p. 134-136.

Norton, K. P., Blanckenburg, F. v., and Kubik, P. W., 2010, Cosmogenic nuclide-derived rates of diffusive and episodic erosion in the glacially sculpted upper Rhone Valley, Swiss Alps: Earth Surface Processes and Landforms, v. 35, p. 651-662.

Norton, K. P., Blanckenburg, F. v., Schlunegger, F., Schwab, M., and Kubik, P. W., 2008, Cosmogenic nuclide-based investigation of spatial erosion and hillslope channel coupling in the transient foreland of the Swiss Alps: Geomorphology, v. 95, p. 474-486.

Ouimet, W. B., Whipple, K. X., and Granger, D. E., 2009, Beyond threshold hillslopes: Channel adjustment to base-level fall in tectonically active mountain ranges: Geology, v. 37, no. 7, p. 579-582.

Palumbo, L., Hetzel, R., Tao, M., and Li, X., 2009, Topographic and lithologic control on catchment-wide denudation rates derived from cosmogenic ^{10}Be in two mountain ranges at the margin of NE Tibet: Geomorphology, v. 117, p. 130-142.

Peel, M. C., Finlayson, B. L., and McMahon, T. A., 2007, Updated world map of the K¨oppen-Geiger climate classification: Hydrology and Earth System Sciences, v. 11, p. 1633-1644.

Perg, L., Anderson, R., and Finkel, R., 2003, Use of cosmogenic radionuclides as a sediment tracer in the Santa Cruz littoral cell, California, USA: Geology, v. 31, p. 299-302.

Placzek, C. J., Matmon, A., Granger, D. E., Quade, J., and Niedermann, S., 2010, Evidence for active landscape evolution in the hyperarid Atacama from multiple terrestrial cosmogenic nuclides: Earth and Planetary Science Letters, v. 295, p. 12-20.

Portenga, E. W., Bierman, P. R., Trodick, C. D. J., and Rood, D. H., 2010, Low rates of bedrock outcrop erosion in the central Appalachian Mountains inferred from *In Situ* ^{10}Be concentrations, *in* 2010 GSA Denver Annual Meeting, Denver, Colorado.

Quigley, M., Sandiford, M., Fifield, K., and Alimanovic, A., 2007a, Bedrock erosion and relief production in the northern Flinders Ranges, Australia: Earth Surface Processes and Landforms, v. 32, no. 6, p. 929.

Quigley, M., Sandiford, M., Fifield, L. K., and Alimanovic, A., 2007b, Landscape responses to intraplate tectonism: Quantitative constraints from [10]Be nuclide abundances: Earth and Planetary Science Letters, v. 261, no. 1-2, p. 120-133.

Reinhardt, L. J., Bishop, P., Hoey, T. B., Dempster, T. J., and Sanderson, D. C. W., 2007, Quantification of the transient response to base-level fall in a small mountain catchment: Sierra Nevada, southern Spain Journal of Geophysical Research, v. 112, no. F03S05, p. 20.

Reuter, J. M., 2005, Erosion rates and patterns inferred from cosmogenic [10]Be in the Susquehanna River basin: University of Vermont, 172 p.

Riebe, C. S., Kirchner, J. W., and Finkel, R. C., 2003, Long-term rates of chemical weathering and physical erosion from cosmogenic nuclides and geochemical mass balance: Geochimica et Cosmochimica Acta, v. 67, no. 22, p. 4411-4427.

Riebe, C. S., Kirchner, J. W., Granger, D. E., and Finkel, R. C., 2000, Erosional equilibrium and disequilibrium in the Sierra Nevada, inferred from cosmogenic [26]Al and [10]Be in alluvial sediment: Geology, v. 28, no. 9, p. 803-806.

-, 2001a, Minimal climatic control on erosion rates in the Sierra Nevada, California: Geology, v. 29, no. 5, p. 447-450.

-, 2001b, Strong tectonic and weak climatic control of long-term chemical weathering rates: Geology, v. 29, no. 6, p. 511–514.

Safran, E. B., Bierman, P. R., Aalto, R., Dunne, T., Whipple, K. X., and Caffee, M., 2005, Erosion rates driven by channel network incision in the Bolivian Andes: Earth Surface Processes and Landforms, v. 30, no. 8, p. 1007-1024.

Saunders, I., and Young, A., 1983, Rates of surface processes on slopes, slope retreat, and denudation: Earth Surface Processes and Landforms, v. 8, p. 473-501.

Schaller, M., von Blanckenburg, F., Hovius, N., and Kubik, P. W., 2001, Large-scale erosion rates from In situ-produced cosmogenic nuclides in European river sediments: Earth and Planetary Science Letters, v. v. 188, p. 441-458.

Small, E. E., Anderson, R. S., Repka, J. L., and Finkel, R., 1997, Erosion rates of alpine bedrock summit surfaces deduced from in situ [10]Be and [26]Al: Earth and Planetary Science Letters, v. 150, no. 3-4, p. 413-425.

124

Stock, G. M., Frankel, K. L., Ehlers, T. A., Schaller, M., Briggs, S. M., and Finkel, R. C., 2009, Spatial and temporal variations in denudation of the Wasatch Mountains, Utah, USA: Lithosphere, v. 1, no. 1, p. 34-40.

Stone, J., 2000, Air pressure and cosmogenic isotope production: Journal of Geophysical Research, v. 105, no. b10, p. 23753-23759.

Sullivan, C. L., 2007, [10]Be erosion rates and landscape evolution of the Blue Ridge Escarpment, southern Appalachian Mountains: University of Vermont, 76 p.

Syvitski, J. P. M., Vorosmarty, C. J., Kettner, A. J., and Green, P., 2005, Impact of Humans on the Flux of Terrestrial Sediment to the Global Coastal Ocean: Science, v. 308, p. 376-380.

Tomkins, K. M., Humphreys, G. S., Wilkinson, M. T., Fink, D., Hesse, P. P., Doerr, S. H., Shakesby, R. A., Wallbrink, P. J., and Blake, W. H., 2007, Contemporary versus long-term denudation along a passive plate margin: the role of extreme events: Earth Surface Processes and Landforms, v. 32, no. 7, p. 1013.

Trimble, S. W., 1977, The fallacy of stream equilibrium in contemporary denudation studies: American Journal of Science, v. 277, p. 876-887.

Vanacker, V., von Blanckenburg, F., Hewawasam, T., and Kubik, P. W., 2007, Constraining landscape development of the Sri Lankan escarpment with cosmogenic nuclides in river sediment: Earth and Planetary Science Letters, v. 253, no. 3-4, p. 402-414.

Vance, D., Bickle, M., Ivy-Ochs, S., and Kubik, P. W., 2003, Erosion and exhumation in the Himalaya from cosmogenic isotope inventories of river sediments: Earth and Planetary Science Letters, v. 206, p. 273-288.

von Blanckenburg, F., Hewawasam, T., and Kubik, P. W., 2004, Cosmogenic nuclide evidence for low weathering and denudation in the wet, tropical highlands of Sri Lanka: Journal of Geophysical Research, v. 109, no. F3.

Walling, D. E., 1983, The sediment delivery problem: Journal of Hydrology, v. 65, no. 1-3, p. 209-237.

Ward, I. A. K., Nanson, G. C., Head, L. M., Fullagar, R. L. K., Price, D. M., and Fink, D., 2005, Late Quaternary landscape evolution in the Keep River region, northwestern Australia: Quaternary Science Reviews, v. 24, no. 16-17, p. 1906-1922.

Weissel, J. K., and Seidl, M. A., 1998, Inland propagation of erosional escarpments and river profile evolution across the southeast Australian passive continental margin: Geophysical Monograph, v. 107, p. 189-206.

Wilkinson, B.H., 2005, Humans as geologic agents: A deep-time perspective: Geology, v. 33, no. 3, p. 161-164.

Wittmann, H., Blanckenburg, F. v., Guyot, J. L., Maurice, L., and Kubik, P. W., 2009, From source to sink: Preserving the cosmogenic ^{10}Be-derived denudation rate signal of the Bolivian Andes in sediment of the Beni and Mamoré foreland basins: Earth and Planetary Science Letters, v. 288, p. 463-474.

Wittmann, H., Blanckenburg, F. v., Kruesmann, T., Norton, K. P., and Kubik, P. W., 2007, Relation between rock uplift and denudation from cosmogenic nuclides in river sediment in the Central Alps of Switzerland: Journal of Geophysical Research, v. 112, no. F04010.

Zeitler, P. K., Meltzer, A. S., Koons, P. O., Craw, D., Hallet, B., Chamberlain, C. P., Kidd, W. S. F., Park, S. K., Seeber, L., Bishop, M., and Shroder, J., 2001, Erosion, Himalayan geodynamics, and the geomorphology of metamorphism: GSA Today, v. 11, no. 1, p. 4-9.

Figure Captions

Figure DR-1. Bivariate plot of CRONUS-derived erosion rates versus published erosion rates for (A) bedrock outcrops and (B) drainage basins. Grey lines represent a one-to-one relationship and red lines are the regressions through the data points.

Figure DR-2. Bivariate plots of CRONUS-derived erosion rates for bedrock outcrops versus (a) Latitude, (b) Elevation, (c) Relief, (d) Seismicity, (e) Mean Annual Precipitation, (f) Mean Annual Temperature, (g) Precipitation Seasonality, (h) Rock Type, (i) Seismic Regime, and (j) Climate Zone.

Figure DR-3. Bivariate plots of CRONUS-derived erosion rates for drainage basins versus (a) Latitude, (b) Mean Basin Elevation, (c) Basin Relief, (d) Mean Basin Slope, (e) Basin Area, (f) Seismicity, (g) Mean Annual Precipitation, (h) Mean Annual Temperature, (i) Percent Vegetation Coverage, (j) Precipitation Seasonality, (k) Rock Type, (l) Seismic Regime, and (m) Climate Zone.

Figure DR-4. Results of Student's t-Tests comparing the means of bedrock outcrop (O) and drainage basin (B) erosion rates at locations or in regions where both have been measured. Sample populations are given for each sample type below the corresponding boxplot.
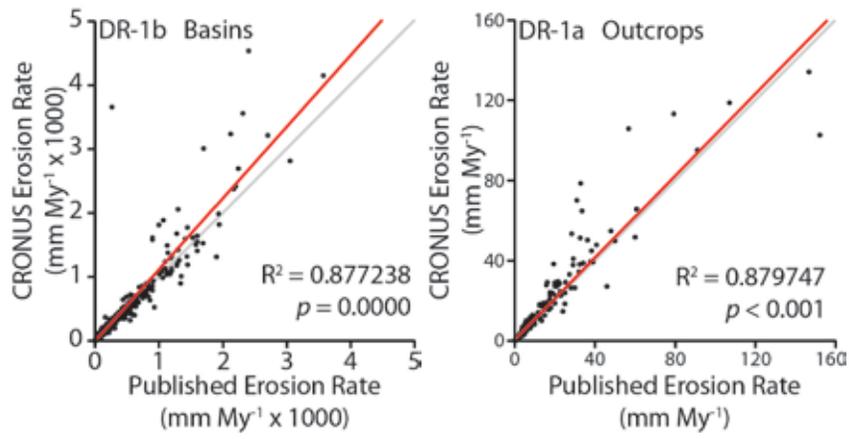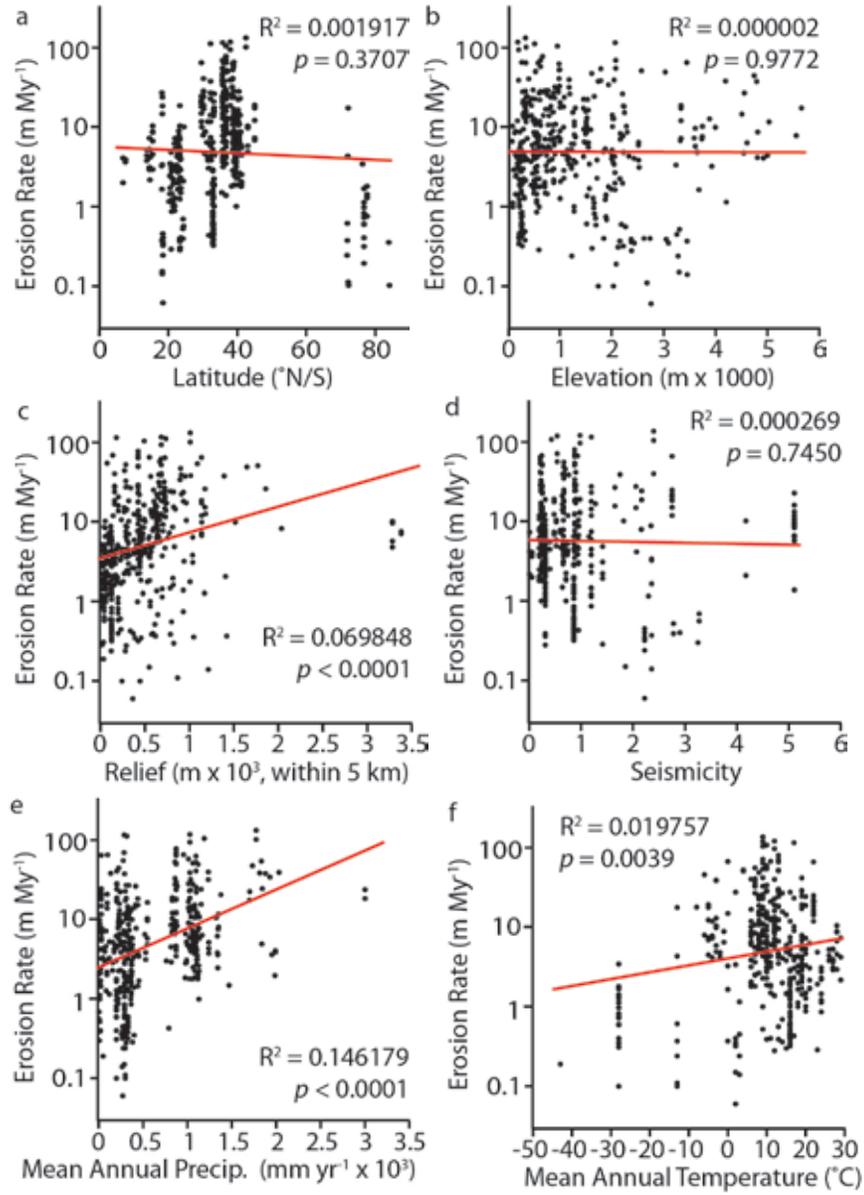
Figures
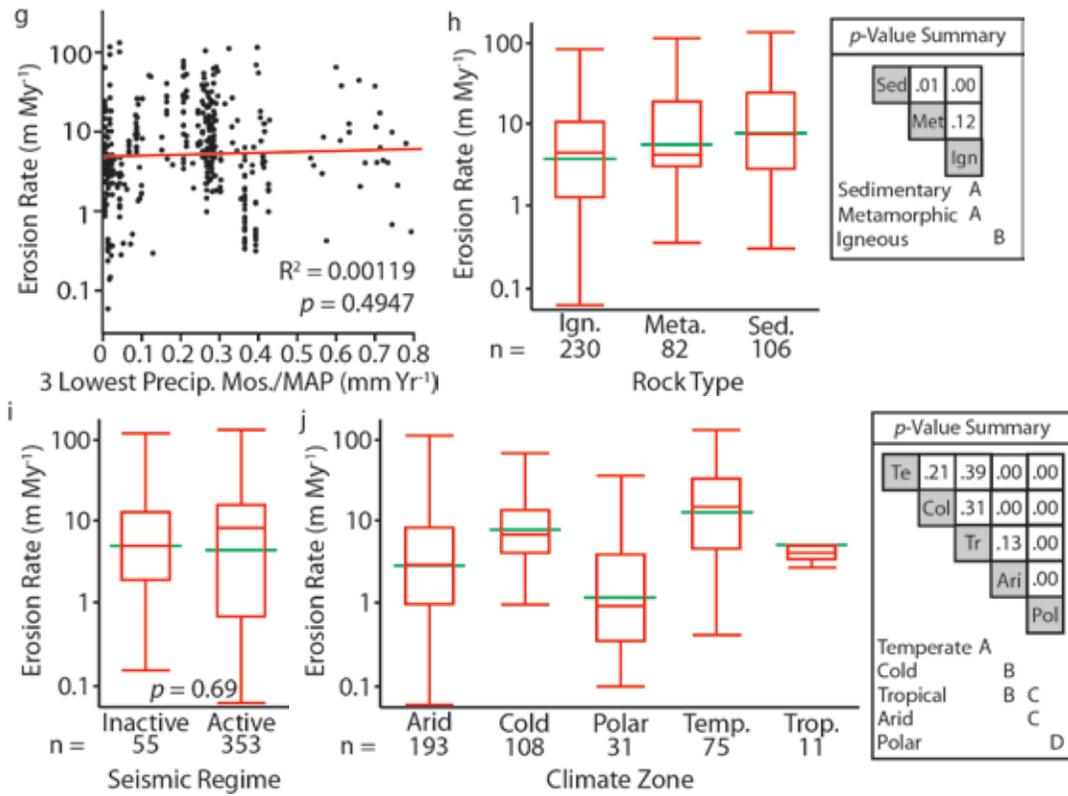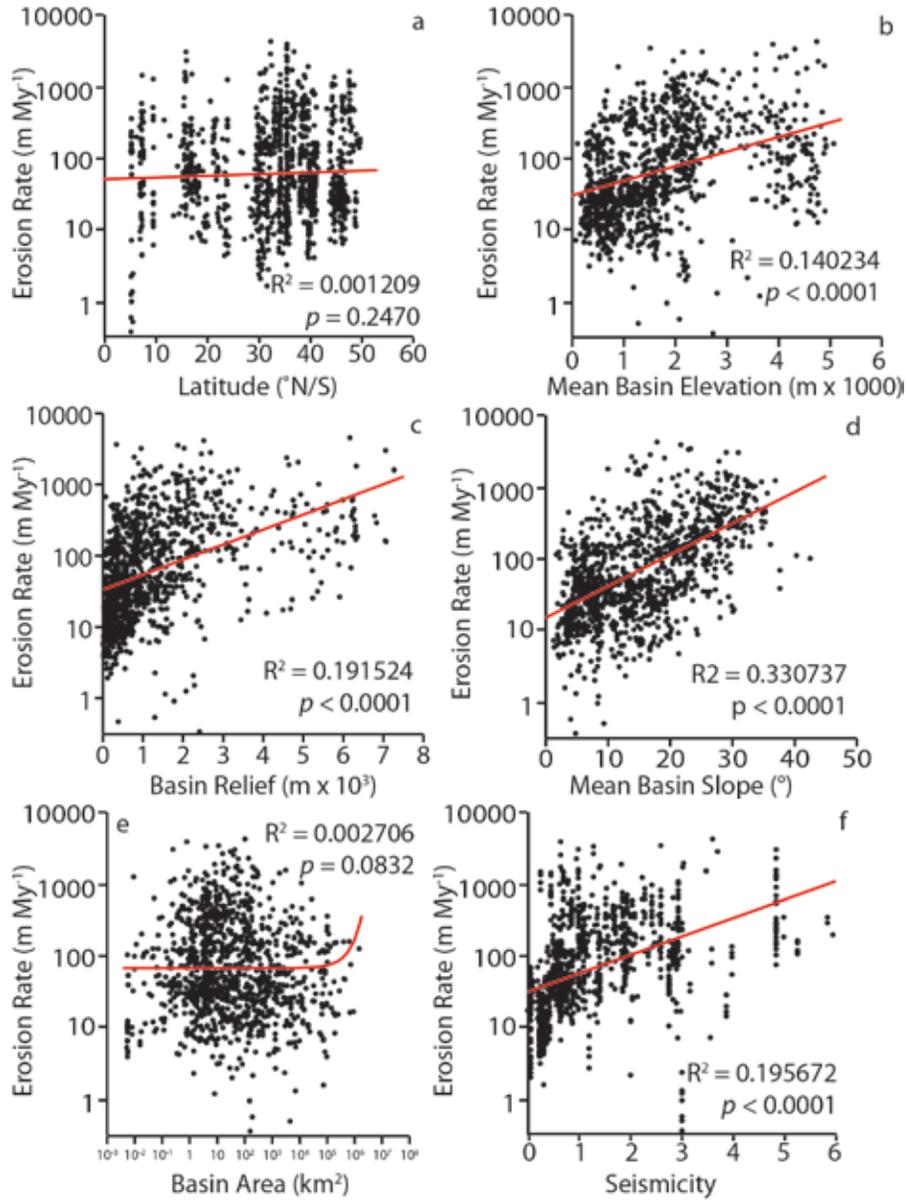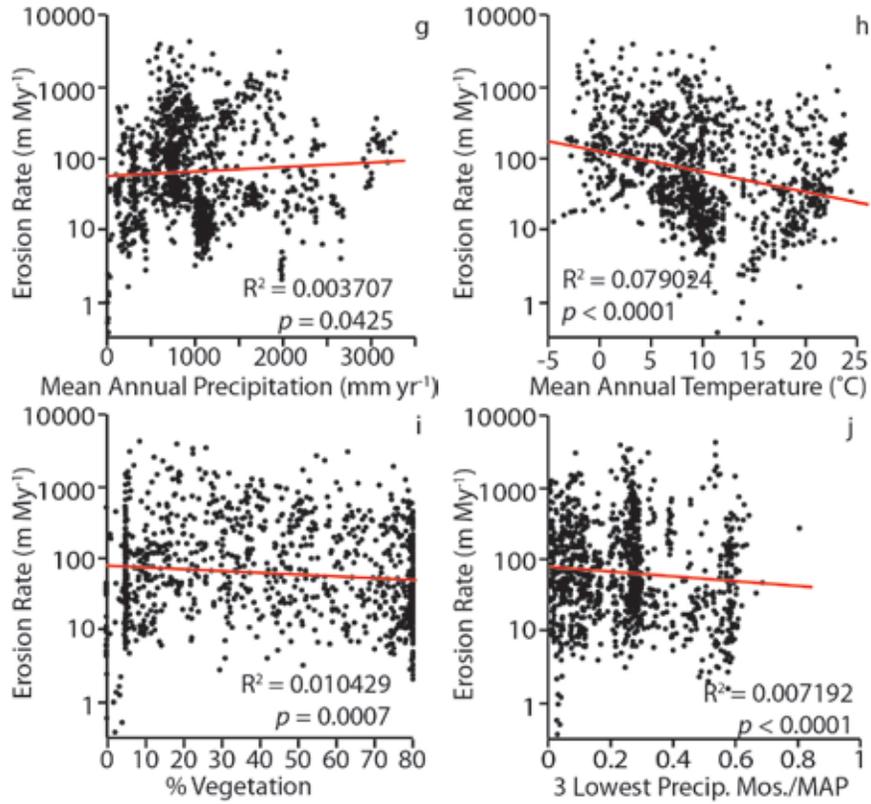
Figure DR-1.

Figure DR-2.

Figure DR-2 (continued).

Figure DR-3.

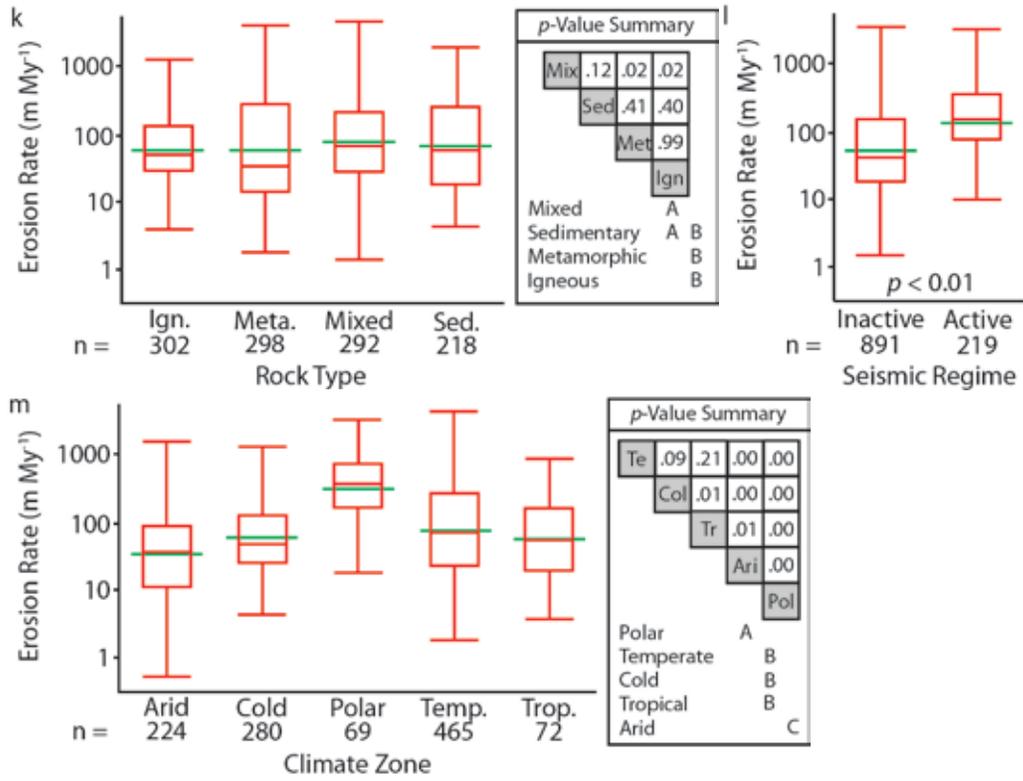Figure DR-3 (continued).

Figure DR-3 (continued).

Figure DR-4.